UCL Université catholique de Louvain

École polytechnique de Louvain (EPL)

epl

Particulate Matter Emissions of Automobiles

Development of a Low-cost Measurement System

Dissertation presented by
Séverine CASSIERS , Antoine GLORIEUX

for obtaining the Master's degree in
Mechanical Engineering

Supervisors
Francesco CONTINO, Hervé JEANMART

Readers
François BOVEROUX, Thomas WALEWYNS

Academic year 2017-2018

Abstract

Particulate matter emissions of vehicles have become a matter of great concern due to their adverse health effects and to the inability to measure them correctly. Actual vehicle inspection tests are indeed unable to detect the presence of a particulate filter on modern diesel cars although this after-treatment device allows to reduce the particulate matter emissions with 90 %. Particulate matter is moreover laborious to quantify since it is characterized by a number and mass concentration that depend on the size of the measured particles. The "Dieselgate" has also questioned the reliability of the current vehicle emission tests. There is consequently a need for reliable and representative measurements of particulate matter emissions of vehicles that are affordable for automobile inspection tests.

The objective of the present Master's thesis is to develop a low-cost PM measurement system that is able to detect the presence of a diesel particulate filter and to assess its efficiency. In addition, a general idea of the amount of particulate matter present in the exhaust gases of an on-road vehicle is also pursued.

In order to have an order of magnitude of particulate matter concentrations in exhaust gases, the present Master's thesis develops a conversion model based on the Euro norms. The conversion model is applied to two cars of the same model but complying with the Euro 3 and Euro 6b norm. As expected, the mass concentrations computed for the most recent car are more severe and within the order of magnitude of 1 mg/m^3, as opposed to 5-20 mg/m^3 for the car complying with Euro 3.

In this paper, two low-cost measurement systems that quantify a particulate mass concentration of PM2.5 based on the optical backscatter principle are compared to three state-of-the-art measurement systems made available by GOCA. These sensors are compared during tests at low load on two diesel cars dating from 2001 and 2016 and characterized respectively by the absence and presence of a particulate filter. The tests at low load include a low and high idle speed test. A packaging for the low-cost sensors is developed for the experiments and it includes a dilution, a measurement chamber and two pumps. The improved setup of the sensor allows to minimize the clogging, condensation and to tackle the temperature limits imposed by the low-cost sensor.

The present Master's thesis addressed the feasibility of using low-cost optical sensors for measuring particulate matter emissions of diesel cars. Further experiments with low-cost sensors on a recent car with and without DPF should indicate whether the distinction obtained during the experiments is indeed due to the absence of a particulate filter.

Acknowledgements

First and foremost, we are very grateful to our thesis supervisors Professor Hervé Jeanmart and Professor Francesco Contino for their expert opinion, availability and guidance throughout this year.

Furthermore, we are indebted to thank François Boveroux and Thomas Walewyns for accepting the role of reader, but also for their support given during the realization of the present Master's thesis.

Of great value were Lily, Frank and Julien from the LEFT laboratory for their help in the installation of the test bench and low-cost sensors as well as for their availability for using the laboratory equipments. Their precious recommendations were appreciated.

We would like to express our gratitude to the GOCA center in Sint-Agatha-Berchem for the possibility to use their state-of-the-art particulate matter measurement systems. Without their instruments, the present Master's thesis would probably not have reached the same conclusions. We would like to thank Bart Veldeman in particular for his availability.

Many thanks to Mederic Van Genechten from the Autosécurité group for his assistance for an appointment at the periodic technical inspection station of Rhisnes.

The tests performed in the cleanrooms of the Maxwell Building would not have been possible without Christian Renaux's availability. We thank him for his time.

Last but not least, we express our gratitude to our family and friends for providing us with unfailing support and continuous encouragement throughout the years of study and during the realization of the present Master's thesis.

Without all their valuable input and participation, this Master's thesis would not have been successfully conducted.

Séverine Cassiers and Antoine Glorieux

Contents

Introduction **1**

1 Interpretation of Regulations and Control of Particulate Matter **6**
1.1 Vehicle Emission Regulations . . . 7
1.1.1 European Norms regarding M1 Vehicles . . . 7
1.1.2 European Test Procedures for Light Duty Vehicles . . . 8
1.1.3 Low Emission Zone . . . 10
1.2 Control of PM Emissions of Diesel Engines . . . 11
1.2.1 After-treatment Devices for PM Emissions . . . 12
1.2.2 Controlling the Combustion Process of Diesel Engines . . . 13
1.3 Characterization of Particulate Matter in Engine Exhaust . . . 14
1.3.1 Particle Size Distribution . . . 15

2 Conversion of the Euro Norms into Volume Concentration **18**
2.1 Model for Computing Exhaust Volume Flow . . . 18
2.1.1 Volumetric Efficiency . . . 19
2.1.2 Pressure and Temperature in the Cylinder . . . 20
2.2 Results of the Conversion Model Applied to Two Volvo V40 Cars . . . 25
2.3 Summary . . . 26

3 Measurement Techniques of Particulate Matter **28**
3.1 Optical Sensors . . . 28
3.1.1 Optical Backscatter Sensor . . . 28
3.1.2 Opacimeter . . . 30
3.2 Accumulation Particulate Mass Measurement System . . . 32
3.2.1 Dilution Sampling System . . . 32
3.2.2 Micro Electromechanical Sensor Mass Scales Requiring Micro-dilution of the Exhaust . . . 33
3.2.3 Micro Emectromechanical Particulate Mass Sensor *Without* Micro-dilution of the Exhaust . . . 34
3.3 Scanning Mobility Particle Sizer . . . 36
3.4 Electrical Low Pressure Impactor +, Dekati ® . . . 36

4 Experimental Purpose and Methodology **39**
4.1 Motivation and Purpose of the Experiments . . . 39
4.2 Test Protocol for Car at Low Load . . . 41
4.2.1 Low Idle Speed Test . . . 41
4.2.2 High Idle Speed Test . . . 41
4.2.3 Free Acceleration Test . . . 42
4.2.4 Pre- and Post-Tests . . . 42
4.3 Setup of the Test Bench . . . 42
4.3.1 Description of the Test Bench . . . 42

4.3.2 Interest of Dilution . . . 43
4.4 Studied Low-cost Sensors . . . 44
4.4.1 Nova Laser PM2.5 Sensor SDS011 . . . 44
4.4.2 Makeblock Me PM2.5 sensor . . . 47
4.4.3 Shinyei PPD42NS Dust Sensor . . . 48

5 Experiments with Low-cost PM2.5 Sensors 51
5.1 Experiments with Nova Laser PM2.5 Sensor SDS011 at Low Load . . . 52
5.1.1 Low Idle Speed Test . . . 52
5.1.2 High Idle Speed Test . . . 57
5.1.3 Summary . . . 61
5.2 Experiments on MakeBlock Me PM2.5 Sensor at Low Load . . . 62
5.2.1 Low Idle Speed Test . . . 62
5.2.2 High Idle Speed Test . . . 64
5.2.3 Summary . . . 65
5.3 Laboratory Tests . . . 67
5.3.1 Citroën Gasoline Laboratory Engine . . . 68
5.3.2 Incense . . . 68
5.3.3 Summary . . . 69
5.4 Review of the Experimental Study . . . 69

Conclusion 72

Acronyms 75

Nomenclature 78

Bibliography 80

List of Figures 84

List of Tables 89

A Technical Details of the Cars of the Conversion of the Euro Norms 92
A.1 Volvo V40 1.9 D 102ch Summum . . . 92
A.2 Volvo V40 II D2 102ch Kinetic . . . 92

B Experiments with State-of-the-art Measurement Systems 93
B.1 High Idle Speed Test of MakeBlock Sensor on Opel Astra . . . 93
B.2 Schedule of the Tests at the GOCA Center . . . 94

Introduction

Particulate Matter (PM) causes each year the early death of about 2,500 people in Belgium and 450,000 in Europe [1]. A study of the Harvard Medical School performed in December 2017 showed a direct correlation between the daily expectation of death of elderly people and days with high PM2.5 and ozone concentrations [2]. PM is qualified by the World Health Organisation (WHO) as the pollutant that affects more people than any other one. The exposure to PM is responsible for cardiovascular and respiratory diseases such as asthma, hypertension, myocardial infarction and lung cancer.

The transport sector is one of the three biggest sources of PM in the world alongside with the residential and industrial sector [3]. In Figure 1, the distribution of emitted PM2.5 in the aforementioned sectors is shown for different parts of the world. In Africa, the burning of biomass is at the basis of cooking, heating and lighting which explains the major contribution of the residential sector to their PM2.5 emissions (78 %). China, Southeast Asia and India rely to a large extent on coal from nearby countries explaining the high contributions of the residential and industry sector in their PM2.5 emissions. In Europe, the United States and the Middle East the transport sector contributes with an important part to the PM2.5 emissions.

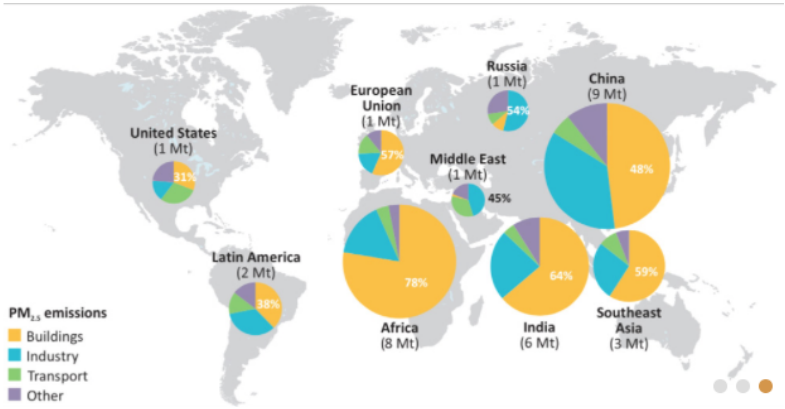

Figure 1: *Energy-related PM2.5 by region in 2015 considering 3 major sectors: buildings, industry and transport. The transport sector contributes with a significant amount to the PM2.5 emissions In Europe, the United States and the Middle East. [3]*

Historically, PM emissions have been an important issue for diesel engines. Since the introduction of the duty to have a Diesel Particulate Filter (DPF) on newly produced cars, the PM emissions of diesel cars have dropped significantly. Gasoline Port Fuel Injected (PFI) engines are characterized by low PM emissions but they are replaced nowadays by Gasoline Direct Injection (GDI) engines that are emitting up to 100 times more PM as concluded in a Study of the European Commission's Joint Research Centre [4]. Gasoline particles are also smaller than diesel particles making them more harmful for the health. Figure 2 displays a visual comparison of PM deposition for, on the one hand, diesel engines with and without DPF and, on the other hand, gasoline PFI and direct injection engines [5]. Modern diesel engines equipped with a DPF

are emitting less PM than modern gasoline direct injection engines without Gasoline Particulate Filter (GPF). The importance of a DPF is strongly highlighted with this visual comparison.

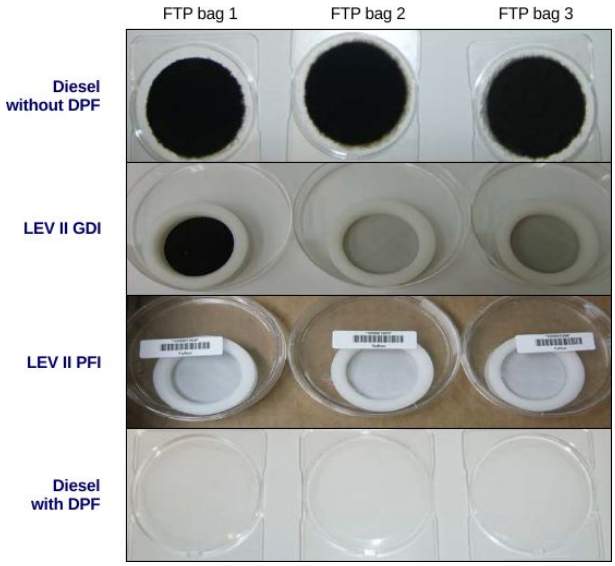

Figure 2: *Visual comparison of the PM emissions for modern and old diesel and gasoline light duty vehicles. Diesel engines with DPF emit considerably less PM emissions than diesel engines without a DPF. Old gasoline PFI engines are characterized by low PM emissions whereas modern GDI engines are emitting significantly more PM especially during the cold start phase (see FTP bag 1). [5]*

Legislative standards for the emissions from the transport sector have emerged in the early nineties and are known in Europe as the Euro norms. The standards try to decrease as much as possible the various noxious fumes. Figure 3 gives the history of limiting values for Nitrogen Oxides (NOx) and PM emissions from 1992 until 2014 covering the Euro norms 1 until 6. The norms evolve exponentially with the years making it more and more stringent to car manufacturers to succeed the tests that allow them to commercialize a car.

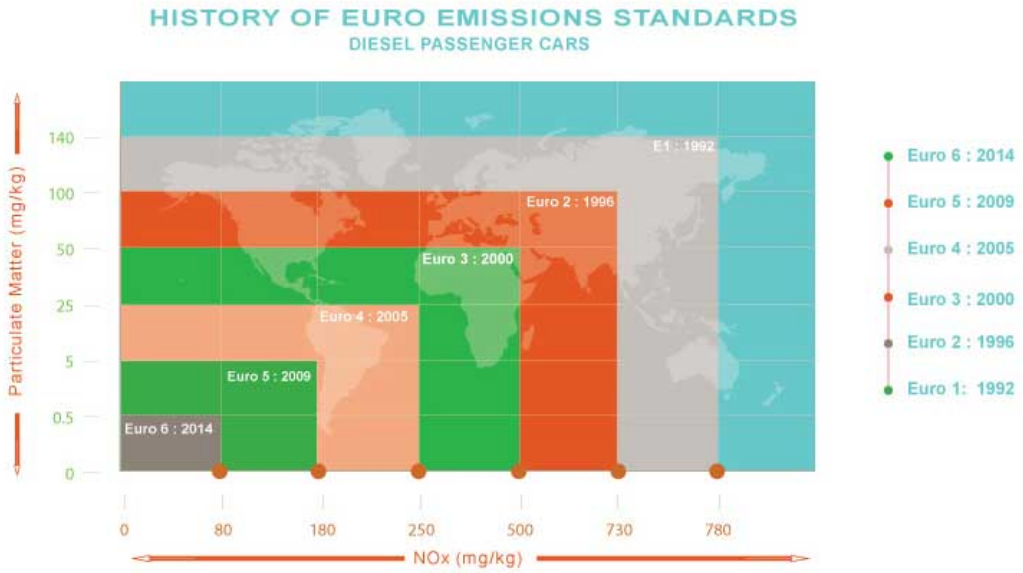

Figure 3: *History of Euro emissions standards for diesel passenger cars concerning NOx and PM emissions from 1992 until 2014 covering the Euro norms 1 until 6. The non-scaled graph shows that the norms have decreased exponentially with the years. [6]*

The "Dieselgate" has shed a new light on the reliability of the Euro norms. In September 2015, the United States Environmental Protection Agency (US EPA) officially revealed the defeat device used by Volkswagen. This cheating device inherent to the car detected when the latter was undergoing an emission test and decreased its NOx emissions by a factor up to 35 during the test [7]. Fudged NOx emissions were afterwards observed on cars of many other manufacturers among which the French car manufacturer PSA where the emissions norms were largely exceeded during real driving emissions tests.

In July 2017, the Flemish Radio and Television Broadcasting Organization VRT addressed in a documentary the relevance of a low emission zone, which prohibits old polluting cars to enter the city. They investigated whether a car without DPF would fail the Periodic Technical Inspection (PTI) tests [1]. Replacing a DPF costs approximately 2,000 € whereas illegally withdrawing it and deleting the software of the DPF from the Engine Control Unit (ECU) cost a mere 450 €, making it a cheaper alternative. Due to outdated measurement techniques, tests performed by the PTI are not able to detect the absence of a DPF which is shown with a real case of cheating during the documentary. Withdrawing a DPF, however, increases the soot and PM emissions with 90 % [1]. Due to the extensiveness of the Volkswagen scandal, this fraud has not been as much mediatized.

Consequently, the group of recognized enterprises for PTI and driving licenses GOCA has been commissioned by the Belgian authorities to prevent this fraud by identifying affordable PM measurement systems that are able to detect the presence of a DPF. GOCA studies also whether an alternative test to the one performed nowadays could help detect the presence of a DPF. The importance of a reliable measurement swiftly reporting whether or not the car is conform to the norm is highlighted as well as the need of a simple and easily reproducible test.

The tests performed by car manufacturers for getting the Euro norm are moreover not representative of real driving emissions since the car is optimized for the test conditions. Tires are, for instance, overinflated in order to reduce the ground resistance and thus the fuel consumption. The aerodynamics of the car are enhanced by gluing the air intakes. The engine is moreover perfectly greased when performing the emission test [8].

The cheated laboratory tests, as revealed by the Volkswagen scandal, and the optimized car for the test conditions have introduced the need of a real driving emission test. On-road tests require mobile measurement systems that are relatively compact and adaptable to non-laboratory conditions. Various new parameters, such as the meteorological conditions and the surrounding traffic conditions, need to be taken into account in the measurement results. Moreover, unlike laboratory tests, it is not possible to study one parameter at a time or exclude one. Consequently, there is a need of numerous test results allowing to observe trends. On-road tests also require measurement systems that are affordable to PTI stations and car manufacturers in order to apply it to the entire automobile fleet.

Since 1st September 2017, the emission test procedure of the Euro norm has been replaced by a new test procedure still performed in a laboratory and an additional emission test in real driving conditions, named respectively the World harmonised Light vehicle Test Procedure (WLTP) and the Real Driving Emissions (RDE). The latter emission test is done with a Portable Emmision Measurement System (PEMS) on public roads under various conditions among which differences in altitude, temperatures and vehicle payload, up- and down-hill driving and low-medium-high speed [9].

As a result of the adverse health effects of PM and the failing of vehicle emission standards in the previous years, a series of citizen science projects emerged. Their goal is to let citizens measure the PM concentration in their environment, to sensitize them to the exposure and, in some cases, to adapt the local traffic in order to limit the PM emissions in very polluted

streets. The community based project "*ik adem*", for instance, was created in 2014 in Ghent and organized workshops to help people build their own sensor kit for PM emissions [10]. OK Lab, on the other hand, is a group of private people in Stuttgart that developed a large scale citizen science project seeking to map the PM concentration in Europe [11]. They organize workshops that help all interested citizens in building a cheap PM measurement system. These sensors map the PM concentration by sending the measurement data through Wi-Fi. Figure 4 gives a map of the PM emissions in Belgium with the detailed measurements of the sensor in Louvain-la-Neuve on the right hand side. The city of Leuven subsidizes an extension of the project of OK Lab named Leuvenair and offers the sensor kit to their citizens in order to map the PM concentration [12]. The city of Leuven's intention is to adapt the traffic in highly polluted streets when possible in order to limit the exposure of PM nearby schools and other facilities.

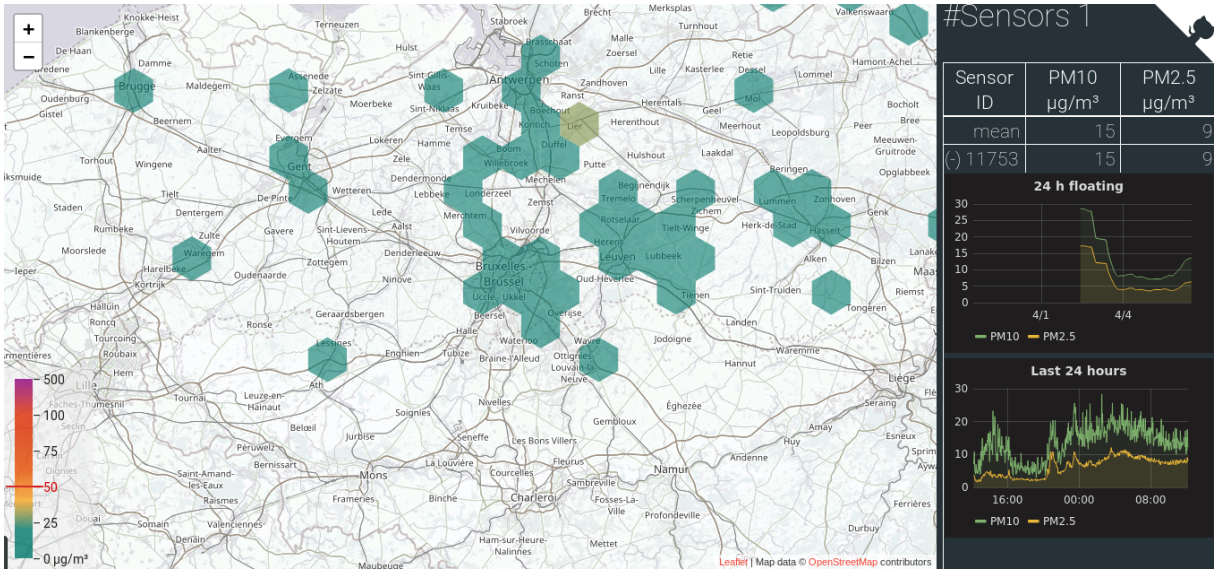

Figure 4: *The PM concentration in Northern Belgium with the measurement system developed by OK Lab based on the optical backscatter sensor Nova Laser PM2.5 on 6th April 2018. The detailed measurement of the sensor in Louvain-la-Neuve is given on the right side of the Figure. The guideline values fixed by the WHO for 24-hour mean and annual mean are respectively 25* $\mu g/m^3$ *and 10* $\mu g/m^3$ *for PM2.5 and 50* $\mu g/m^3$ *and 20* $\mu g/m^3$ *for PM10. [11]*

The present Master's thesis objective is to concentrate on PM emissions originating from the automobile sector and to conceive a low-cost measurement system for PM emitted by a car. A balance between cost, size and preciseness is pursued for the low-cost sensor. The original objective was to focus on on-road tests in order to confront the real PM measurements to the norms. However, due to the difficulty to validate the reliability of the low-cost sensors, tests at rest have been performed instead, which minimizes the amount of confounding parameters. Moreover a collaboration with GOCA was possible since they were investigating on the presence of a DPF and they allowed us to use their precise state-of-the-art PM measurement systems. The Master's thesis objective has therefore been altered to low load tests with the aim to investigate the efficiency and presence of a DPF. A comparison of the low-cost sensors with the measurement systems of GOCA will foremost allow to determine the feasibility of a low-cost measurement system.

This Master's thesis is composed of five chapters. The first chapter is performing a state of the art concerning the regulations of PM emissions and their control on diesel cars. In particular, the Euro norms are detailed and will be used as references for the study. The second chapter relates to the conversion of these Euro norms, expressed per kilometer, to concentrations per volume

unit. It will explain how to manipulate these norms in order to have more appropriate limits for the study. The third chapter gives a state of the art concerning the different types of PM measurement systems, focusing firstly on optical and accumulation sensors. Precise measurement systems giving the particle size distribution are thereafter described. The fourth chapter will detail the experimental structure. An explanation of the use of the tests and how they are performed is given. There is also a description of the test bench and the low-cost sensors selected for this Master's thesis. The fifth chapter provides the results obtained from the tests on cars and in a laboratory. A comparison with state-of-the-art measurement systems is performed on a car with and without DPF in order to assess the low-cost sensors.

Chapter 1

Interpretation of Regulations and Control of Particulate Matter

The WHO defines PM as a complex mixture of solid and liquid particles of organic and inorganic substances suspended in the air [13]. PM is physically classified based on its size in PM1.0, PM2.5 and PM10 where 50 % of particles have an aerodynamic diameter[1] less than respectively 1.0 µm,2.5 µm and 10 µm(Fig. 1.1). The mass of particles is proportional to its aerodynamic diameter. PM is also the only pollutant that is not defined chemically by US EPA [14].

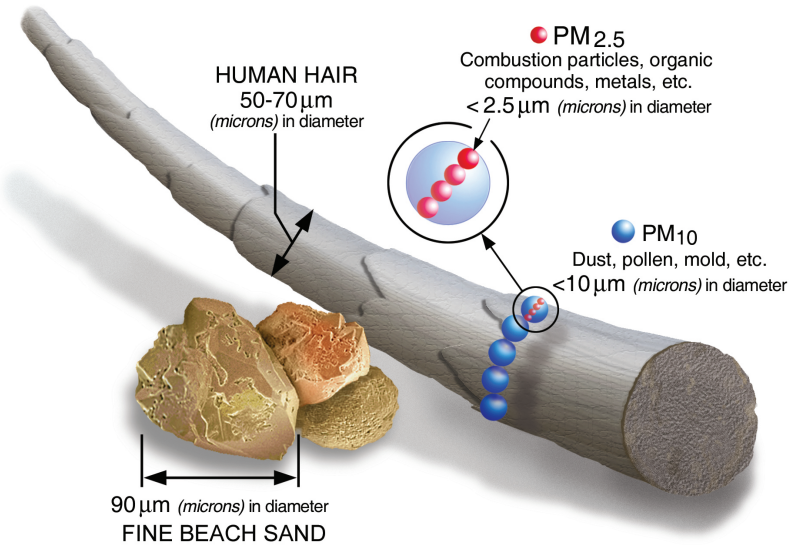

Figure 1.1: *Size comparisons for PM between fine sand beach, human hair, PM2.5 and PM10 as defined by US EPA. [15]*

The present chapter firstly details the European emission regulations related to PM and pursues with a characterization of the control devices influencing PM emissions of car engines with a peculiar interest for diesel particulate filters. A final section characterizes PM and presents particle size distributions.

[1]The aerodynamic diameter is defined as the equivalent volume diameter corresponding to the diameter of a sphere that has the same volume as the irregular particle.

1.1 Vehicle Emission Regulations

This section focuses on the European emission regulations of M1 category vehicles which are defined by the European Parliament as "motor vehicles with at least four wheels designed and constructed for the carriage of passengers comprising no more than eight seats in addition to the driver's seat" [16].

1.1.1 European Norms regarding M1 Vehicles

In 1992, the European Union introduced the first norm, named Euro 1, regarding the emissions' rate of vehicles. The latest norm, the Euro 6c and Euro 6d-TEMP, applies only to newly produced cars that are being sold presently. Old car models are not restricted by the latest norm but they have to meet the emission limits of the Euro norm of the year in which the car was produced. This is tested by the PTI but, as mentioned in the introduction, the performed verifications are not completely impervious. Euro norms define the maximum allowable limits for the following emissions: NOx, HC, CO and PM. Given the subject of the present Master's thesis, a focus will be performed on PM emissions.

As it appears from Table 1.1, there was initially only a limit to the mass of PM for diesel engines. Only 17 years after Euro 1, the European Union decided to apply the same limit for gasoline engines but only for those with a direct injection.

A sharp drop is observable over time for the limit of the mass of PM from 140 mg/km in 1992 to 4.5 mg/km in 2014. Euro 5b introduced a limit for the particle number of diesel engines and it is furthermore the only difference with Euro 5a. The limit on Particulate Number (PN) is introduced to avoid that car manufacturers focus on reducing the particulate mass concentration by having a small amount of big particles and an important amount of small particles. This would favour the amount of small particles but these are more noxious for health than bigger particles. Indeed, the smaller the particles are, the further they can go in the respiratory system and thus the more dangerous they are for people's health. DPFs and their regeneration are furthermore responsible for the emission of much smaller particles which are not measured precisely with particulate mass measurements.

M1	**Date of**	**Gasoline**		**Diesel**	
Category	**application**	**PM** [mg/km]	**PN** [#/km]	**PM** [mg/km]	**PN** [#/km]
Euro 1	1/07/1992	-	-	140	-
Euro 2	1/01/1996	-	-	80	-
Euro 3	1/01/2000	-	-	50	-
Euro 4	1/01/2005	-	-	25	-
Euro 5a	1/09/2009	5	-	5	-
Euro 5b	1/09/2011	-	-	5	6×10^{11}
Euro 6b	1/09/2014	5	6×10^{12}	4.5	6×10^{11}
Euro 6c	1/09/2018	5	6×10^{11}	4.5	6×10^{11}

Table 1.1: *The Euro norms of the European Union for vehicles from category M1 corresponding to passenger cars with a mass that is greater or equal to 2,500* kg *[17]. A sharp drop is observable over time for the limit of the mass of PM from 140* mg/km *in 1992 to 5* mg/km *in 2014.*

Concerning the latest norms, Euro 6c is an update of Euro 6b and it is based on a new test procedure, i.e. the WLTP instead of the New European Driving Cycle (NEDC) (see detailed test procedures below). Euro 6d-TEMP is a temporary Euro norm preparing for Euro 6d. This temporary norm is based on the RDE test that allows a deviation of 110 % also known as the CF. By 2020, the Euro 6d norm will become applicable with a conformity factor of 50 % between RDE and WLTP.

1.1.2 European Test Procedures for Light Duty Vehicles

The European norms are meaningless without a properly defined test procedure. Except the RDE test, all European test procedures impose laboratory test cycles performed on a chassis dynamometer where the PM emissions are expressed in g/km or #/km. A driving cycle is a series of data points representing the speed versus time and it is used to assess the performances of vehicles in various ways. The Motor Emissions Vehicle Group A (MEVG-A) test cycle is the original test procedure imposed by the European Union (EU) and consists of urban and extra-urban segments performed on a hot engine. The Urban Driving Cycle (UDC) aims at representing city driving conditions and is characterized by low vehicle speed, low engine load, and low exhaust gas temperature (Table 1.2). The Extra-Urban Driving Cycle (EUDC), on the other hand, is characterized by aggressive and high speed driving modes [18]. MEVG test cycles are characterized by one EUDC and four repetitions of the UDC. In the year 2000 when Euro 3 was the prevailing standard, the MEVG-B test cycle, better known as the NEDC, is introduced whose only difference with the MEVG-A test cycle is the cold start.

	UDC	**EUDC**	**MEVG**
Distance [km]	0.994	6.954	10.931
Total time [s]	195	400	1,180
Idle (standing) time [s]	57	39	267
Average driving speed (incl. stops) [km/h]	18.35	62.59	33.35
Average driving speed (excl. stops) [km/h]	25.93	69.36	43.10
Maximum speed [km/h]	50	120	120
Average acceleration [m/s^2]	0.599	0.354	0.506
Maximum acceleration [m/s^2]	1.042	0.833	1.042

Table 1.2: *Characterization of the MEVG cycle test composed of urban and extra-urban segments. MEVG test cycles are characterized by one EUDC and four repetitions of the UDC. The NEDC follows the MEVG cycle test and imposes a cold start.*

Since September 2017, a new test procedure, the WLTP, is introduced and will be completely replacing the NEDC from September 2018 on. The WLTP is composed of several World harmonized Light vehicle Test Cycle (WLTC) depending on the type of car, i.e. hybrid, electric or combustion engine, and depending on the Power-to-Mass Ratio (PMR). Figure 1.2 represents the Class 3b test cycle that concerns typical vehicles driven in Europe (PMR $\geq$ 34 W/kg and $v_{\max} \geq$ 120 km/h).

Figure 1.3 displays the differences between the NEDC and the WLTP whose main one is that the WLTP is more dynamic having higher average and maximum speeds and including motorways and freeways. As opposed to NEDC, WLTP does not fix gear shift points but determines optimal shift points computed with an algorithm based on the vehicle characteristics (vehicle weight and load power curves).

RDE testing requirements were introduced in September 2017 together with WLTP. These measurements need to be done during vehicle operation with a PEMS and last between 90 and 120 minutes [19]. The test is composed of three parts of each minimum 16 km. An urban segment with a maximum velocity of 60 km/h is followed by a rural segment with speeds comprised between 60 km/h and 90 km/h. The last part of RDE tests has to be performed on a motorway at a minimum speed of 90 km/h.

Switzerland is a pioneer worldwide in RDE tests by introducing in 2013 on-site PN emission testings of off-road construction machinery (SR 941.242) [20].

The test procedure for particule number is based on the Particle Measurement Program (PMP) method. The PMP is a a collaborative program of government sponsored research projects

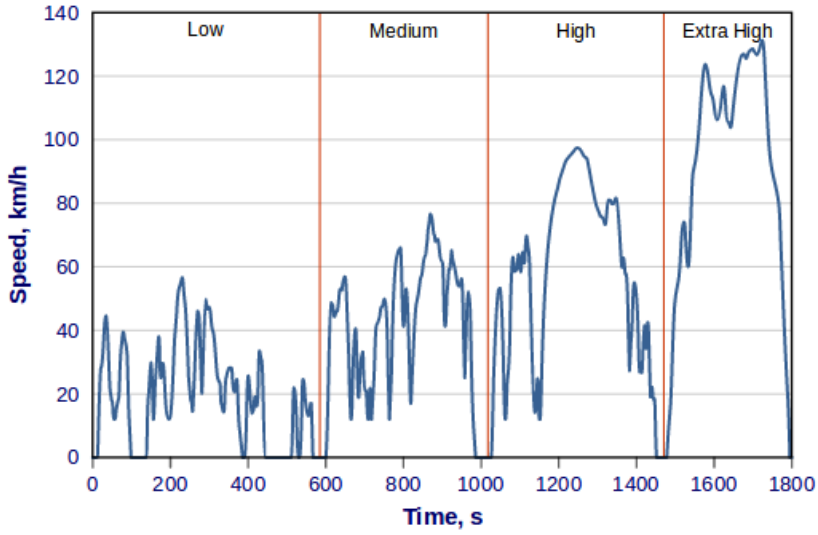

Figure 1.2: *The WLTC concerning Class 3b vehicles, i.e. typical vehicles driven in Europe (PMR* $\geq$ *34* W/kg *and* $v_{max} \geq$ *120* km/h*).*

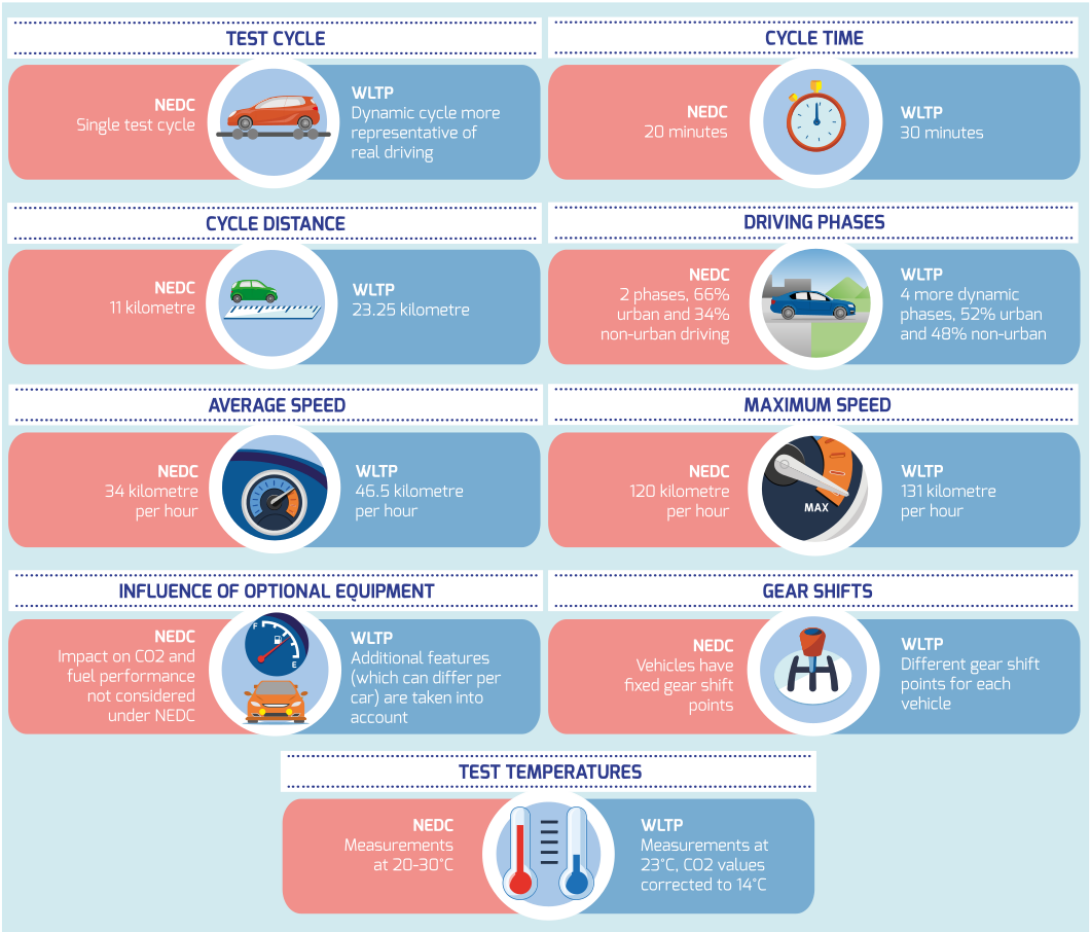

Figure 1.3: *Differences between NEDC and WLTP introduced respectively in the year 2000 and 2017. The main difference is that WLTP is more dynamic reaching higher average and maximum speeds and including motorways and freeways.*

among which the Joint Research Center of the European Commission. The PMP method defines a minimum threshold for the particle's aerodynamic diameter of 23 nm. All particles greater

than 23 nm should be measured in order to have a representative number concentration because it excludes the volatile fraction. Indeed, an aerodynamic diameter of 23 nm is "larger than the size of typical volatile nucleation mode particles but smaller than the main accumulation mode of solid diesel particles" [20], as will be clear when the particle size distribution is discussed. This threshold allows to have stable and repeatable particle number measurements. This limit is not unanimously accepted as a representative threshold because, among others, the regeneration of a diesel particulate filter can produce solid particles smaller than 23 nm. The existence of solid particles below this threshold has also been observed in the literature [20] and it is accounted on average for "30–40% [of the total particle number concentrations] without considering the particle loss in the sampling system" [21].

1.1.3 Low Emission Zone

In spite of relatively good PM emissions in Belgium compared to other European countries (Fig. 1.4), the European Commission has repeatedly sent a warning for not transposing in time the amendments, brought to the directive related to car's emissions, to the national law [22]. Moreover the European Union seeks to standardize the PTI. By doing so all the vehicles in Europe would have to fulfill the same constraints to ride on the roads. In Belgium the opposite is done in 2014. Indeed, since the 6th reform of the government, the PTI in Belgium became a regional competence [23]. Thus, the adaptation to the Euro norms does not proceed in the same way everywhere and it takes more time although ultimately the same objectives should be reached.

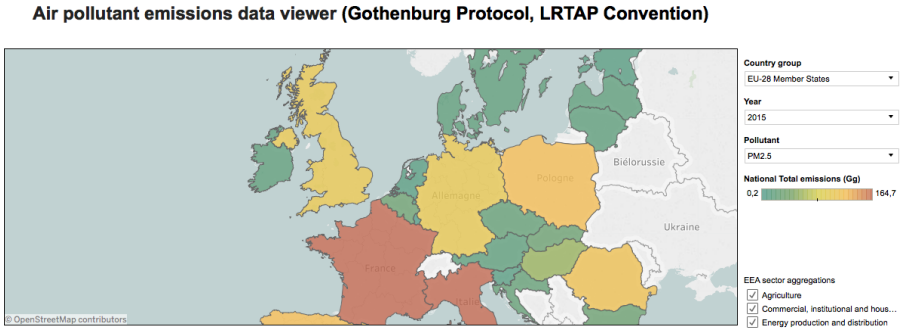

Figure 1.4: *Small particle emissions (PM2.5) of European countries in 2015 [24]. The more the color tends to green, the lower is the rate of emission of particles of matter and vice versa when the color tends towards the red. Belgium being colorized in green, it is among the countries that emitted the lowest PM concentration.*

With the pressure of the European Commission, drastic measures have been adopted by the different cities and regions in Belgium. The city of Antwerp has introduced in February 2017 a Low Emission Zone (LEZ) forbidding vehicles that do not meet the emissions criteria to drive in the city 24 hours a day and 7 days a week. Diesel cars and buses that satisfy Euro 4 and any more recent Euro norm are allowed to drive inside the city. This applies also to diesel cars and buses with particulate filters that comply with Euro 3. Concerning gasoline, CNG and LNG cars and buses, the restriction applies to vehicles that comply with a norm that is older than Euro 1. Recent balances since 2017 of Black Carbon (BC) and NOx emissions in Antwerp, showed a positive impact on the air quality thanks to the LEZ [25]. The greatest decrease in soot and NOx emissions as a result of the LEZ is observed in the parts of the city that are characterized by a dense traffic. A maximum drop of 19.2 % and 27.6 % are observed for respectively the soot and NOx emissions (Fig. 1.5).

Brussels introduced a low emission zone in January 2018, being the second city in Belgium. Diesel engines satisfying the Euro 2 norm or ≥ 2 are allowed to drive in Brussels whereas older diesel cars will be restricted. As for the LEZ of Antwerp, some of the non-accepted vehicles will

be allowed to enter the city if they pay a daily pass of 35 € that can be renewed at a maximum of eight times a year. The permit system is a transitional measure and applies until the end of 2019 for the LEZ of Antwerp. Table 1.3 reports the evolution of the prohibited vehicles in Brussels until 2025 [26]. It shows that more and more vehicles driven nowadays, diesel as well as gasoline, will not be allowed to drive freely in Brussels anymore. The Walloon Minister for the environment, Carlo Di Antonio proposed to create LEZ in Wallonia too and, at the same time, to introduce conditions of progressive ban on diesel cars in their current technological conception [27].

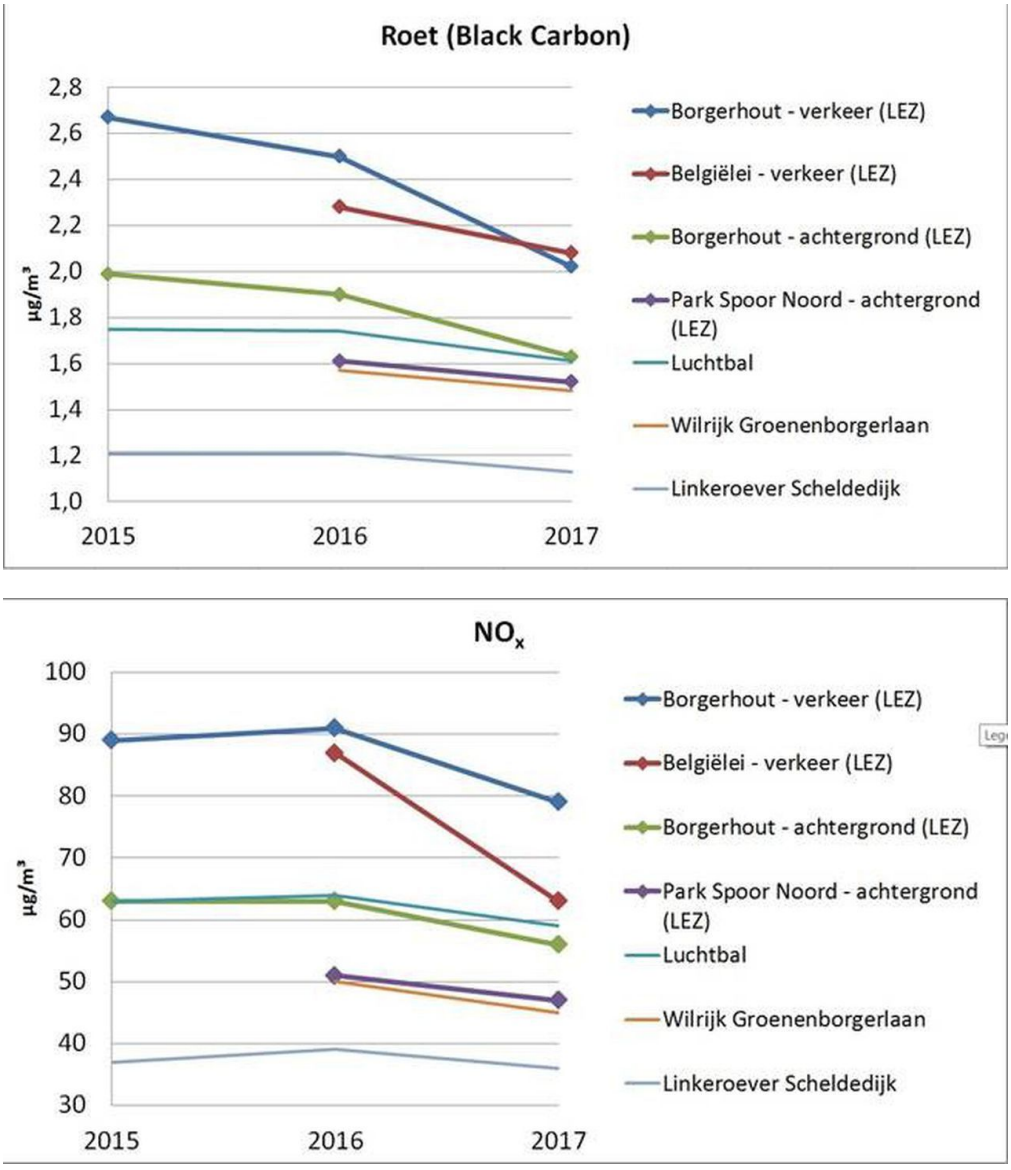

Figure 1.5: *Decrease of the soot and NOx emissions in Antwerp since the introduction of the LEZ. The observed decrease is at its highest at places with a lot of congestion. A maximum decrease of 19.2 % for soot emissions is observed in Borgerhout whereas the maximum decrease of NOx emissions (27.6 %) is observed in de Belgiëlei.*

1.2 Control of PM Emissions of Diesel Engines

Engine emissions can be controlled in two ways: either indirectly by using after-treatment devices, either directly by controlling the combustion in itself. Exhaust after-treatment does not solely

	2018	2019	2020	2021	2022	2023	2024	2025
Euro 6	Access	Access	Access	Access	Access	Access	Access	Access
Euro 5	Access	Access	Access	Access	Access	Access	Access	Pass
Euro 4	Access	Access	Access	Access	Pass	Pass	Pass	Pass
Euro 3	Access	Access	Pass	Pass	Pass	Pass	Pass	Pass
Euro 2	Access	Pass	Pass	Pass	Pass	Pass	Pass	Pass
Euro 1	Pass	Pass	Pass	Pass	Pass	Pass	Pass	Pass
Without Euro	Pass	Pass	Pass	Pass	Pass	Pass	Pass	Pass

Table 1.3: *Table with the evolution of the prohibition of the most polluting diesel vehicles in Brussels' LEZ.*

reduce emissions but it also alters the chemical composition and particle size distribution of PM emissions. Little is known nor defined about the influences of all exhaust after-treatment on PM since they all influence one another. An attempt is done to study the most relevant influences.

1.2.1 After-treatment Devices for PM Emissions

The principle of a DPF consists of separating the particles from the car's exhaust gases by depositing on a surface. This type of after-treatment device is mandatory for diesel cars since the introduction of the Euro 5 norm. DPFs are made from a ceramic or metallic medium. Several geometric configurations exist for DPFs among which the wall-flow honeycomb is the most popular (Fig. 1.6). The advantages of this type of geometric configuration is its compactness resulting in a low pressure drop without reducing the filtration rate nor the available space [28].

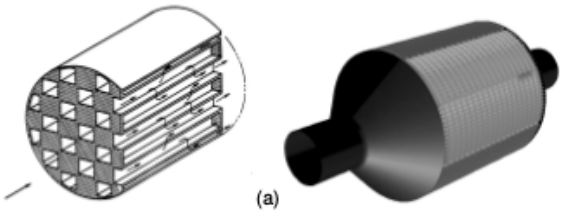

Figure 1.6: *The honeycomb wall-flow monolith is the most popular geometric configuration for actual DPFs since its compactness allows to have a low pressure drop without reducing the filtration rate nor the available space. [28]*

Particles are trapped by a DPF thanks to a combination of filtration mechanisms among which diffusional and inertial deposition and flow-line interception [29]. Figure 1.7 details the filtration mechanisms and represents graphically the filtration efficiency of each mechanism regarding the particle's aerodynamic diameter. Small particles are characterized by a high filtration efficiency for flow-line interception and inertial deposition and a low filtration efficiency is observed for filtration through diffusion. The opposite is true for particles with a high aerodynamic diameter.

Diesel particulate filters are characterized by good mechanical and thermal durability as well as very high filtration efficiencies for solid fractions of PM ($\geq$ 90 %). Liquid fractions of PM such as the Soluble Organic Fraction (SOF) and sulfate particles cannot be trapped by a DPF. The latter emission can be minimized by using ultra low sulfur fuels.

Diesel particles have a low bulk density ($\leq$0.1 g/cm^3) which results in the accumulation of considerable volumes of soot in the filter. Old heavy-duty truck or bus engines can trap up to a

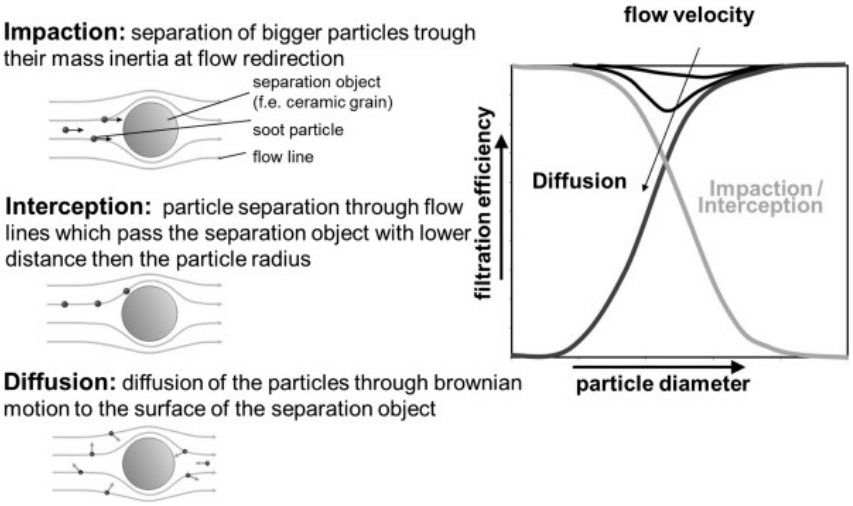

Figure 1.7: *Particles are trapped by a DPF thanks to a combination of filtration mechanisms among which diffusional and inertial deposition and flow-line interception [29]. The filtration efficiency of each filtration mechanism varies according to the particle's aerodynamic diameter. [30]*

couple of liters of soot every day [29]. Thermal regeneration of the filter is therefore essential in order to keep the DPF efficient. This process consists of increasing the exhaust temperature in order to burn off the soot with O_2 or N_2 to CO_2 ($T_{\text{exh}} \geq 550°C$ without catalysts). Passive regeneration is performed thanks to the help of catalysts and occurs continuously when the exhaust temperature is high enough whereas active regeneration is triggered periodically. For passive regeneration a catalyst is added either in the fuel either in the filter media so that the soot oxidation temperature is lowered. The catalyst promotes carbon oxidation through an oxygen or nitrogen dioxide mechanism. This type of regeneration occurs when the car drives at high speed ($\geq$ 65 km/h) during at least 10 minutes. Active regeneration, on the other hand, is triggered by increasing the soot temperature. This is done either through electric heaters in the filter media, either by injecting additional fuel in the exhaust gases or either by using in-cylinder management techniques [31]. The different types of regeneration of a particulate filter are summarized in Table 1.8.

When a blocked filter is not regenerated a risk of excessive back pressure on the engine may occur damaging among others the DPF [14]. Some types of oil and low quality fuel may destroy the DPF as well.

The Diesel Oxidation Catalyst (DOC) is another exhaust after-treatment that is mandatory since Euro 5. The main purpose of DOC is to convert HC and CO into H_2O and CO_2. However, DOC has also an indirect effect on the PM concentration and distribution. By removing the hydrocarbons, the oxidation catalyst avoids potential condensation of the hydrocarbons on the soot particles as well as nucleation of the hydrocarbons. Let's notice that there is no risk of condensation of water vapour on the soot particles since the latter are hydrophobic.

The DOC also oxidizes SO_2 to SO_3 which forms sulfuric acid in the presence of water vapor [14]. On the other hand, sulfuric acid can potentially nucleate or condense on soot particles. The very low sulfur levels of nowadays' diesel fuel imply a limited effect of sulfuric acid caused by a DOC on PM emissions. Finally, the DOC is located upstream of the DPF and it also oxidates NO to NO_2 which promotes the passive regeneration of the filter.

1.2.2 Controlling the Combustion Process of Diesel Engines

Combustion parameters can be adapted to decrease the PM emissions of diesel engines but this influences the engine performances and other emissions such as NOx and CO.

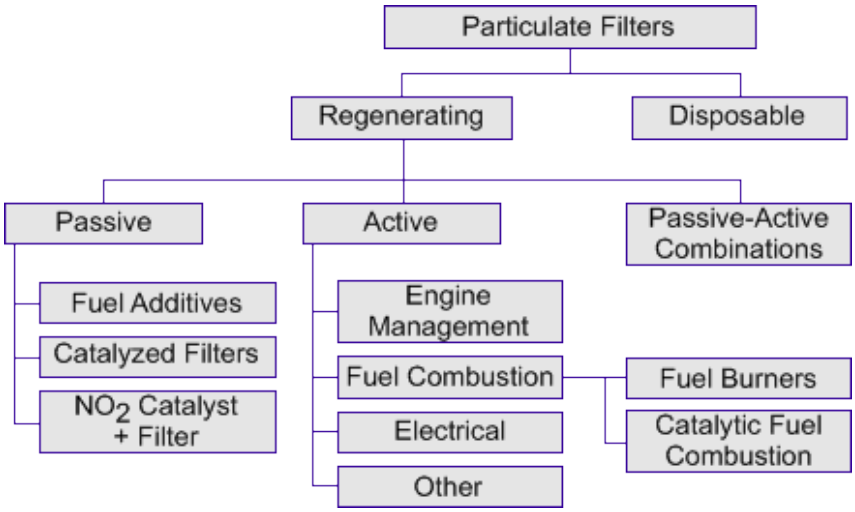

Figure 1.8: *A tree-shape summary of the different types of options in the case of a blocked diesel particulate filter. The filter can then either be replaced, either be regenerated through active and passive processes. The latter process consists in lowering the soot oxidation temperature with a catalyst whereas active regeneration consists in increasing the soot temperature.*

The evolution of diesel indirect injection systems to direct injection systems reduced the PM emissions on top of decreasing the fuel consumption thanks to the significant improvement in mixture formation [30]. The high injection pressure and the use of several injection holes atomizes the fuel droplets avoiding incomplete combustion products. Direct injection systems also allow to control the injection timing which is beneficial for PM emissions.

Exhaust Gas Recirculation (EGR) increases PM emissions because it decreases the available amount of oxygen. EGR also lowers the NOx concentration as a consequence of the reduction of the peak combustion temperature. A particle-NOx trade-off should therefore be pursued. External EGR is preferred to in-cylinder EGR with regard to PM emissions because the recirculated exhaust gases are cooled down in the first type of EGR. This allows to decrease the combustion temperature and increase the charge density which increases on its turn the combustion air ratio.

Altering the charge movement in the cylinder by inducing more or less swirl can also decrease PM emissions since it favors fuel mixing and fluid turbulence. The optimal amount of swirl depends on the combustion and injection system which varies during operation. A variable swirl is therefore preferred for reducing the PM emissions and it can be obtained through a variable geometry and arrangement of the inlet ports and piston head [30]. Increasing the swirl level has the drawbacks of increasing the fuel consumption and CO emissions because the increase in swirl impairs the volumetric efficiency.

1.3 Characterization of Particulate Matter in Engine Exhaust

PM emissions of cars are either volatile, semi-volatile or solid having an organic or inorganic composition. Carbon material contributes significantly to the PM emissions. Carbonaceous PM, also known as Total Carbon (TC), can be subdivided into three categories: Elementary Carbon (EC), Organic Carbon (OC) and Inorganic Carbon (IC) mostly present as carbonate carbon [32].

Vehicle's PM emissions is primarily composed of EC which results from incomplete combustion. EC does not volatilize up to a very high temperature and includes particles with light and non-light absorbing properties. OC and IC are present in vehicle's PM emissions "as condensed

or adsorbed aerosols or as discrete particles formed through gas-to-particle nucleation" [33]. The organic fraction of PM emissions consists among others of "atomized and evaporated lubracting oil" [34] that did not oxidate and it is present as the SOF of PM. During dilution the organic fraction can condense and trap soot. Hence, expensive and precise PM measurement systems include a catalytic stripper eliminating the volatile materials. The OC/EC fraction can be determined through a thermal/optical analysis since OC can be distinguished thanks to its thermal properties.

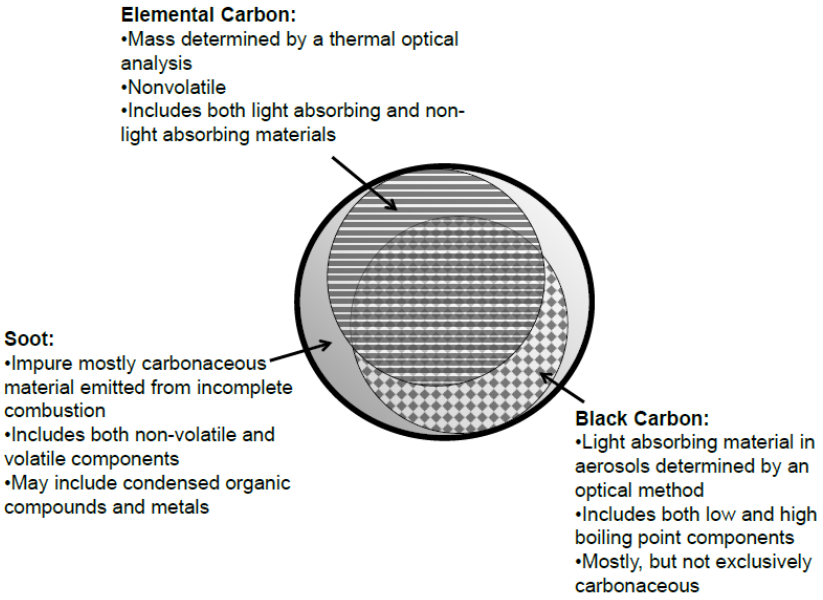

Figure 1.9: *Comparison between EC, BC and soot. [33]*

Figure 1.9 explicits the relationship between EC, BC and soot. The latter refers to the mixture of volatile and non-volatile components resulting of incomplete combustion and mainly composed of carbonaceous material. EC and BC are both a subset of soot and differ from each other by their light absorbing properties.

1.3.1 Particle Size Distribution

The number and mass weighted Particulate Size Distribution (PSD) of diesel aerosol is displayed in Figure 1.10. The lognormal distribution has three different modes based on the aerodynamic diameter of the particles [35].

The particles in the nuclei mode are mainly composed of volatile condensates such as hydrocarbons, sulfuric acid and sulfur compounds and they are formed during the dilution and cooling process of the exhaust. Small solid carbon and metal compounds are also part of the nuclei mode. Particles in the nuclei mode have an aerodynamic diameter between 0.005 µm and 0.05 µm and contain 1-20 % of the particle mass and more than 90 % of the particle number [35].

Particles in the accumulation mode have an aerodynamic diameter between 0.05 µm and 1.0 µm [35] and they are composed of particles of the nuclei mode that have grown by coagulation and vapor condensation to agglomerates of solid material (carbon and metallic ash), condensates and adsorbed materials (heavy carbons and sulfur species). These agglomerates are formed during the in-cylinder combustion process. This mode as well as the nuclei mode are a threat for the health since they are too small to be trapped by the nose but large enough to precipitate in the alveoli of the lungs.

Particles in the coarse mode are accumulation mode particles that have deposited on the cylinder surface and are later re-entrained resulting in larger particles (aerodynamic diameter around 1µm). Five to twenty percent of the particle mass consists of PM in the coarse mode.

The number distribution is thus mainly composed of particles in the nuclei mode whereas the mass distribution is mainly composed of particles in the accumulation mode. PM is in this manner composed of a considerable amount of small, and therefore lightweight, particles and only a limited amount of heavier particles.

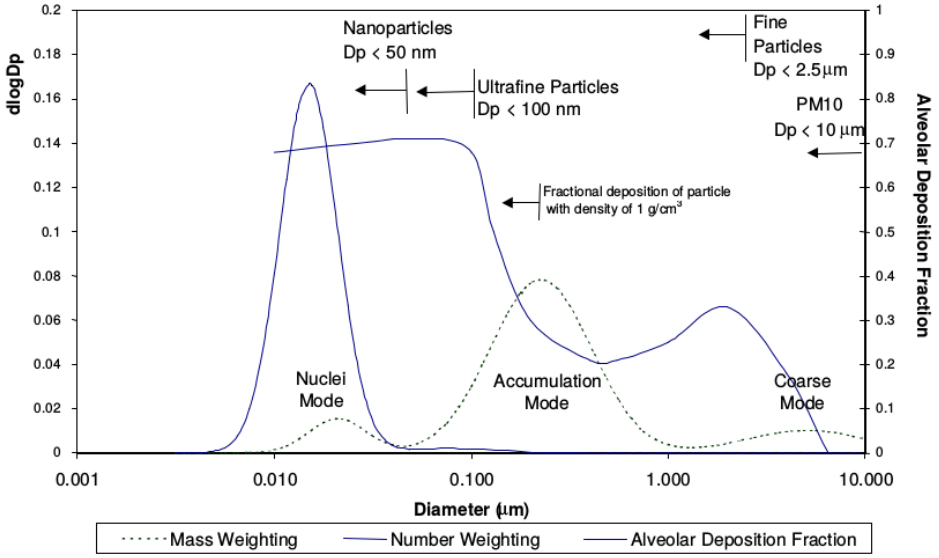

Figure 1.10: *The particle size distribution of diesel exhaust expressed in mass and number weightings have three distinctive modes. The nucleation mode contains more than 90 % of the number weighting whereas the accumulation mode contains a considerable amount of the mass weighting. The coarse mode particles are formed through deposition and re-entrainement of accumulation mode particles. [35]*

The particle size distribution when varying EGR and injection timing is displayed in Figure 1.11. The PM emissions of a four-cylinder, four-stroke diesel engine are measured after a two-stage dilution with a Scanning Mobility Particle Sizer (SMPS) (see Chapter 3 for a detailed description of the measurement instrument) [36]. The limit between nucleation and accumulation mode is in this case set at 70 nm and is represented by a vertical line on the graphs.

At zero EGR, the nuclei mode is predominant on a logarithmic plot and it is not affected by a varying injection timing. Delaying the injection timing from −23 ° Crank Angle (CA) to −10 °CA After Top Dead Center (ATDC), increases the amount of PM in the accumulation mode. When still increasing the injection timing from −10 °CA to 0 °CA ATDC, an increase is observed in accumulation mode particles with an aerodynamic diameter smaller than approximately 200 nm whereas the amount of particles greater than approximately 200 nm in diameter decreases.

At an EGR of 40 %, the accumulation mode is predominant on a logarithmic plot for early injection timings except at −23 °CA ATDC. Due to the exhaust gas recirculation, some particles are re-entrained in the combustion chamber and form agglomerates resulting in an increase of particles in the accumulation mode. Delaying the injection timing from −23 °CA to −10 °CA ATDC, increases the accumulation mode whereas delaying the injection timing from −10 °CA to 5 °CA ATDC decreases it. Retarding the injection at positive crank angles after the top dead center leads to a particle size distribution that is dominated by the nucleation mode.

The present chapter reported a state of the art concerning PM emissions of automobiles with a main interest on the European regulations and methods for controlling the PM emissions of diesel vehicles.

A first section detailed the existing European emission regulations of vehicles regarding PM. The Euro norms and the related test procedures are described in addition to their history. The measures introduced by the European Commission are thereafter addressed by giving the example of the low emission zones of Antwerp and Brussels.

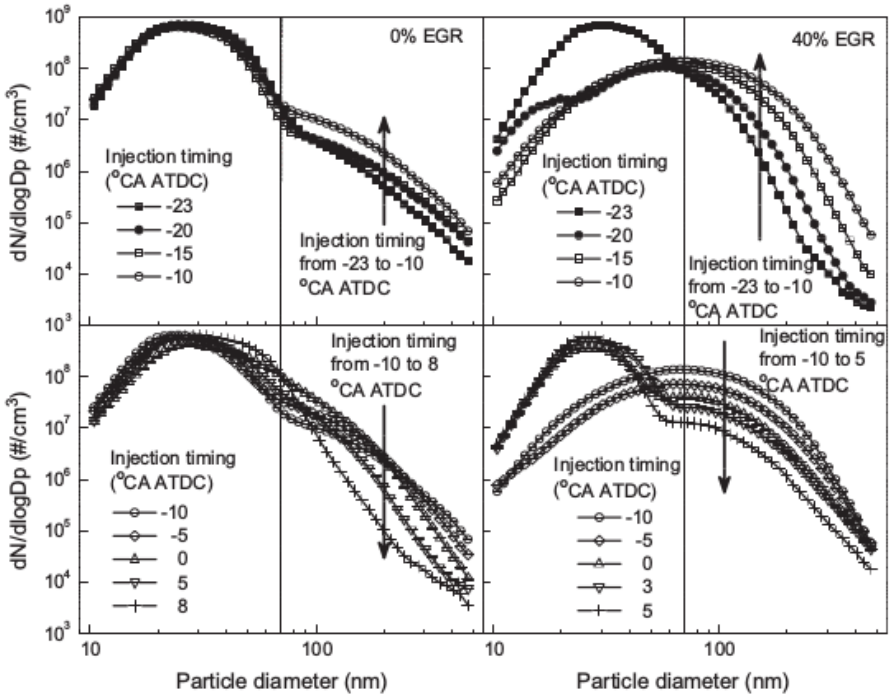

Figure 1.11: *The effects of EGR and injection timing, expressed in CA ATDC, on particle size distribution. The PM emissions of a a four-cylinder, four-stroke diesel engine are measured with a scanning mobility particle sizer after a two-stage dilution. [36]*

The second section specified the ways of controlling PM emissions of diesel engines. Indirect control is firstly addressed explaining the influences of a DPF and a DOC on PM emissions. Direct control of PM emissions of vehicles is afterwards detailed by addressing the influences of the injection system, EGR and charge movement.

The last section characterized PM by clarifying the difference between OC, EC, BC and soot. This section also included a detailed analysis of the PSD of diesel engines.

Chapter 2

Conversion of the Euro Norms into Volume Concentration

The present chapter aims to convert the Euro norms, expressed in g/km, to volume concentrations expressed in g/m^3. In order to perform this conversion, the exhaust volume flux needs to be computed or measured. The purpose of this conversion is to determine the expected particulate mass concentration of the exhaust gases which allows to choose appropriate sensors for the experiments. PM sensors have indeed a limited concentration range expressed in g/m^3. A dilution can potentially be performed in order to tackle the concentration limit but it is restricted by a physically possible dilution ratio.

This conversion model computes the intake and exhaust volume flow using a theoretical model for the volumetric efficiency. After describing the conversion method, the present chapter applies it to two Volvo V40 engines dating from the years 2000 and 2016. Comparisons are done with the density of dry air and the ratio of produced PM emissions to the mass of diesel fuel.

An alternative to this conversion method would be to perform a direct measurement of the intake mass flow and fuel consumption.

2.1 Model for Computing Exhaust Volume Flow

Euro norms are bound to a test procedure as detailed in Chapter 1. The present conversion model focuses on the Euro 6 norm following the NEDC. As a short reminder, this type of test procedure is separated into two different cycles: the UDC and the EUDC. The first one represents typical driving conditions in large cities and the second one represents high speed driving modes. Figure 2.1 represents the evolution of speed during the NEDC. For this study, we only took into account the urban driving cycle segment which corresponds to driving the car during 780 s (13 min) at a mean speed of 33 km/h.

The exhaust volume flow at the tailpipe of a four-stroke engine can be expressed by multiplying the intake volume flow by a factor depending on the temperature of the exhaust gases (Eq. (2.2)). The expression for the intake flow is, on its turn, directly derived from the engine's rotational speed, the engine's displacement V_c and the volumetric efficiency η_{eff} [37]. The engine's displacement and the temperature of the exhaust gases are respectively expressed in inches and degrees Fahrenheit in the following expressions for the intake and exhaust volume flow:

$$\dot{V}_{\text{in}} = \frac{V_c \text{ RPM } \eta_{\text{eff}}}{3456} \qquad [\text{feet}^3/\text{rot}] \tag{2.1}$$

$$\dot{V}_{\text{ex}} = \left(\frac{T_{\text{ex}} + 460}{540}\right) \dot{V}_{\text{in}} \qquad [\text{feet}^3/\text{rot}] \tag{2.2}$$

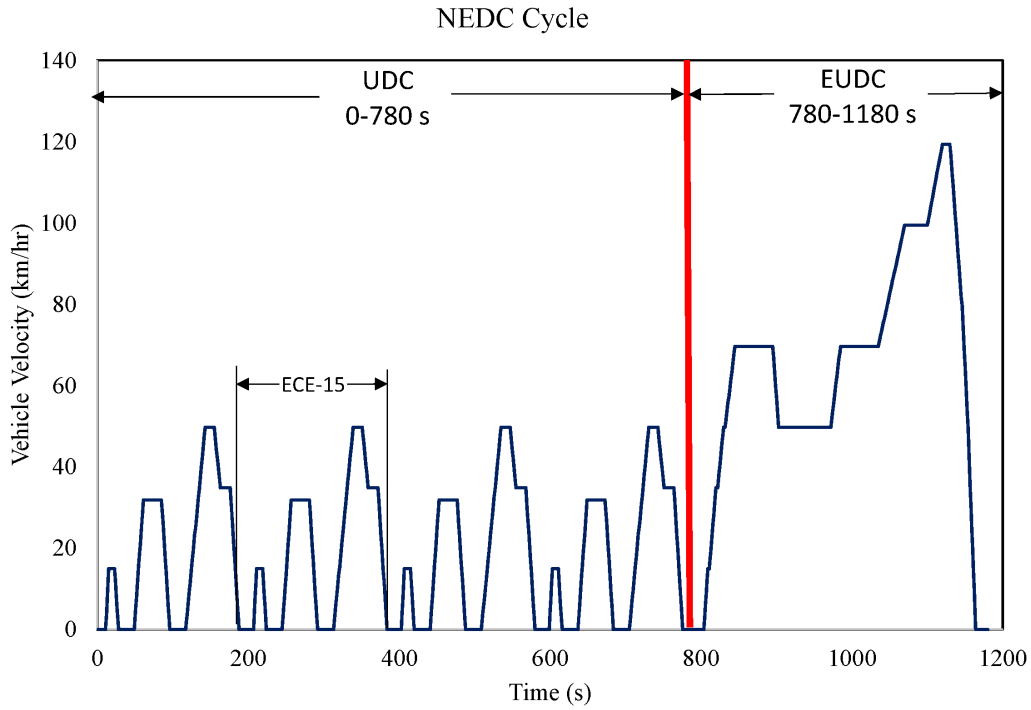

Figure 2.1: *Representation of the speed during the NEDC which is composed of four urban driving cycle and one extra-urban driving cycle. ECE-15 represents one elementary urban cycle.*

Based on the test conditions of the NEDC, the engine rotational speed is computed as follows and depends on the car's characteristics:

$$\mathrm{RPM} = \frac{88 \text{ mph } i_2 \; i_\mathrm{f}}{\mathrm{circ}_\mathrm{feet}} \tag{2.3}$$

where mph is the car speed, i_2 is the gear ratio for the second gear, i_f the final gear ratio and $\mathrm{circ}_\mathrm{feet}$ is the circumference of the tire in feet.

2.1.1 Volumetric Efficiency

No simplified equation can be used for the volumetric efficiency for this model since it depends on the engine's operational parameters. The volumetric efficiency is not constant due to acceleration and it exceeds unity on modern cars as a result of the presence of a turbocharger. A model for the volumetric efficiency developed by Raymond C. Turin from SimuQuest incorporation and Rhong Zhang and Man-Feng Chang from the R&D department of General Motors [38], is used as reference for this conversion model. The starting point of the model is that the volumetric efficiency is defined and non-zero only between the Intake Valve Opening (IVO) and Intake Valve Closing (IVC). At those moments, the energy conservation reads:

$$\begin{array}{ccccccccccc} m_{\mathrm{c,IVC}} c_\mathrm{v} T_{\mathrm{c,IVC}} & = & m_\mathrm{fg} c_\mathrm{p} T_\mathrm{m} & + & m_\mathrm{rg} c_\mathrm{v} T_\mathrm{ex} & + & m_{\mathrm{bf_{ex}}} c_\mathrm{p} T_\mathrm{ex} & - & W_\mathrm{pi} & + & Q \\ \downarrow & & \downarrow & & \downarrow & & \downarrow & & \downarrow & & \downarrow \\ \text{energy at time of IVC} & = & \text{fresh gas energy} & + & \text{residual gas energy at time of IVO} & + & \text{exhaust backflow gas energy} & - & \text{piston work} & + & \text{net heat transfer} \end{array}$$

In this expression, the mass terms should be eliminated because they are very difficult to measure. They are therefore replaced by other values that are known or measurable. For example, for the energy at time IVC and the residual gas energy at time of IVO, the perfect gas law allows

to express the mass regarding pressure and volume. This results in the following expression for the energy conservation:

$$\begin{aligned} p_{\text{ram}} \left(\frac{V_{\text{c}_0}}{V_{\text{IVC}}}\right)^{\kappa_{\text{p}}} V_{\text{IVC}} \frac{c_{\text{v}}}{R} = \eta_{\text{eff}} p_{\text{m}} V_{\text{c}} \left(1 + \frac{1}{F_{\text{st}}\lambda} + r_{\text{EGR}}\right) \frac{c_{\text{p}}}{R} \\ + V_{\text{IVO}} \frac{c_{\text{v}}}{R} \sum_{i=1}^{3} p_{\text{i}}(\phi_{\text{IVO}}) + c_{\text{p}} T_{\text{ex}} k_{\text{bf}} \sum_{\text{i}=1}^{4} m_{\text{ex}_{\text{i}}} - k_{\text{w}} \overline{W}_{\text{pi}} \\ + \frac{k_{\text{cg}} \eta_{\text{eff}}}{\omega_{\text{e}}} \left(\frac{n}{n_{\text{ref}}}\right)^{k_{cn}} \left(\frac{p}{p_{\text{ref}}}\right)^{k_{cp}} (T_{\text{clt}} - T_{\text{fg}})[2A_{\text{pi}}(\phi_{\text{IVC}} - \phi_{\text{IVO}}) + B\pi\chi_{\text{pi}}] \end{aligned} \tag{2.4}$$

with

$$\begin{aligned} p_{\text{ram}} &= p_m \, \exp\left[\frac{1}{2RT_m}\left(k_{v0}\frac{V_c}{A_r}\frac{N_{\text{cyl}}}{2}\frac{\min(n_e, k_{\text{rpm}})}{60}\right)^2\right] \\ \chi_{pi} &= \int_{\phi_{\text{IVO}}}^{\phi_{\text{IVC}}} r\left(1 - \cos\phi + \frac{r}{2L}\sin^2\phi\right) d\phi \end{aligned}$$

The volumetric efficiency is isolated as follows in the adapted equation of the energy conservation (Eq. 2.4).

$$\eta_{\text{eff}} = \frac{p_{\text{ram}} \left(\frac{V_{\text{c}_0}}{V_{\text{IVC}}}\right)^{\kappa_p} V_{\text{IVC}} - V_{\text{IVO}} \sum_{i=1}^{3} p_i(\phi_{\text{IVO}}) - k_{\text{bf}} R\kappa T_{\text{ex}} \sum_{i=1}^{4} m_{\text{ex}_i} + k_w \frac{R}{c_v} \overline{W}_{\text{pi}}}{\kappa p_m V_c \left(1 + \frac{1}{F_{\text{st}}\lambda} + r_{\text{EGR}}\right) + \frac{k_{cg}}{\omega_e}\left(\frac{n}{n_{\text{ref}}}\right)^{k_{cn}} \left(\frac{p}{p_{\text{ref}}}\right)^{k_{cp}} (T_{\text{clt}} - T_{\text{fg}})[2A_{\text{pi}}(\phi_{\text{IVC}} - \phi_{\text{IVO}}) + B\pi\chi_{\text{pi}}]} \tag{2.5}$$

Lots of new parameters are introduced in the computation of the volumetric efficiency and they can be separated into geometric and thermodynamics quantities. The first category includes among others the volumes and the crankshaft angles which are generally constant values. The thermodynamics parameters are usually not constant and laborious to determine, such as the temperature and the pressure of the gas inside the cylinder. These non constant thermodynamic variables are the result of a series of phenomena occurring in the cylinder among which the combustion of the fuel.

2.1.2 Pressure and Temperature in the Cylinder

To obtain the expression of the pressure and temperature in the cylinder in function of the crank angle, the thermodynamic cycle is separated in different time or crank angle intervals. These intervals are delimited by the IVO and the IVC but also by the Exhaust Valve Opening (EVO) and the Exhaust Valve Closing (EVC) (Fig. 2.2). The studied thermodynamic cycle has an overlap around the TDC between IVO and EVC which means that both the intake and the exhaust valves are opened at the same time.

From IVC to EVO

The first considered interval is between IVC and EVO and is the time interval during which both valves are closed. It is also during that time interval that the combustion occurs. The 0D model of an engine cycle including in-cylinder heat transfer losses gives the following dimensionless expression for the evolution of the pressure regarding the crankshaft angle:

$$\frac{d\tilde{p}}{d\phi} = -\kappa\frac{\tilde{p}}{\tilde{V}} + \frac{\kappa - 1}{\tilde{V}}\left[\tilde{Q}\frac{dx}{d\phi} - \tilde{h}(1 + \beta\tilde{V})(\tilde{p}\tilde{V} - \tilde{T}_{\text{wall}})\right] \tag{2.6}$$

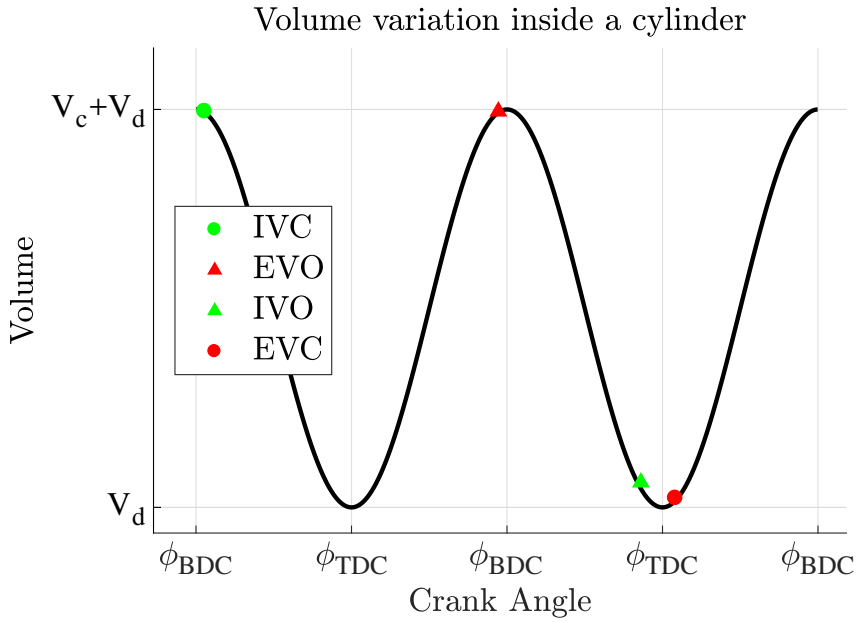

Figure 2.2: *The evolution of the cylinder volume in function of the CA with the specified opening and closing times of the inlet and exhaust valves of a four-stroke engine.*

where the nondimensional quantities are defined as follows and where the heat transfer coefficient h is approximated by the Woschni expression:

$$\tilde{h} = \frac{h\, T_{IVC}(A_{\mathrm{TDC}} - 4V_{\mathrm{TDC}}/B)}{p_{\mathrm{IVC}}\, V_{\mathrm{IVC}}\, \omega},$$

$$\beta = \frac{4V_{\mathrm{TDC}}}{B(A_{\mathrm{TDC}} - 4V_{\mathrm{TDC}}/B)},$$

$$\tilde{p} = \frac{p}{p_{\mathrm{IVC}}}, \qquad \tilde{V} = \frac{V}{V_{\mathrm{IVC}}}, \qquad \tilde{Q} = \frac{Q}{p_{\mathrm{IVC}}\, V_{\mathrm{IVC}}}, \qquad \tilde{T}_{\mathrm{wall}} = 1.3.$$

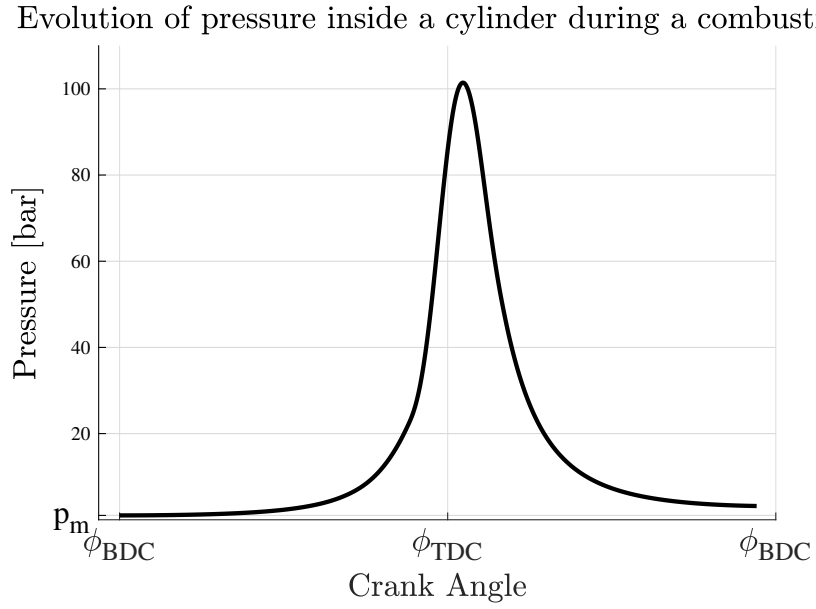

Figure 2.3: *The evolution of the pressure inside the cylinder from IVC to EVO. The peak in pressure is not aligned with the crank angle at top dead center ϕ_{TDC} because the combustion is delayed which is generally the case in cars.*

The resulting evolution of the pressure inside the cylinder between IVC and EVC does not line up with ϕ_{TDC}, the crank angle at TDC (Fig. 2.3). It is due to the fact that the considered time of combustion is not symmetrical with respect to ϕ_{TDC} but slightly retarded, in this case by 10 °.

After computing the cylinder pressure by integrating the 0D model (Eq. 2.6), the evolution of the temperature in the cylinder is calculated based on the Van der Waals equation (Eq. 2.7). In this expression, n corresponds to the amount of moles, the variables a and b correspond to the properties of the gas molecules and T_c and p_c correspond to the pressure and temperature at the critical state. This Van der Waals model is preferred to the perfect gas law because of the combustion products and the pressures reached during combustion ($p \geq 30$ bar). The perfect gas law is indeed rather representative for small molecules at low pressures and high temperatures.

$$p + \frac{an^2}{V^2} = \frac{nRT}{V - nb} \tag{2.7}$$
$$\text{with} \quad a = \frac{27R^2T_c}{64p_c} \quad \text{and} \quad b = \frac{RT_c}{8p_c}$$

From EVO to BDC

During the interval between EVO and Bottom Dead Center (BDC), the temperature stays constant because it is just after the combustion and the temperature of the walls are high enough to neglect the heat loss through them. The pressure inside the cylinder decreases due to the two following phenomena: the piston is going down in the cylinder increasing the volume and the exhaust valve is opening. It is assumed that the pressure loss can be split in the two following terms:

- A pressure loss due to the increase of volume in a closed adiabatic system: $pv^{\gamma} = constant$.
- A pressure loss due to the loss of mass through the exhaust ports.

From BDC to IVO

During the interval between BDC and IVO, the gain in pressure due to the ascent of the piston is assumed equal to the loss due to the opening of the exhaust valve. This results in assuming a constant pressure inside the cylinder. The temperature remains constant too for the same assumptions as in the previous interval.

From IVO to EVC

During the interval between IVO and EVC, both valves are open. The evolution of cylinder pressure is approximated by two independent constant pressure segments with, between them, a pressure peak close to ϕ_{TDC} as it is done in the volumetric efficiency model [38]. The total cylinder pressure across these particular intervals can be seen as the superposition of three elementary piece-wise linear pressure functions which all depend on the prevailing operating conditions (Fig. 2.4).

The equations of the three elementary piece-wise linear pressure functions are detailed in Equations (2.8), (2.9) and (2.10) and define four new crank angles : ϕ_s, ϕ'_s, ϕ_1 and ϕ_2.

$$p_1(\phi) = \begin{cases} 0 & \phi < \phi_s \text{ or } \phi > \phi'_s \\ k(\phi - \phi_s) & \phi_s \leq \phi \leq \phi_{\text{TDC}} \\ k(2\phi_{\text{TDC}} - \phi_s - \phi) & \phi_{\text{TDC}} < \phi \leq \phi'_s \end{cases} \tag{2.8}$$

$$p_2(\phi) = \begin{cases} p_{\text{ex}} - p_m & \phi < \phi_1 \\ p_{\text{ex}} - p_m - m(\phi - \phi_1) & \phi_1 \leq \phi \leq \phi_2 \\ 0 & \phi > \phi_2 \end{cases} \tag{2.9}$$

$$\begin{aligned} p_3(\phi) &= p_m \\ p_c(\phi) &= \sum_{i=1}^{3} p_i(\phi) \end{aligned} \tag{2.10}$$

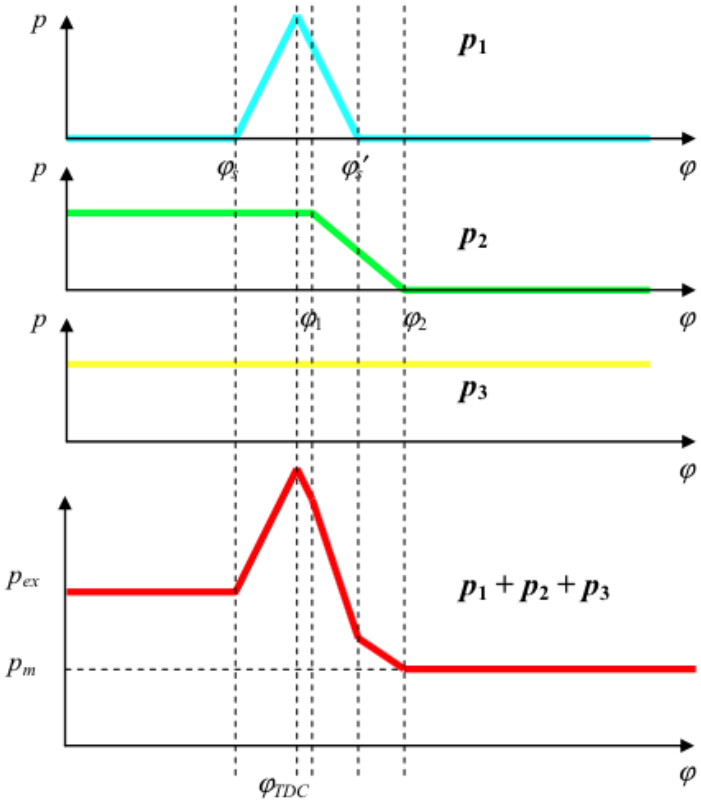

Figure 2.4: *The cylinder pressure between IVO and EVO approximated as the superposition of three linear pressure functions. [38]*

The newly defined crank angles depend on the engine geometry. The angle ϕ_s represents the instant at which the mass displacement due to the piston motion is higher than the maximum possible flow out of the intake and exhaust port. At this moment, the flow at the exhaust port becomes subject to choked flow conditions and can be approximated with the following equation [38]:

$$\left| r\omega_e \left(\sin\phi + \frac{r}{2L} \sin 2\phi \right) \right| \approx \frac{4\sqrt{RT_c}}{B^2} \left[D_{\text{inv}} L_{\text{inv}}(\phi_s) + D_{\text{exv}} L_{\text{exv}}(\phi_s) \right] \psi_{\max}$$

where

$$\psi_{\max} = \sqrt{\frac{2\kappa}{\kappa - 1} \left[\alpha^{\frac{2}{\kappa}} - \alpha^{\frac{\kappa+1}{\kappa}} \right]} \quad , \quad \alpha = \left(\frac{2}{\kappa + 1} \right)^{\frac{\kappa}{\kappa-1}}$$

Once ϕ_s is known, the others crank angles can be computed easily as follows:

$$\begin{aligned} \phi_s' &= \phi_{\text{TDC}} + |\phi_{\text{TDC}} - \phi_s| \\ \phi_1 &= \phi_{\text{IVO}} + \Delta\phi_{\text{off}} \\ \phi_2 &= \phi_1 + \Delta\phi_{\text{len}} \end{aligned}$$

where the angle shift values $\Delta\phi_{\text{off}}$ and $\Delta\phi_{\text{len}}$ are used as regression parameters.

From EVC to IVC

In the last interval between EVC and IVC, the intake valve is open whereas the exhaust valve is closed. The pressure remains constant and its value is equal to the manifold pressure while the temperature is decreasing until the temperature of the fresh gases.

Complete Cycle

Figure 2.5 depicts the (p,V)-diagram of the complete cycle and results from the assumptions that were aforementioned. Figure 2.6 illustrates the corresponding evolution of the temperature inside the cylinder. Both graphs are close to what is obtained in the literature [39], [40].

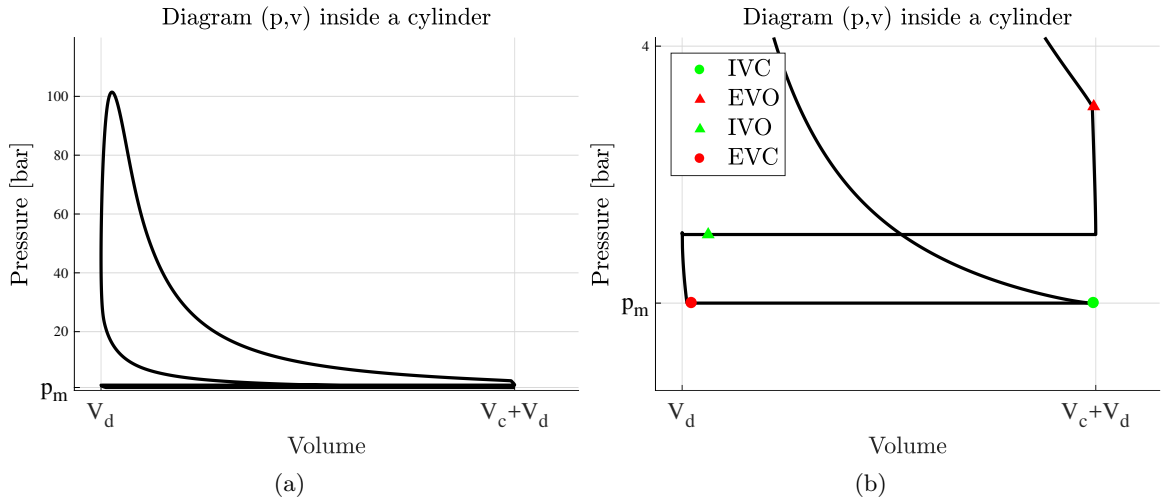

Figure 2.5: *The pressure inside the cylinder in function of the cylinder volume for a four-stroke engine. Figure (b) is a zoom at low pressure of Figure (a) and allows to have a better image of the corresponding valve timings.*

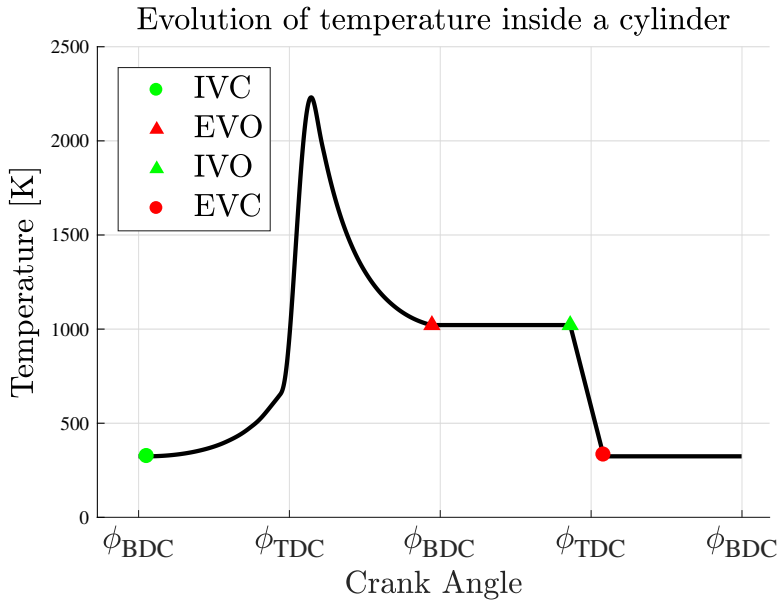

Figure 2.6: *Representation of the temperature variation versus the crank angle with the valve timings represented in red and green.*

The valve timing is not the same for all the cars because it depends of the wanted characteristics for the car. The car manufacturers have to choose between several characteristics such

as the performance of the car or the pollution emitted. Moreover, the values are not generally communicated in the datasheets found on their website. So, to apply this conversion model to specific cars in the next section, the following values have been imposed:

- $\phi_{\mathrm{IVC}} = 10°$ after BDC
- $\phi_{\mathrm{EVO}} = 10°$ before BDC
- $\phi_{\mathrm{IVO}} = 25°$ before TDC
- $\phi_{\mathrm{EVC}} = 15°$ after TDC

2.2 Results of the Conversion Model Applied to Two Volvo V40 Cars

The present section converts the Euro norm to a mass concentration of two Volvo V40 cars by using the previously developed equations for the engine's exhaust volume flux (Eq. (2.2)), volumetric efficiency (Eq. (2.5)) and rotational speed (Eq. (2.3)). The results of the conversion model are engine-specific since the engine's geometry and volumetric coefficient is taken into account. The two Volvo V40 engines have similar engine models and are respectively dating from the years 2000 and 2016 complying therefore with the Euro 3 and Euro 6 norms. The limit in particulate mass concentrations of the two norms is 50 mg/km and 4.5 mg/km for respectively the Euro 3 and Euro 6 norm, as stated in Chapter 1. A limit for the particle number is only imposed for the Euro 6 norm and is fixed to 6×10^{11} #/km. The two cars to which the conversion model is applied are the following (for detailed characteristics see Appendix A):

- Volvo V40 1.9 D 102ch Summum commercialized in 2000
- Volvo V40 II D2 120ch Kinetic commercialized in 2016

The mass concentration, the volumetric efficiency and the exhaust volume flow resulting from the conversion model of both Volvo V40 models is depicted in Table 2.1 and Table 2.2. Intake pressures ranging from one to three atmospheres are compared for both engines. The conversion of the particle number limit is only computed for the model dating from the year 2016. The converted mass norms show the impact of technological improvements of the engine's model. The ratio of both mass norms gives a factor of 10 whereas the ratio of the converted mass concentrations gives a value of 12 to 14. The computed ratio is moreover varying with the intake pressure. These results show that the technological progresses obtained by car manufacturers are better than what the EU expected. This conclusion should, however, be done with caution since the conversion model includes several constant parameters and approximations.

Volvo V40 - 2000	**Intake pressure [atm]**		
	1	2	3
Volumetric efficiency	0.684	1.666	2.277
Exhaust flow [m^3/s]	0.021	0.051	0.070
Mass norm [mg/m^3]	21.78	8.959	6.560

Table 2.1: *Conversion of the norms into volume concentration for a Volvo V40 commercialized in 2000.*

Since it is difficult to report whether the obtained concentrations are high or not, the following ratios are computed comparing the results to known quantities. The computed volume flow rate can firstly be compared to the product of the displacement volume and the engine regime showing that both are within the same order of magnitude of 10^{-2} m^3/s. The calculated mass

Volvo V40 - 2016	**Intake pressure [atm]**		
	1	2	3
Volumetric efficiency	0.912	1.910	2.513
Exhaust flow $[m^3/s]$	0.030	0.063	0.083
Mass norm $[mg/m^3]$	1.360	0.651	0.495
Number norm $[\#/m^3]$	18.14×10^{10}	8.670×10^{10}	6.597×10^{10}

Table 2.2: *Conversion of the norms into volume concentration for a Volvo V40 commercialized in 2016.*

concentrations can furthermore be compared to the density of dry air ($\rho_{\text{air}} = 1225$ $[g/m^3]$). The ratio of both densities gives a concentration of 10^{-4} % to 10^{-5} % of particles in air which is physically acceptable.

Another way of interpreting the converted particle concentrations is by computing the ratio between the Euro norm (g/km) and the mass of fuel consumed. Let's recall that a Compression Ignition (CI) engine uses heat of compressed air to burn the fuel that is considered to be liquid. The mass flow of air and fuel that is required for the engine is therefore expressed as follows:

$$\begin{aligned} \dot{m}_{\text{air}} &= \rho_0 \, \dot{V}_{\text{in}} \\ \dot{m}_{\text{fuel}} &= \varphi \frac{\dot{m}_{\text{air}}}{m_{\text{a1}}} \end{aligned}$$

where $\dot{V}_{\text{in}}$ (Eq. 2.1) is expressed as $[m^3/s]$ and ρ_0 is the air density at the intake which is easily computed with the ideal gas law. The stoichiometric air-fuel ratio m_{a1} is computed based on the stoichiometric combustion reaction of $C_{16}H_{34}$, an approximation of diesel fuel. The air-fuel equivalence ratio ϕ varies a lot for diesel engines and is computed based on its definition ($\varphi = \text{AFR}/m_{\text{a1}}$) and an Air-Fuel Ratio (AFR) varying between 17 and 29.

Table 2.3 and Table 2.4 depict the mass of PM emitted by the two studied Volvo V40 cars when burning one mass or volume unit of diesel fuel for different intake pressures. The obtained mass ratios are higher than expected, particularly for the Volvo car commercialized in 2000. Indeed, the computed ratio for an intake pressure of one atmosphere indicates that 0.5 g of particulate matter is produced when 1 g of fuel is burned which is too high. The lowest computed ratio for the Volvo car of the year 2000 is 0.004 $g_{\text{PM}}/g_{\text{diesel}}$ and it is still a considerable amount. Indeed, when this ratio is converted back into g_{PM}/km by using the diesel urban consumption of the corresponding car, the value is around 30 times higher than the Euro 6 norm. These surprising results are most probably due to the approximated values such as the AFR which was considered constant at 23.

Volvo V40 - 2000	**Intake pressure [atm]**		
	1	2	3
$[g_{\mathbf{PM}}/g_{\mathbf{diesel}}]$	0.505	0.104	0.051
$[g_{\mathbf{PM}}/L_{\mathbf{diesel}}]$	426.45	87.58	42.70

Table 2.3: *Ratios of the allowable mass of particulate matter to the mass of diesel fuel for a Volvo V40 commercialized in 2000.*

2.3 Summary

The previously developed conversion model allows to convert the Euro norm following the NEDC expressed in g/km to mass concentrations expressed in g/m^3 regarding particulate matter emissions. The established conversion model computes a car's exhaust volume flow based on

Volvo V40 - 2016	**Intake pressure [atm]**		
	1	2	3
$[g_{PM}/g_{diesel}]$	0.033	0.008	0.004
$[g_{PM}/L_{diesel}]$	28.11	6.71	3.40

Table 2.4: *Ratios of the allowable mass of particulate matter to the mass of diesel fuel for a Volvo V40 commercialized in 2016.*

the car's characteristics. This is done by using the volumetric efficiency model developed by Raymond C. Turin from SimuQuest incorporation and Rhong Zhang and Man-Feng Chang from the R&D department of General Motors [38]. The volumetric efficiency model required to compute the evolution of the cylinder pressure and temperature in function of the crank angle.

The conversion model is applied to two diesel Volvo V40 cars dating from the years 2000 and 2016, complying respectively with Euro 3 and Euro 6b. The obtained particulate mass concentrations indicated a realistic percentage of particles in dry air of 10^{-4} to 10^{-5}. The results showed moreover that the more recent Volvo V40 has done more improvements in terms of PM emissions than expected by the Euro norm. This conclusion has to be considered with caution since several parameters are assumed constant in this conversion model such as the timing valve. The present chapter allows eventually to give an order of magnitude of the expected PM concentration in a car's exhaust gases which gives an idea of the required dilution ratio for the chosen low-cost sensors.

Chapter 3

Measurement Techniques of Particulate Matter

Four main types of measurement techniques are discussed. The two first ones, optical sensors and sensors based on accumulation of PM, are relatively small in size and measure a mass or number concentration. The two last ones, the Scanning Mobility Particle Sizer (SMPS) and the Electrical Low Pressure Impactor (ELPI)+, measure a size distribution, mass and number concentration. They are very accurate as well as expensive ($\geq$ 50,000 €) and are more appropriate to laboratory conditions.

3.1 Optical Sensors

Optical sensors have the advantage of small size and a relatively low cost. The major drawback is the limit in the particle's detected size as discussed below.

3.1.1 Optical Backscatter Sensor

The working principle of this sensor is based on the *scattering* of light by PM. The intensity of the scattered light is a measure of the particle concentration or number. The measurement system is composed of a light source, e.g. Light-Emitting Diode (LED), a photomultiplier detector and collimating or focusing lenses. The light source is oriented by an angle of 90 ° or less with the detector (Fig. 3.1). Some sensors also include purge lines to allow air or N_2 to withdraw the particles from the probe and a heater or fan in order to create air circulation (esp. for indoor sensors).

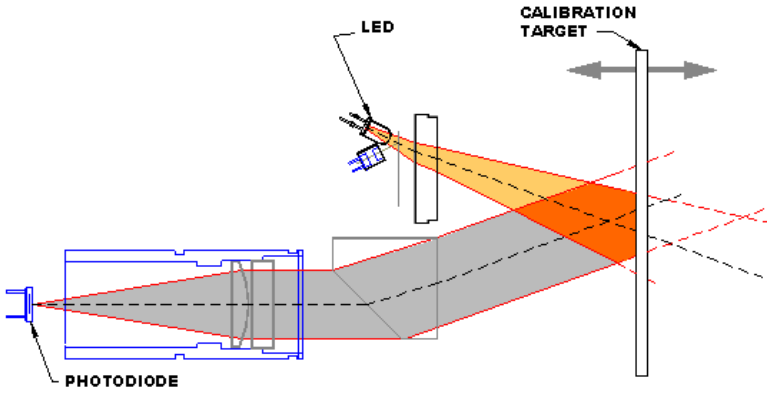

Figure 3.1: *The optical backscatter sensor is composed of a photodiode which measures the light emitted by the LED source whenever a particle scatters its light beam. The output signal is directly proportional to the amount of particles.*

A lot of low-cost optical backscatter PM sensors exist on the market but they are mainly for indoor applications. Three optical backscatter PM sensors are tested on vehicles in Chapter 5 and compared to accurate, state-of-the-art measurement instruments, relying on the principles described below.

The Oak Ridge National Laboratory (U.S. Department of Energy) has developed an optical backscatter PM sensor for the exhaust manifold of vehicles, before the DPF [41]. The sensor design based on optic fibers is detailed in Figure 3.2. A comparison is done with an opacimeter showing a non-zero baseline level for the optical backscatter. This is due to light scattering from the wall and can be solved by changing the geometry of the sensor in the intake. The test conditions occur before the DPF where relatively many particulate matter is present (compared to indoor conditions).

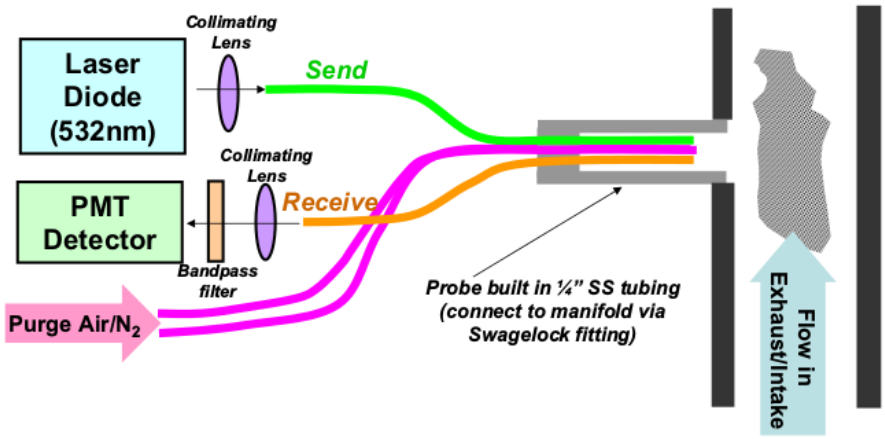

Figure 3.2: *The optical backscatter PM sensor developed by the Oak Ridge National Laboratory (U.S. Department of Energy) that is based on the light scattering principle. The sensor uses optic fibers for the signal transmission and measures a PM concentration at the exhaust manifold, i.e. before a DPF. [41]*

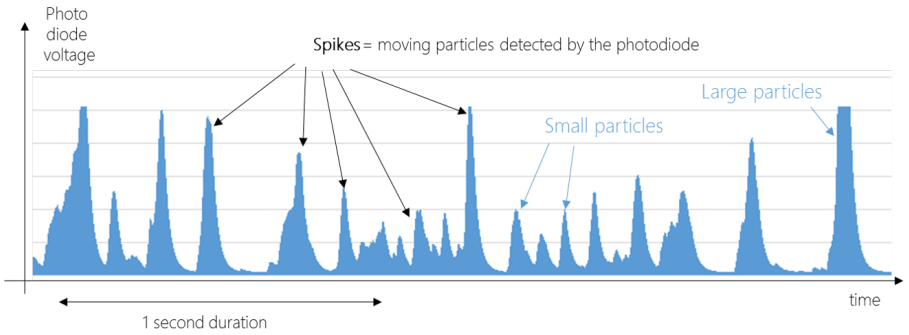

Figure 3.3: *The photodiode voltage in function of time for the Shinyei PM2.5 PPD42NS sensor, a low-cost PM2.5 sensor. The measurement principle of the sensor is based on the scattering of light by particles. The more scattered light the photodiode intercepts, the higher the spikes and also the greater the particle's size. [42]*

Accurate optical backscatter sensors, such as the Dylos monitor, count individual particles and classify them by size. Low-cost optical backscatter sensors, such as the three selected sensors for the experiments, measure on the other hand the duration during which the photodiode detects the particles that are passing by. This amount of time is analogous to an opacity percentage and is called Low Pulse Occupancy (LPO). Figures 3.3 and 3.4 portray respectively the photodiode voltage and the Low Pulse Occupancy (LPO) of the Shinyei PM2.5 PPD42NS sensor, a low-cost optical backscatter sensor that is used in the experiments of this Master's thesis. The sensor firstly applies a pass band filter to get rid of the noise and the very small particles which is

represented by the red line in Figure 3.4. The spikes of the photodiode voltage represent moving particles and the higher the spikes are, the greater the size of the particles. The pass band filter is thus adjusted depending on which particle's size the sensor measures (PM2.5 or PM10). After applying the pass band filter, the LPO is measured independently of the height of the spikes. For the Shinyei sensor, the LPO is assumed to be proportional to the particle number concentration whereas the two other selected low-cost sensors assume it proportional to the mass concentration.

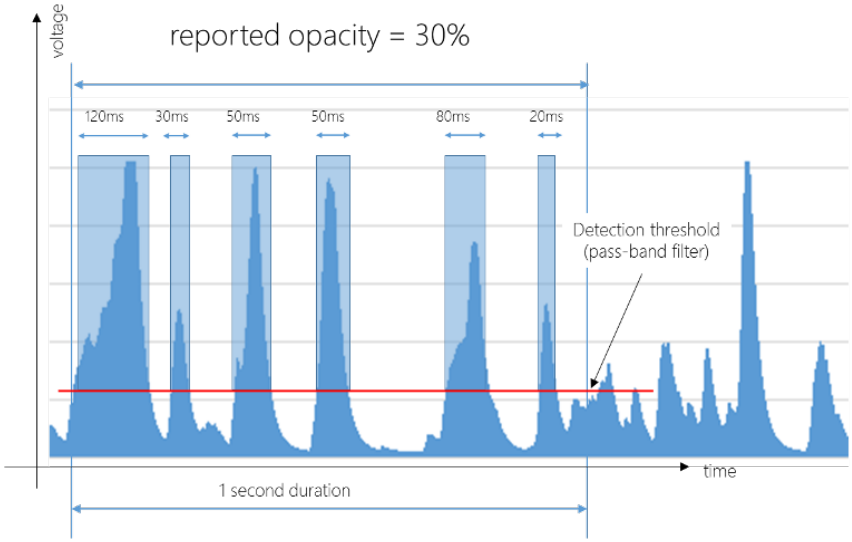

Figure 3.4: *The photodiode voltage in function of time for the Shinyei PM2.5 PPD42NS sensor with a representation of the LPO. The latter represents the amount of time the photodiode detects a moving particle and is analogous to an opacity percentage. The red line represents the pass band filter excluding small particles and noise. [42]*

3.1.2 Opacimeter

The working principle of this sensor is based on the *extinction* of light by PM. The opacity of the exhaust is given in percentage or with a coefficient of absorption k [m^{-1}]. It is a measure of the PM in the flow and unlike the optical backscatter sensor it is inversely proportional to the amount of PM. The k-value has a range of 0-10 m^{-1} and a margin, depending on the sensor, of 0.5 m^{-1} [43]. The measurement system is composed of a light source and a photodiode or photoelectric cell with filter if necessary. The emitter and receiver are located on each side of the intake unlike the optical backscatter sensor (Fig. 3.5). An opacimeter is the legally demanded measurement technique for the exhaust test of the PTI [44]. During PTI, a free acceleration test is performed where the accelerator needs to be pressed down during 1 second by the driver. Whether this type of test is representative of the real driving emissions is not commonly accepted in the literature. This type of test has not been chosen for the experiments of this Master's thesis as described in Chapter 4.

The measurement technique of an opacimeter was historically developed for diesel engines without diesel particulate filter where k-values were of the order of 1.5 to 2.5 m^{-1} and where a margin of 0.5 m^{-1} was physically acceptable [43]. In Table 3.1 the maximum allowed k-values during PTI are shown. A mean margin of 0.3 m^{-1} is achieved on the first generation opacimeters of Belgian PTI centers and this margin becomes problematic when the maximum allowed k-value is 0.7. Moreover diesel engines with DPF have k-values not exceeding 0.05 m^{-1} [43]. Improvements have been done in opacimeter's margin but the emission test performed at the PTI with an opacimeter is still not able to prove whether a modern vehicle has a DPF or

not at a reasonable price. During PTI, the performance of a DPF is not precisely monitored with the car's current On-Board Diagnostics (OBD)-system because the PID 7A, 7B and 7C are only made accessible by a few car manufacturers. The PTI only verifies that no error codes are displayed by the emission systems, e.g. EGR and DPF. This can however be forged by a garage keeper allowing cars without DPF, whereas they need to have a particulate filter, to succeed the tests.

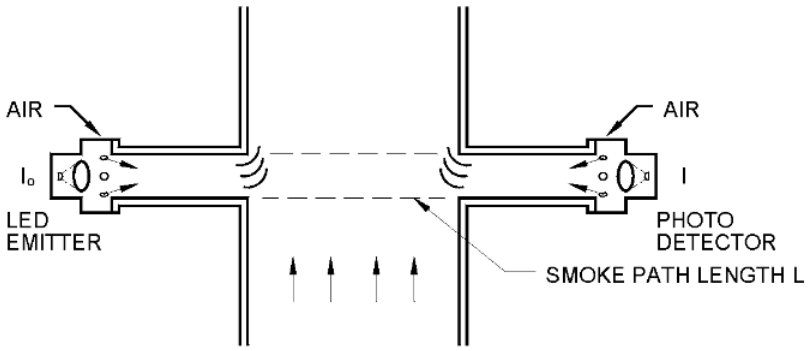

Figure 3.5: *The measurement technique of the opacimeter that is distinguished from optical backscatter sensors by the location of the receiver and emitter on either side of the exhaust pipe.*

	Year	**Maximum allowed k-value** [m^{-1}]
With turbocharger	1980	3.0
Without turbocharger	1980	2.5
Diesel Euro 4 and 5 (with turbo)	2008	1.5
Diesel Euro 6[1]	2018	0.7

Table 3.1: *During the PTI, the maximum allowed smoke emissions becomes very close to the margin of error (0.5* m^{-1}*) for recent vehicles. [43]*

The first generation opacimeters used in Belgian PTI centers are the CAPELEC 3600, CRYPTON 700 series and TEN EDA 2. These opacimeters are not all able to detect the presence of a DPF. GOCA is investigating whether second generation opacimeters and particle counters could detect the presence of a DPF. The considered second generation opacimeters are the TEN LPA and the AVL DITEST SMOKE 2000 whose latter one is based on the light scattering method and measures an opacity percentage. Table 3.2 compares the first and second generation opacimeters and lists their LED's wavelength, their smoke density's accuracy and their price. A decrease in LED's wavelength as well as an increase in smoke density accuracy is observed. The LED's wavelength evolves from green for first generation opacimeters to near violet for second generation ones.

The weaknesses of optical sensors are the cross sensitivity to nitrogen dioxide and the insensitivity to small particles.

Nitrogen oxide absorbs light in the ultraviolet, blue and green spectrum and can therefore affect the measurement of optical sensors. Opacimeters are the most affected because NO_2 instead of PM will cause extinction of light. For opacimeters using green light, the coefficient of absorption k per ppm of NO_2 is, depending on the sensor bandwidth, between 1.6×10^{-4} and 2.4×10^{-4} m^{-1} [45]. Considering a NO_2 concentration of 300 ppm, it will increase the measured absorption coefficient with 0.06 m^{-1} which is not negligible considering a k-value of 0.05 m^{-1} at the exhaust. The PM measured with an optical sensor is therefore dependant of the NO_2 emissions. Exhaust after-treatment such as DOC and fast Selective Catalytic Reduction (SCR) reaction, can alter the amount of NO_2.

	LED's wavelength	Smoke density accuracy	Price
First Generation Opacimeters			
Capelec 3030-2	565 nm	0.01 m^{-1}	8,800 €
Crypton 700	560nm	1% full scale	second hand 1,800 £
TEN EDA2	N/A	$\leq$ 0.1 m^{-1}	N/A
Second Generation Opacimeters			
TEN LPA	300-440 nm	$\sim$ 0.001 m^{-1}	4,000 €
AVL ditest	*light scattering*	$\sim$ 0.001 m^{-1}	N/A

Table 3.2: *Comparative table between first and second generation opacimeters which are respectively used during PTI and investigated by GOCA for their ability to detect the presence of a DPF.*

As mentioned in Chapter 1, the PSD shows that a major proportion of particles are smaller than 1 µm. In order to obtain a correct number concentration of PM, the minimum detected particle size should be 23 nm as explained with the PMP method in Section 1.1.2 on page 8. A drawback of optical sensors is their insensitivity to small particles. Optical sensors use green or red light ($\lambda \in [500 - 700$ mm]) and the light beam is refracted or blocked in proportion to the particle's size. For green light approximatively 15% of particles with a diameter smaller than 50 nm, are blocked resulting in an underestimated measurement of the opacimeter [45].

The sensitivity to NO_2 can be reduced by increasing the wavelength of the light source, e.g. red light, but this decreases on its turn the sensitivity of the optical sensor to small particles. Eliminating one negative effect increases the other one which suggests a calibration of the sensor taking into account the NO_2 concentration or size distribution.

3.2 Accumulation Particulate Mass Measurement System

A PM measurement system based on accumulation can occur through a filter or by measuring the resonance frequency or difference in electric field in the sensor. The two first measurement techniques require micro-dilution of the exhaust flow. Such measurement systems have three key elements : a dilute sampling system, an exhaust flow meter and a mass scale for which accumulation of the PM is needed.

The advantages of a portable micro-dilution system compared to a non-portable full-flow tunnel based Constant Volume Sampler (CVS) are a reduction of the measurement equipment's size and cost as well as a reduction in power demands since a smaller quantity of exhaust is used.

3.2.1 Dilution Sampling System

Micro-Proportional Sampling (MPS) systems extract a part of the engine's exhaust gas flow and keep the ratio of the exhaust flow to the sampled flow constant (constant dilution ratio). The sampled flow is thereafter mixed with dilution air which can be ambient air or recirculated gases.

Micro-dilution Tunnel PM Measurement System [46]

The Model 7610 Mott Corporation used for the micro-dilution tunnel PM measurement system [46] consists of a 25.4 cm-long porous tube sample with two entrances (Fig. 3.6). A minimum length is imposed to the micro-dilution system in order to achieve a fully developed flow. The micro-dilution tunnel has a cross-flow design which "keeps most particles in the gas stream and away from the porous walls" [46]. This design avoids that the porous walls get clogged rapidly. The sampled flow is in this case diluted with recirculated gases which reduces the number of pumps to one. The dilute exhaust is drawn through the tunnel thanks to the vacuum created by the pump upstream. In order to use the recirculated gases as dilution air it needs to be 'cleaned' before entering the dilution sampling system. For this reason the micro-dilution tunnel

PM measurement system developed by the West-Virginia University consists also of a High Efficiency Particulate-free Air (HEPA) filter and a chiller to remove the moisture and the heavier hydrocarbons as well as a filter that is gravimetrically analyzed (see next subsection on mass scales). A block diagram of the micro-dilution tunnel PM measurement system is illustrated in Figure 3.7.

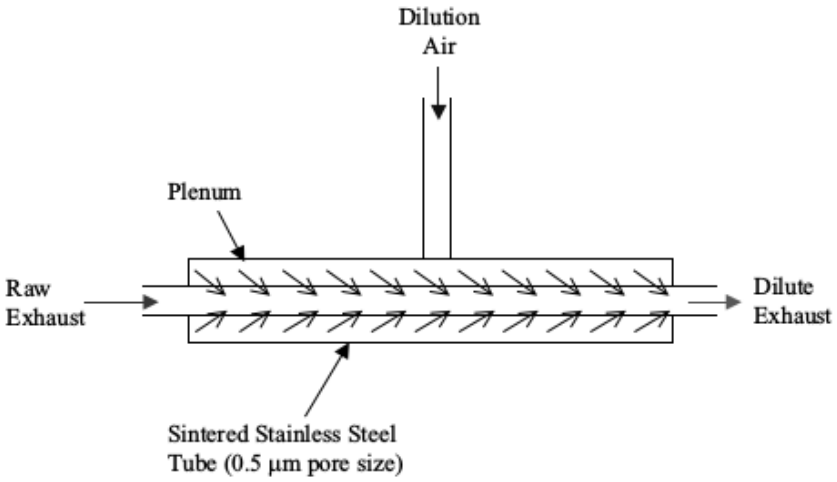

Figure 3.6: *The model 7610 Mott Corporation Micro-Proportional Sampling (MPS) of the Micro-dilution Tunnel PM Measurement System. The cross-flow design of the micro-dilution tunnel avoids that the porous walls get clogged. [46]*

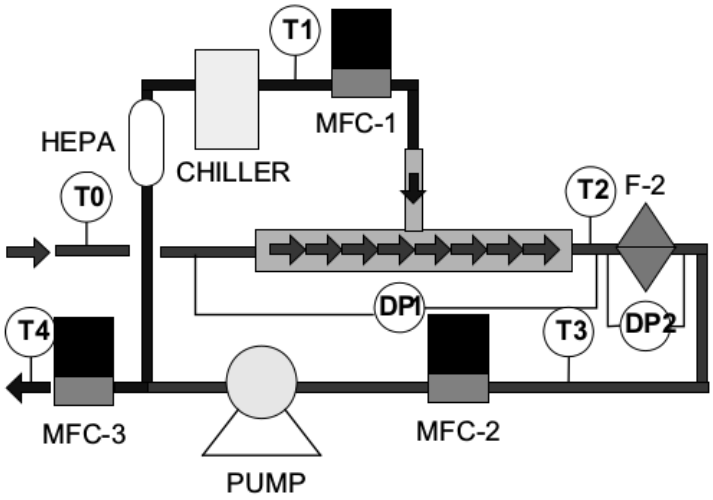

Figure 3.7: *The block diagram of the micro-dilution tunnel PM measurement system developed by West-Virginia University. Next to a MPS, the measurement sensor is composed of a HEPA filter, a chiller and a filter. [46]*

3.2.2 Micro Electromechanical Sensor Mass Scales Requiring Micro-dilution of the Exhaust

The particulate mass of diluted exhaust can be measured by measuring the differential pressure of a filter, by measuring the change in resonance frequency of the material constituting the microbalance or by combining both.

Differential Pressure at Filter - Micro-dilution Tunnel PM Measurement System

The Micro-dilution Tunnel PM Measurement System (Fig. 3.7) uses a 47 mm T60A20 Fiberfilm filter [46]. The filter is gravimetrically analyzed by measuring the increase in the filter's pressure drop. The filter's efficiency is determined by the total number and size of particulates in the filter; for an identical pressure differential a clean filter will have a higher flow rate than a filter with PM. According to literature, filter-based technologies are not suitable anymore to PM emissions measurements after the DPF since "the mass on the filter is that small that there is practically no difference between measurements with ambient air ('background') and exhaust gas from the engine" [47].

Quartz Crystal Microbalance

The Quartz Crystal Microbalance (QCM) is composed of a piezoelectric quartz crystal that is "externally driven by an electric oscillator attached to two metal plates placed on either side of the crystal". The crystal therefore oscillates at a frequency that depends on the thickness of the electrodes, of the quartz crystal and of the deposited PM on the top electrode [48] (Fig. 3.8). The mass of the PM is measured in real-time as a difference in resonance frequency of the piezoelectric quartz crystal. The amount of deposited PM is inversely proportional to the resonance frequency of the QCM. This type of microbalance has a small mass range (10^{-9}-10^{-5} g) but a great sensitivity [49] which makes it more appropriate to the current emission levels focused on ultrafine particles (particle size 100 nm). A drawback of this microscale for on-road measurement is its cost [48].

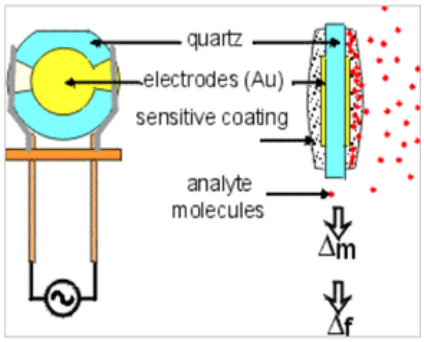

Figure 3.8: *QCM where the externally driven crystal oscillates at a frequency depending on the thickness of the electrodes, the crystal and the deposited PM.*

Tapered Element Oscillating Microbalance

The Tapered Element Oscillating Microbalance (TEOM) is a combination of the two mass scales described above and is composed of a hollow glass tube with a filter at its tip. The particulate mass is measured through the change in resonance frequency of the filter. Mechanical noise such as vibration and considerable temperature fluctuations affects the measurements which makes this microbalance rather suitable for laboratory conditions than for on-road testing.

3.2.3 Micro Emectromechanical Particulate Mass Sensor *Without* Micro-dilution of the Exhaust

Leaving out the dilution sampling system reduces the size and cost of the measurement system. The following MEMS all work on a similar principle in which the deposit of PM on an electrode alter the electric field.

Delphi PM Sensor

The Delphi PM sensor is composed of a non conductive substrate and two conductive electrodes (Fig. 3.9). PM accumulates on the electrodes and lowers the conductance of the electrodes giving a measure of the particulate mass.

This sensor is still in development; Delphi ® has released a light duty version in 2017 and the implementation of a controller is in pipeline in order to handle sensor anomalies. Large particles may create undesirable spikes in the output signal and the effects of high exhaust flow velocity may cause temporarily adherence of the PM on the electrodes leading to wrong sensor measurements [50].

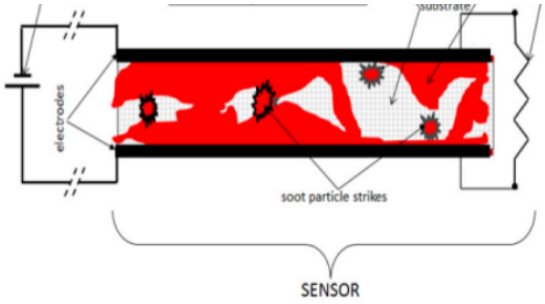

Figure 3.9: *The measurement technique of the Delphi PM sensor that is based on the accumulation of PM on electrodes altering their conductance. [50]*

Soot Deposit Spark Sensor

The University of Texas developed an electronic PM sensor for vehicle exhaust gas that operates on a similar principle as the Delphi PM sensor described previously. The Soot Deposit Spark Sensor (SDSS) measures a change in minimum spark discharge voltage which is a measure of the soot deposited on the electrodes [48]. The two electrodes have an insulated casing establishing a total electric isolation. One electrode is kept at a voltage of 1,000 Volt Direct Current (VDC) and generates an electric field. The charged particles alter the charge of the other electrode and are amplified downstream. A correlation is established linking particle mass concentration to the output voltage, the distance between the two electrodes, the electrode length, the flow velocity and the bias voltage used in the charge amplifying and signal conditioning circuitry.

Charge Induced Electrodynamic MEMS

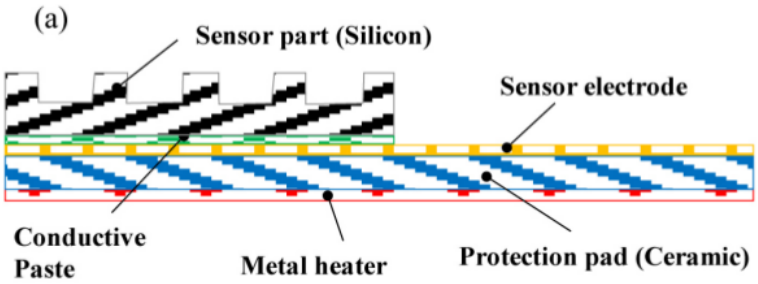

Figure 3.10: *The charge induced electrodynamic MEMS composed of a heater to remove the deposited particles and a semiconductor that measures a change in electric field as particles move along. [51]*

The charge induced electrodynamic MEMS is composed of a sensor part made of a semiconductor and a heater part made of platinum that removes the deposited PM on the sensor [51]. The charged particles induce a charge in the semiconductor as they pass along. The induced charge

is increased by the charge amplifier an gives a measure of the PM concentration. In order to increase the sensitivity of the sensor the surface area of the sensor is increased through grooves (Fig. 3.10).

The sensor is in development and has the advantages of both high sensitivity and small size. The effect of mechanical vibration as well as the scarce sensitivity at small fluctuations of charge still need to be improved.

3.3 Scanning Mobility Particle Sizer

A SMPS measures the particle size distribution in the sub-micron scale and is composed of a Differential Mobility Analyzer (DMA) and a Condensation Particle Counter (CPC) (Fig. 3.11). It is an expensive measurement system that is suitable for laboratory conditions and would therefore rather be used as a calibration measurement system for this Master's thesis. SMPS Model 3034 detects particles in the range of 10 to 487 nm and can measure concentrations up to 10^7 particles per cubic centimeter.

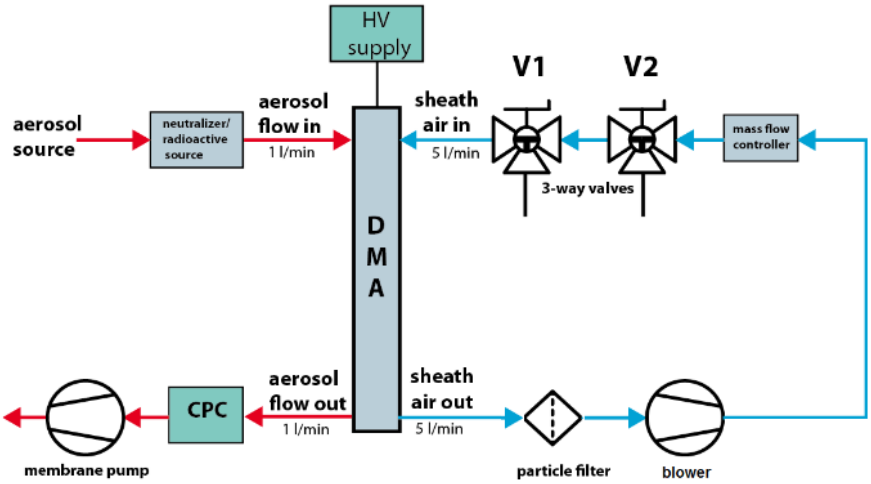

Figure 3.11: *Block diagram of the SMPS composed of a DMA to size the particles and a CPC to count them. [52]*

The DMA is made of a cylindrical capacitor consisting of an inner and outer electrode and separates the particles according to their electrical mobility which varies in function of the particle size and the electrical charge of the particles [52].

The CPC counts the particles selected by the DMA through an optical method. Since the particles are in the sub-micron scale (below 500 nm) they are not visible by a laser light as described in Section 3.1. When the flow enters the CPC (Fig. 3.12), it is saturated with alcohol vapor (butanol) and it becomes supersaturated as it is cooled in the condenser tube. The alcohol vapor therefore condenses on the particles increasing the size of the particles to a diameter of about 10 µm [53]. As a result the optical backscatter sensor upstream is able to detect these particles. This optical method including an alcohol pool is sensitive to mechanical noise and very sensitive to temperature changes making it only adequate to laboratory conditions. Moreover, it requires a non negligible maintenance.

3.4 Electrical Low Pressure Impactor +, Dekati ®

The ELPI+ of Dekati ®, introduced in 2010, measures a size distribution and concentration. It has 14 stages of particle size ranging from 6 nm to 10 µm [54].

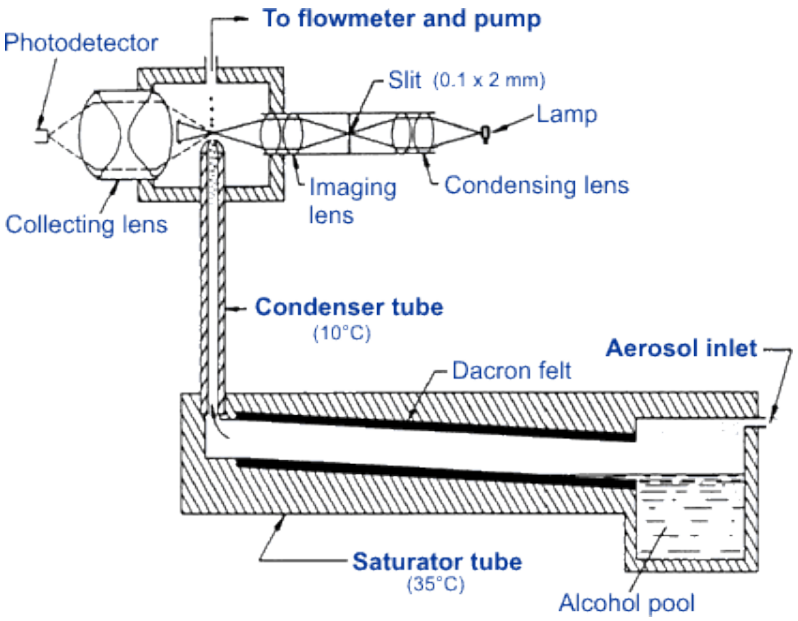

Figure 3.12: *Schematic illustrating the working principle of a CPC. The pool saturated with alcohol vapor allows to increase the size of the sub-micron particles which makes them visible to the lamp of the optical system. [53]*

The ELPI+ is composed of three main components : an unipolar charger, a low pressure impactor and electrometers.

Whereas a charge amplifier and a semiconductor material is used for the charge induced electrodynamic MEMS (see previously), the ELPI+ charges the particles through a diode type corona charger which affects the particles by a relatively strong electric field. The particle's charge increases through a corona discharge where a zone of plasma is created around the electrode. A current flows from the electrode with high potential into air by ionizing the air creating a zone of plasma. The ions generated in this process either give their charge to areas of lower potential or recombine to form neutral gas molecules [55].

A size classification of the particles is done in the low pressure cascade impactor. The 14 stages are separated by electrical insulators and each stage is connected to an electrometer. The electric current from each stage is measured with the electrometer and is directly proportional to the particle number concentration and size [54]. The electric current thus detects the deposit of unipolarly charged particles on the stages. Large particles are removed in the first stage, the pre-separator, and the smallest particles are captured by the filter in the final stage. A small pump is located after the filter and the downstream pressure has a value of 40 mbar [56]. A detailed schematic of the ELPI+ is presented in Figure 3.13.

Chapter three analyzed four types of measurement systems of PM. The two first ones measure a particulate mass concentration whereas the two latter systems measure a particle size distribution including mass and number concentrations. Firstly, optical sensors are described making a distinction between optical backscatter sensors and opacimeters. Secondly, measurement systems that are based on the accumulation of PM are detailed including the importance or not of a dilution for the developed mass scales. Finally, the SMPS and ELPI+ are described.

From this short state of the art concerning PM measurement techniques, optical backscatter sensors have been identified as corresponding the most to the Master's thesis objective thanks to, inter alia, their simplicity.

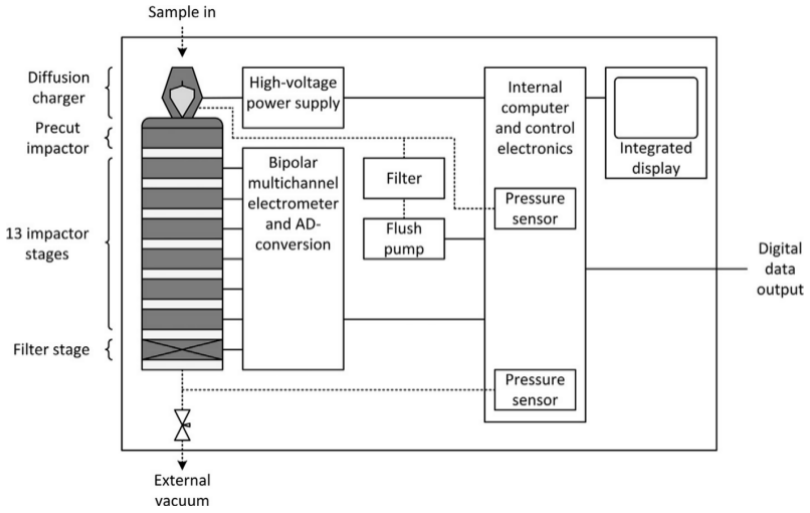

Figure 3.13: *The block diagram of the ELPI+ of Dekati ® which is composed of an unipolar charger, a low pressure impactor and electrometers. [56]*

Chapter 4

Experimental Purpose and Methodology

Three low-cost sensors are selected for the present Master's thesis and two of them are tested on cars' exhaust gases at low load following an experimental protocol consisting of low and high idle speeds. The results are analyzed and compared in Chapter 5 with precise, state-of-the-art measurement systems made available by GOCA in Sint-Agatha-Berchem. The purpose of the tests is manifold and is described in details in Section 4.1. Additional elements are added to the sensors in order to obtain a test bench that is suitable to tests with car exhaust gases as described in the third section. The three PM2.5 sensors are based on the optical backscattering method and have prices ranging from 5 € to 50 €. Detailed characteristics of these sensors are given in the last part of the present chapter.

4.1 Motivation and Purpose of the Experiments

The main objective of the experiments is to determine whether the low-cost sensors are able to detect the presence of a DPF and to monitor its efficiency. DPF can indeed get clogged or damaged during operation emitting more particulate matter than allowed and this is not always detected during the PTI's test. The low-cost sensors are therefore firstly validated by observing whether the sensors react similarly as the state-of-the-art measurement systems and show the same trends. Higher relative peaks should indeed be observed with either sensors on cars without DPF compared to cars with DPF. The height of the peaks would then also be a measure of the efficiency of the DPF.

The tests are done at low load when the car is at rest instead of on the road in order to exclude a couple of parameters influencing the measurements such as traffic conditions and the selected gear. These circumstances indeed simplify the tests and allow to reproduce them. Doing the tests at rest also allows to compare the measurements with the state-of-the-art sensors of GOCA since they are only available at their offices. Some of the measurement systems indeed require strict test conditions that cannot be reached during on-road tests (butanol pool of the CPC, compressed air input...). The selected test protocol consists of a low and high idle speed test and is described in details in Section 4.2. On top of the test's simplicity and reproducibility, the relatively short duration of the tests ($\leq$ 400 s) may make of this type of tests the ideal procedure at the periodic technical inspection's test. Our experiments will also point out whether the chosen types of tests, i.e. low and high idle speed tests, can detect the presence of a DPF and assess the efficiency of a DPF in a car's exhaust pipe.

Another purpose of the tests is to observe if the measurements of the low-cost sensors give a plausible absolute measurement of the particulate mass concentration. This comparison will

point out whether the sensor's measurements are influenced by other emissions and whether the low-cost sensors are measuring "real" particles.

The comparison in absolute measurements furthermore allows to calibrate the low-cost sensors whenever possible. A calibration factor will allow to tackle the amount of PM "unseen" by the low-cost sensors and thus to have a measurement closer to the real PM emissions.

The comparison of the low-cost sensors on a relative and absolute basis is done with state-of-the-art measurement systems made available at GOCA: the Pegasor Mi3, the TSI Nanoparticle Emissions Tester (NPET) and the TEN LPA. The Pegasor Mi3 is the most expensive among the measurement systems cited above and measures a particle number and mass concentration for particles ranging in size from 11 nm to 11 µm. The Pegasor Particle Sensor (PPS) technology is based on the escape current measured when the particles, charged by ions that are generated by a corona discharge, leave the sensor. Its measurement principle is close to that of the ELPI+ discussed in Chapter 3. The NPET Model 3795 from TSI consists of a CPC that is preceded by a diluter (10:1), dryer and catalytic stripper. The sensor's detection efficiency is higher than 50 % for particles greater than 41 nm in diameter and lower than 50 % for particles smaller than 23 nm. Moreover, it gives the Swiss Regulation SR 941.242 certification (mentioned in Chapter 1) after one minute of measurement. The TEN LPA is a second generation opacimeter also depicted in Chapter 3.

GOCA also possesses a Bartec DPF Checker, i.e. a very simple measurement system whose core consists of the GP2Y1010AU0F optical dust sensor based on the light scattering principle. The Bartec DPF Checker returns a green or red light telling respectively whether the car possesses a filter or not.

The sensors measure simultaneously the PM emissions in order to have identical test conditions and consist of one low-cost and three state-of-the-art measurement systems. Having more than four probes in the exhaust pipe is geometrically impossible. Indeed, the probe of each sensor needs to be sufficiently inserted in the tailpipe to avoid ambient air "poisoning". An eventual risk that the four probes together absorb more flux than the exhaust gases is not excluded. This would result in the least absorbing sensor, i.e. the low-cost sensor or the opacimeter, to measure exhaust gases diluted with ambient air.

The tests are performed on two diesel cars (M1 category): a Citroën Berlingo without DPF (2001, Euro 3) and an Opel Astra with DPF (2016, Euro 6b). The detailed characteristics of the two cars are given in Table 4.1 including the engine's power, displacement, certification date, emission class and mileage. Testing on a car with and without DPF allows to measure whether the low-cost sensors can detect the presence of the DPF and consequently the influence of the technological evolution.

	Citroën Berlingo	**Opel Astra**
Power	66 kW	81 kW at 3,500 rpm
Engine displacement	1,997 cm^3	1,598 cm^3
Certification date	19-06-2001	19-02-2016
Emission class	Euro 3	Euro 6b
DPF	Absent	Present
Mileage	122,000 km	44,000 km

Table 4.1: *Characteristics of the two diesel M1-category cars used for testing the low-cost sensors during a low and high idle speed test.*

4.2 Test Protocol for Car at Low Load

To reach the objectives stated in the previous section, it is necessary to design an accurate test protocol that can easily be reproduced and for which the influences of external factors are minimized. Tests at rest are therefore preferred to on-road tests. The low-cost sensors are compared with state-of-the-art sensors which are available in the laboratory of GOCA in Sint-Agatha-Berchem thus preventing the comparison to be done during on-road tests. The designed test protocol is separated in four categories: three tests that simulate the behavior of an on-road vehicle and one test that calibrates the test bench and studies the fouling of the low-cost sensor. The first three tests are measuring the particulate mass concentration of a car at low load, which means the car is out of gear, and only the accelerator is used to modify the engine's rotational speed. It is the engine's rotational speed that makes the differences between the three tests.

4.2.1 Low Idle Speed Test

A low idle speed test compares the particulate mass concentration measured in the exhaust pipe when the car is idling to the particulate mass concentration of ambient air. This type of test is sensitive to background concentration originating either from natural sources, either from human activity and it consequently depends on the localization for the measurement in ambient air.

The low idle speed test established for this study practically consists of several 200-second periods during which the probe is either in the exhaust pipe, either on the ground and oriented parallel to the exhaust pipe. A 20-second period is established between the 200-second periods for inserting or extracting the probes from the exhaust pipe.

The probe developed for the low-cost sensor is composed of a simple narrow plastic tube that is not as user-friendly as the probes of the reference measurement systems. Unlike the reference measurement systems, it will not be possible to extract the probe easily from the exhaust pipe. The ambient air conditions are therefore approached by increasing the fresh air flux to its maximum, i.e. 320 L/h. Since a small filter is used at the pump when the fresh air is pushed for the dilution, the effect of background concentration is minimized in the measurements.

Previous low idle speed tests measuring PN concentrations, have shown higher concentrations in the outside air than in the exhaust pipe of modern diesel cars equipped with a DPF. Practically zero concentrations (6-8 particles/cm^3) have been measured in the exhaust pipe compared to a concentration of 9,000 particles/cm^3 in the outside air[1][43].

4.2.2 High Idle Speed Test

During this test, a high idle speed of 3,000 rpm is maintained during 30 seconds followed by an idling period of 280 seconds. For this study, the high idle speed of 3,000 rpm is repeated a couple of times. This type of test is, to a lesser extent than free acceleration tests, sensitive to the acceleration mode. Indeed, some people can reach high idle speed very rapidly whereas others can firstly obtain overshot high idle speeds or can have more difficulties to maintain the high idle speed at a constant value.

[1]The reported value for the outside air is only an order of magnitude since it depends on the background concentration.

This study demonstrates that high idle speed tests were not repeated exactly in the same manner. Alongside the human sensibility of repeating the same test, fouling of the measurement chamber can be responsible for differences in measurements between the different accelerations. Fouling is indeed a more important issue for high idle speed tests and it becomes more important as more accelerations are performed. Indeed, the first high idle speed showed higher particulate mass concentrations compared to the following ones.

The packaging developed for the low-cost sensor does not increase the amount of dilution air when the exhaust gas flux increases. This is however done by the reference sensors during, for instance, the accelerations in order to keep a constant dilution ratio. It is thus very difficult to know the exact dilution ratio performed by the low-cost sensor during a high idle speed test. Comparing absolute measurements for high idle speed tests should accordingly be done with caution.

4.2.3 Free Acceleration Test

The free acceleration test consists of an acceleration peak lasting less than one second: the driver presses the accelerator until reaching a specified rotational speed and releases the pedal directly afterwards. Unlike the high idle speed test, there is no constant motor speed during this test. The free acceleration test is used to study the reaction of the sensors: is the reaction instantaneous or is there a delay between the thrust and the peak measurement?

4.2.4 Pre- and Post-Tests

One of the issues caused by PM emissions is fouling. PM is indeed composed of solid particles and can adhere to the wall of the tubes or, even worse, inside the low-cost sensors and thus falsify the measurements. A way to measure the impact of fouling during the tests is to measure the concentration of PM in the ambient air before and after the tests. Each pre- and post-test is in fact composed of two ambient air measurements that are distinguished by the setting of the test bench.

By performing such tests, the impact of fouling on the measurements can be determined. For the low idle speed test the gas analyzed by the sensors switches between two environments, exhaust gases and ambient air. But it is possible that a fraction of DPF, from the exhaust gases, lays down on the walls of the tubes or measurement chamber during e.g. an acceleration. When these particles are reintroduced into the flow at, for instance, low idle speed which produces a less polluted flux, the additional particles will increase the measured concentration and therefore not represent the real particle mass concentration. By measuring the particulate mass concentration in ambient air before and after the tests, an idea of the fouling of the setup can be determined. The pre- and post-tests will thus be useful to determine a calibration factor between the measurements of the low-cost sensors and the reality. This factor will take into account the fouling if necessary and hence may be time-dependent.

4.3 Setup of the Test Bench

The setup of the test bench results from tests on two engines of the TFL laboratory of EPL: a motor Varimax and a motor Citroën whose characteristics are described in Section 5.3.

4.3.1 Description of the Test Bench

The selected test bench is illustrated in Figure 4.1 where the exhaust gases that are taken at the tailpipe are represented in red. At the T-branch, the exhaust gases encounter a filtered air flux that is used to dilute the exhaust gas flow. The filtered air flow, represented in blue,

goes through two elements before reaching the T-branch: a pump and a valve combined to a rotameter. The pump is necessary to drive the exhaust gases through the tubes to the sensor and guarantees that the filtered air enters the T-branch avoiding reflux of the exhaust gases. The pump also allows to overcome the head losses in the filter and the tubes. The valve on its turn, is used to control the rate of dilution of the exhaust gases.

The mixture of the exhaust gases and the filtered air flow, represented in green, leaves the T-branch to reach the measurement chamber. Inside the chamber, the mixture goes directly to the sensor that measures the particle mass concentration. The measurement chamber is hermetically closed with silicone to isolate it from the outside. Behind the measurement chamber, there is another pump whose role is to ensure a circulation of the gases inside the chamber and to prevent accumulation.

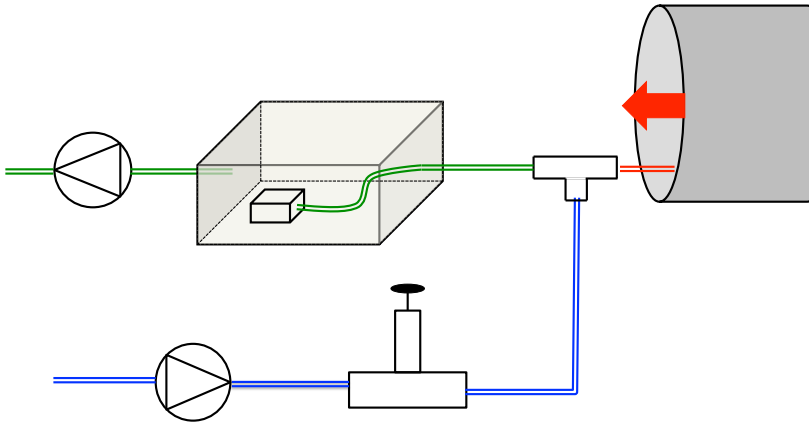

Figure 4.1: *The packaging developed for the low-cost sensors consisting of a measurement chamber, a T-branch, a valve and two membrane pumps. The filtered air flux is represented in blue, the exhaust gases in red and the diluted exhaust gases in green.*

4.3.2 Interest of Dilution

The results obtained for the conversion of the norms in Chapter 2 give concentrations of the order of several milligrams per cubic meter. This is a problem for low-cost sensors such as the Nova PM2.5 sensor whose maximum limit in particulate mass concentration is 1 mg/m^3. So, to assure a system that can be used for nearly all vehicles, a dilution is required. By injecting a filtered air flow, the measured particulate mass concentration is lower than the concentration of PM in the exhaust gases at the tailpipe and saturation of the sensor can be prevented.

Another advantage of dilution is to avoid condensation of water since the appearance of water droplets has been observed before the mixing with filtered air when the red path was too long. Injecting a filtered air flow decreases the partial pressure of water in the mixture or, in other words, the gas obtained by mixing is less saturated with water. Consequently less water droplets appeared in the tubes and inside the sensor, even though the temperature of the flow is also decreased. This is an advantage because the sensors are also limited in temperature range (50°C - 60°C). To counter the formation of water droplets, the red path is as short as possible hence avoiding the cooling of the exhaust gases flow before the dilution.

During the experiments at low load on diesel cars, an air intake flow of 100 L/h is considered. The dilution ratio has been computed by measuring the CO concentration in the exhaust and directly after the measurement chamber. A dilution ratio of approximately 4:1 to 5:1 is obtained.

Dilution has been considered by using a valve directly on the exhaust flux but previous experiments on the Varimax engine showed a significant fouling of the valve with PM reducing the measured concentration. Little fouling of the test bench as a whole will occur anyway but it has to be minimized as much as possible. A constant regime in the fouling of the test bench is supposed, implying that PM deposit equals PM clearance from the walls of the tubes and the measurement chamber. In the case of a fouling regime, the effect of fouling can simply be corrected with a calibration factor.

4.4 Studied Low-cost Sensors

The three studied low-cost sensors are described giving their functional characteristics as well as other pertinent information. The sensors are based on the optical backscattering of light by particles. The first two sensors, i.e. the Nova Laser PM2.5 Sensor SDS011 and the MakeBlock Me PM2.5 Sensor SDS011, measure a particulate mass concentration and are used for the experiments that are analyzed in the next chapter. The Shinyei PPD42NS Sensor, on the other hand, measures an amount of particles and showed too much sensitivity to vibrations and this despite the improvements of the sensor. Although the sensors specify "PM2.5" in their name they measure different particle's size categories among which PM1.0 and PM10.

4.4.1 Nova Laser PM2.5 Sensor SDS011

The Nova laser PM2.5 sensor SDS011 is represented in Figure 4.2 and measures particles whose aerodynamic diameter is comprised between 0.3 µm and 10 µm. The sensor costs approximately 15-20 € and is developed by a spin-off of the Shandong University in China. This low-cost sensor is also used in the citizen science project of OK Lab in Stuttgart, mentioned in the introduction. The sensor returns two mass concentrations for which the particle's aerodynamic diameter is greater than 2.5 µm and 10 µm (resp. PM2.5 and PM10). The sensor measures a Low Pulse Occupancy time that is converted and calibrated to particulate mass concentrations based on "different waveform classification size statistics and conversion formula" [57]. Further characteristics among which the concentration and working temperature range of the sensor are summarized in Table 4.2. Concerning the geometric properties of the sensor, it has a wind inlet to which it is possible to connect a hose. The sensor has also a small ventilator at the exit of the sensor guaranteeing the circulation of air in the sensor. Data transmission and conversion is done through a USB2TTL-chip provided with the sensor and using the Universal Asynchronous Receiver-Transmitter (UART) protocol. Real time measurements are graphically displayed on a computer program similar to labVIEW.

Nova Laser PM2.5 sensor SDS011	
Measurement parameters	PM2.5, PM10
Concentration range PM2.5	0-999.9 µg/m^3
Concentration range PM10	0-1,999.9 µg/m^3
Working Temperature Range	−20 - 50 °C
Serial data output frequency	1 Hz

Table 4.2: *Specifications of the Nova laser PM2.5 sensor including its concentration range and working temperature range which will be a limiting factor for dilution during the experiments.*

The size categories measured by the Nova sensor, PM2.5 and PM10, are compared during

an experiment with incense (Fig. 4.3). An offset is observed at low concentrations whereas higher concentrations rather indicate that two different measurements would have been performed. Since it concerns a simple low-cost sensor, it is supposed that the sensor applies a non-constant offset that depends on the concentration of the reference size category rather than performing two measurements. The reference category is supposed to be PM2.5 due to the presence of this size category in the sensor's name. An inspection inside one of the sensors showed the presence of only one photodiode confirming this hypothesis (Fig. 4.2 (b)).

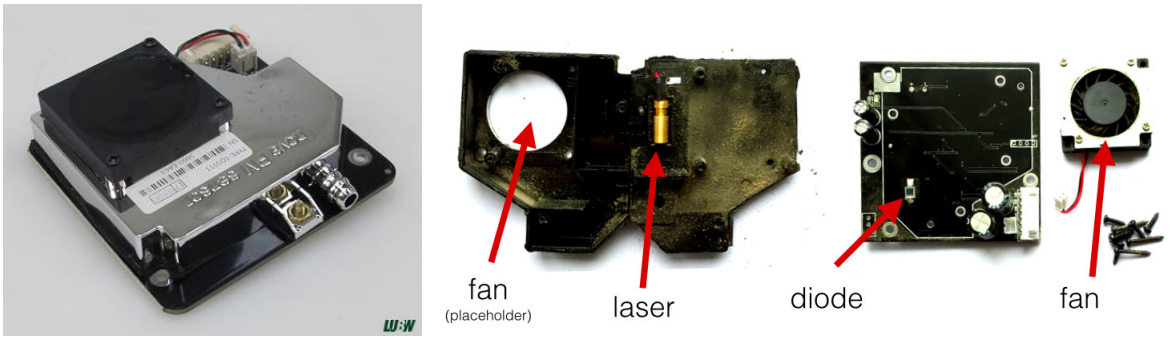

(a) (b)

Figure 4.2: *The Nova laser PM2.5 sensor with its ventilator represented by the black square and its wind inlet with a possible connection to a hose (a). An inside view of the Nova sensor identifies the laser and photodiode (b).*

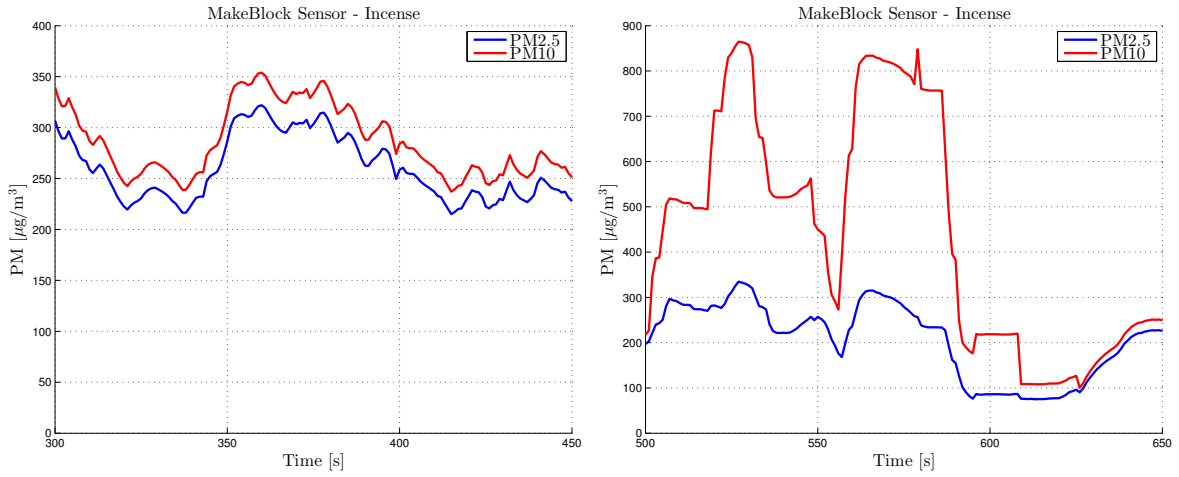

(a) (b)

Figure 4.3: *A comparison of the PM2.5 and PM10 measurement of the Nova sensor during an experiment with incense. Based on the behaviour at low and high concentrations it is supposed that two measurements are done or that a non linear conversion function is applied.*

The Nova laser PM2.5 sensor is being used by a citizen science project in Stuttgart that aims to map the particulate mass concentrations. A study performed by the State Institute for environment, measurement and nature conservation in Baden-Württemberg (LUBW) assessed this low-cost sensor for the citizen science project [58]. Between February and April 2017, they compared the PM10 concentrations measured in ambient air by the Nova sensor and the Grimm Environmental Dust Monitor PM sensor. The air measurements showed a great sensitivity of the Nova sensor to humidity. When the relative air humidity was greater than 70 % as in Figure 4.4 (a), the Nova sensor measured significantly higher concentrations than the reference Grimm sensor. When, on the opposite, the relative air humidity was lower than 50 % as in Figure 4.4

(b), the Nova sensor measured underrated particulate mass concentrations.

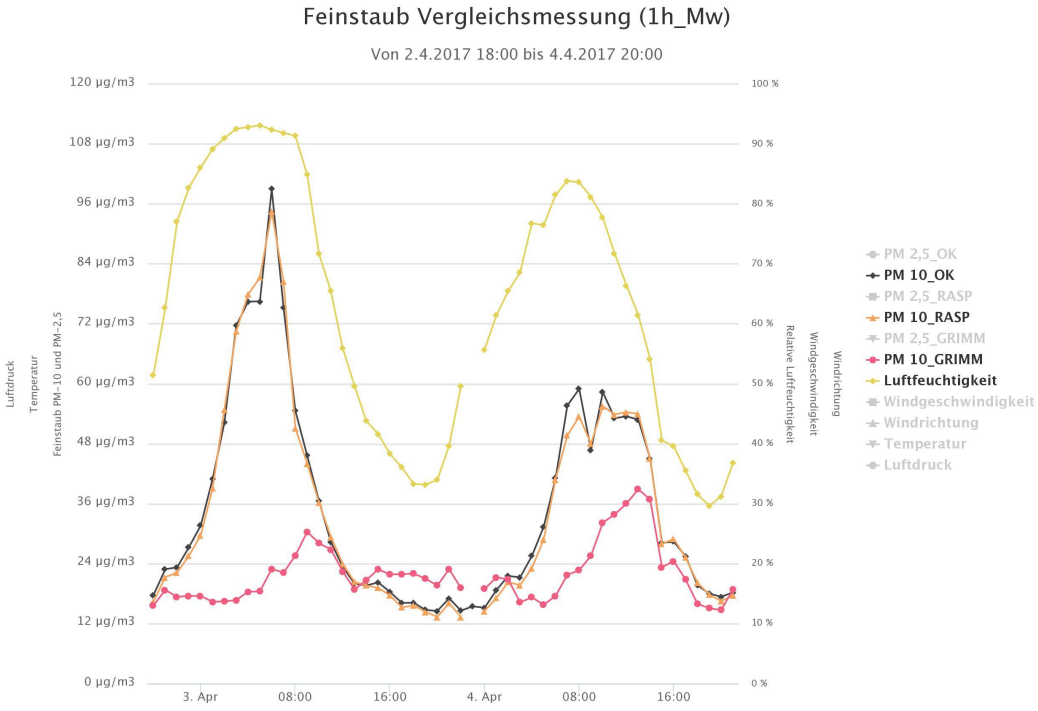

(a)

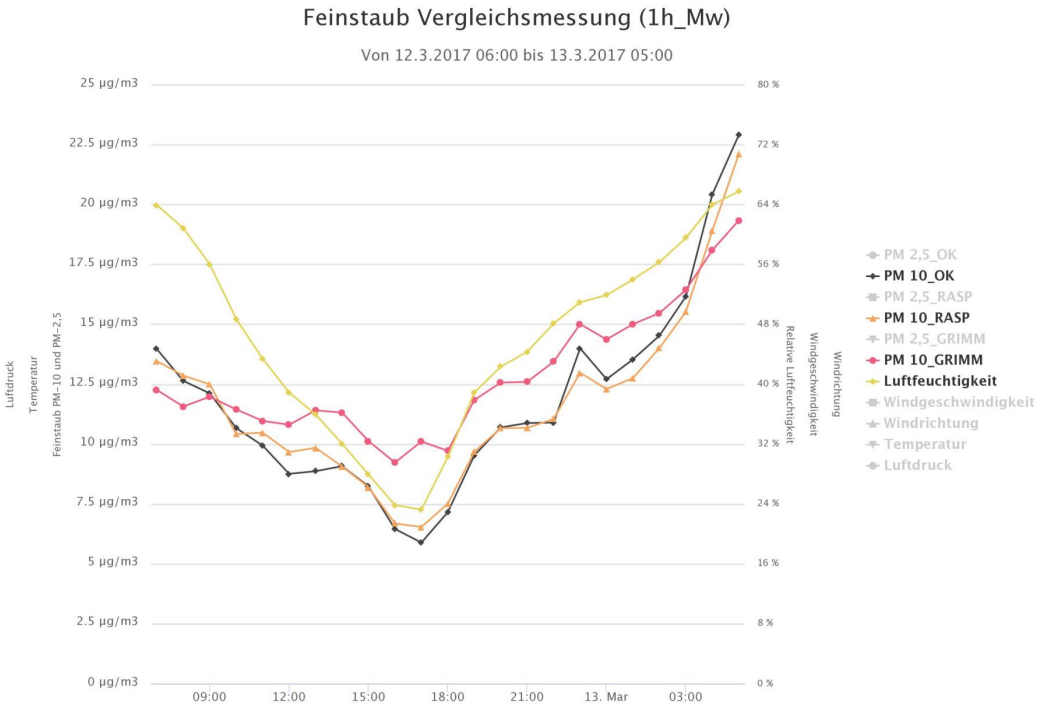

(b)

Figure 4.4: *Both Figures show the influence of air humidity on the PM10 concentrations measured by the Nova sensor, see PM 10_OK, compared to a reference Grimm PM sensor, see PM 10_GRIMM. The air humidity is represented with the Luftfeuchtigkeit curve. Figure (a) shows the overrated particulate mass measurements of the Nova sensor for a relative humidity above 70 % whereas Figure (b) shows the underrated particulate mass measurements for a relative humidity below 50 % compared to the reference Grimm sensor.*

The important sensitivity of the Nova laser PM2.5 sensor to humidity and its concentration and temperature limits make the sensor by itself not applicable to cars' exhaust. A dilution is therefore essential in order to tackle the drawbacks of the sensor.

4.4.2 Makeblock Me PM2.5 sensor

The MakeBlock Me PM2.5 sensor is represented in Figure 4.5 and measures three types of particulate mass concentration, i.e. PM1.0, PM2.5 and PM10. The sensor costs approximately 40-45 € and it is sold by the Chinese makeblock company whose purpose is to develop STEAM (Science, Technology, Engineering, Art and Mathematics) education and entertainment through the selling of DIY kits in robotics and technology. No detailed datasheet therefore exists of the product. Further characteristics among which the concentration and working temperature range of the sensor are summarized in Table 4.3. The sensor has a small circular opening for the inlet and a small ventilator at the exit which guarantees air circulation in the sensor. An Arduino micro-processor is used to transfer the sensor's data using the UART protocol and to convert the raw sensor's signals to particulate mass concentrations. The data is thereafter filtered in Matlab using a moving average with a window size of 200 values determined experimentally.

Makeblock Me PM2.5 sensor	
Measurement parameters	PM1.0, PM2.5, PM10
Range of concentration	0-6,500 $\mu g/m^3$
Working Temperature Range	−10-65 °C
Serial data output frequency	5 Hz

Table 4.3: *Specifications of the MakeBlock Me PM2.5 sensor including its concentration range and working temperature range which will be a limiting factor for dilution during the experiments. The concentration range of the sensor as well as its serial data output frequency is determined from experiments with the sensors.*

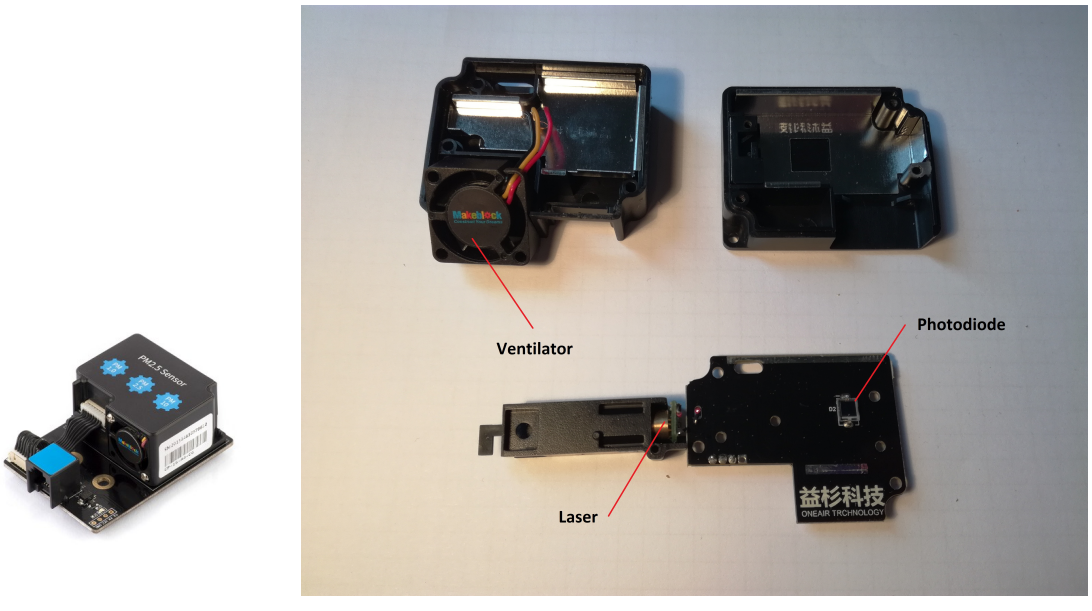

(a) (b)

Figure 4.5: *The MakeBlock Me PM2.5 sensor measuring three types of particulate mass concentration, i.e. PM1.0, PM2.5 and PM10. The sensor has a small circular opening for the inlet on the back of the sensor and a small ventilator at the exit which guarantees air circulation in the sensor.*

The different measurements, i.e. PM1.0, PM2.5 and PM10, are compared during an experi-

ment with incense (Fig. 4.6), showing a proportional offset between the particle's size categories for low as well as high particulate mass concentrations. This is physically not correct since the particle size distribution of the accumulation mode discussed in Chapter 1 has a normal distribution centered at a particle's size of approximately 300 nm with an additional small bump centered below 10 µm. No reference size is mentioned with the sensor's information but a reference of PM2.5 is hypothesized because of the sensor's name.

A dilution is necessary for the MakeBlock PM2.5 sensor due to the temperature and concentration limits. Although no studies have been done related to the sensitivity of the sensor to ambient conditions, a similar sensitivity to humidity is expected as for the Nova PM2.5 sensor.

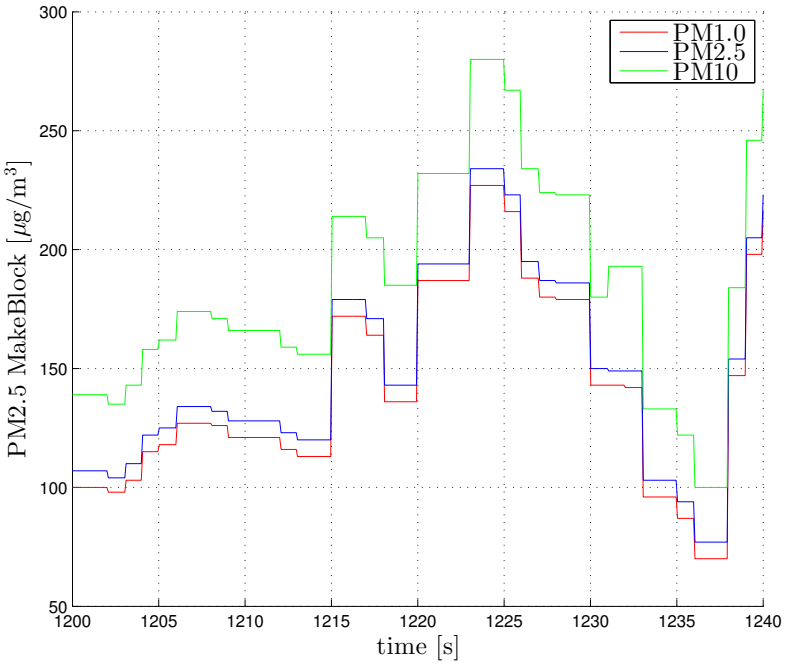

Figure 4.6: *Tests with incense reveal that the different particulate mass measurements of the MakeBlock Me PM2.5 sensor are offset with a proportional factor. This, however, does not represent the reality as observed on the particle size distribution of Chapter 1.*

4.4.3 Shinyei PPD42NS Dust Sensor

The Shinyei PPD42NS Dust Sensor is represented in Figure 4.7 and measures a number concentration for particles whose aerodynamic diameter exceeds 1 µm. The sensor costs approximately 5-10 € and it measures a low pulse occupancy time which is proportional to the particle number concentration as described in Chapter 3. A corresponding transfer function is given graphically in the datasheet [59]. Further characteristics among which the concentration and working temperature range of the sensor are summarized in Table 4.4. An Arduino microprocessor is finally used to transfer the measurement data to a computer.

Shinyei PPD42NS Dust Sensor	
Measurement parameters	PN
Range of concentration	0-28,000 particles/L
Working Temperature Range	0-45 °C
Serial data output frequency	1 Hz

Table 4.4: *Specifications of the Shinyei PPD42NS Dust Sensor including its concentration range and working temperature range.*

During experiments with incense, the sensor has shown a very high sensitivity to vibrations with great variations in the measured concentrations when the sensor was moved or touched. Poor fixing of the sensor's elements and a low quality photodiode detector and light source are identified as potential causes. In order to verify this assumption, the photodiode detector of the sensor has been fixed with glue. Tests in the cleanroom of the Maxwell building of EPL with the "improved" Shinyei sensor have shown a smaller sensitivity to vibrations even though it was still present. The tests have been performed in an ISO3 environment which is considered to have no more than 35 particles/m^3 (aerodynamic diameter $\geq$ 0.5 µm). Further comparisons of the inside of the sensor with the two other low-cost sensors have shown striking differences in the sensor design explaining the high sensitivity of the Shinyei sensor. Unlike the two previous sensors, the Shinyei PPD42NS uses a LED as light source, instead of a laser, which results in a less intense and precise light beam. The Shinyei sensor has furthermore a small resistance for the air circulation which is much less efficient than the ventilator of the two previous low-cost sensors. The measurement of refracted light of the Shinyei sensor is also not isolated from surrounding light as is the case for the two other low-cost sensors. A high sensitivity to the surrounding environment is therefore observed.

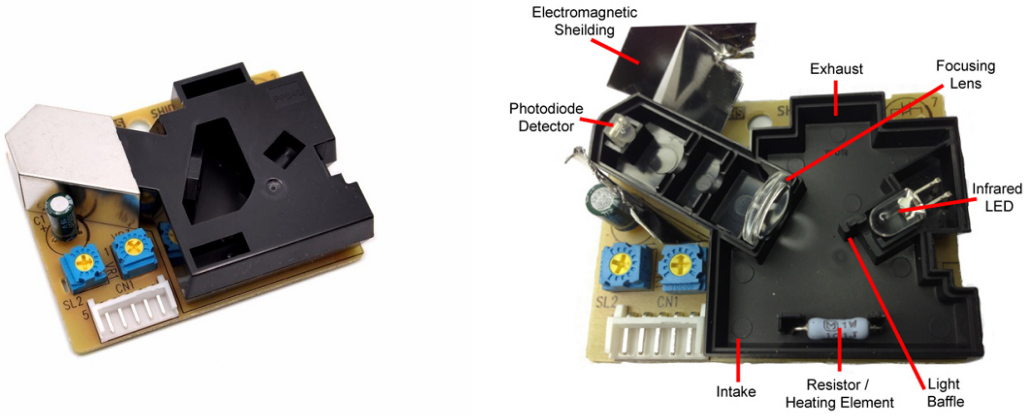

(a) (b)

Figure 4.7: *The Shinyei PPD42NS Dust Sensor (a) with an inside cut of the sensor (b). The sensor measures a particle number concentration and has a small resistance for the air circulation.*

In spite of the poor results obtained for ambient air measurements, the Shinyei sensor has been tested during free acceleration and during on road tests allowing to identify potential additional challenges of low-cost sensors. These tests, performed in January, showed a great sensitivity to humidity and highlighted the need to perform the tests on a hot engine especially during the winter. Droplets were observed on the focusing lens in the beginning of the tests reducing the measured concentration to very low values. Exceeding the sensor's operating temperature limit resulted in the measurement of a zero concentration during the on-road tests. The importance of a measurement chamber, pump and dilution has therefore been identified during the test allowing also to limit the risk of reflux of exhaust gases. No further tests have been done with this sensor due to the lack of reliability.

A comparison between the photodiode and light source of the three low-cost sensors highlights distinctive differences with the Shinyei sensor (Fig. 4.8). The use of a LED for the Shinyei sensor instead of a laser for the Nova and MakeBlock sensor as well as the differences in photodiode are associated with a poorer quality for the measurements of the Shinyei sensor compared to the

Nova and MakeBlock sensors. Moreover, the light source and the photodiode are better fixed on the MakeBlock and Nova sensor using welding instead of glue.

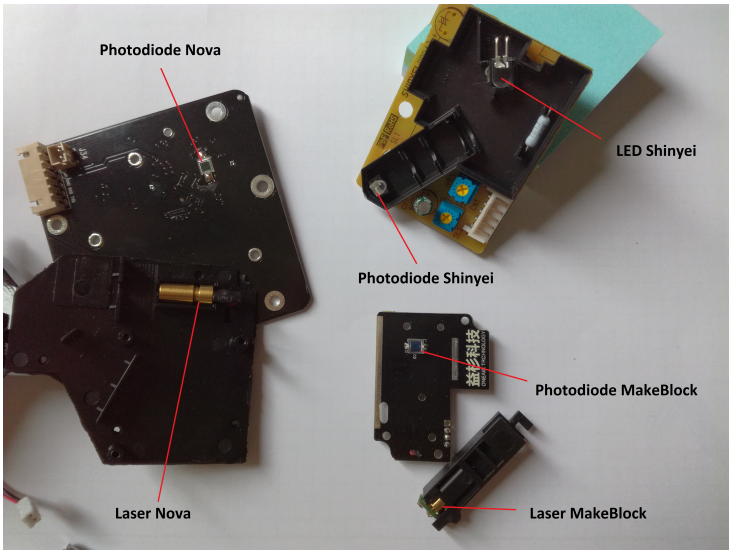

Figure 4.8: *A comparison of the photodiode and laser of the three low-cost sensors, i.e. the Shinyei, MakeBlock and Nova sensors.*

The present chapter addressed the motivation for the experimental study and the established test protocol for cars at low load. The packaging developed around the sensor is subsequently detailed justifying the chosen setup based on experimental observations. The three selected low-cost sensors are finally outlined in detail including inside cuts of the sensors and comparison studies.

Chapter 5

Experiments with Low-cost PM2.5 Sensors

The present chapter analyzes the measurements obtained with two low-cost sensors on diesel cars at low load and on laboratory engines. The measurements made on car engines are compared to the ones of the state-of-the-art sensors made available by GOCA. One low-cost sensor and three state-of-the-art sensors were used in parallel.

However, all sensors do not have the the same frequency and they all need to be filtered with a moving average except for the Nova PM2.5 sensor. A window size of 200 values is set for the MakeBlock sensor. A linear interpolation based on the sensor's frequency is used to determine the window size of the moving average filters of the other sensors. These characteristics are summarized in Table 5.1.

	Measurement's frequency [Hz]	**Window size of the moving average filter**
Nova Laser PM2.5	1	-
MakeBlock Me PM2.5	15	200
Pegasor Mi3	1	13
TSI NPET	1	13
TEN LPA	5	67

Table 5.1: *The measurement's frequency and the window size of the moving average filter for the two low-cost sensors, i.e. the Nova and Makeblock PM2.5 sensors, and the three state-of-the-art measurement systems of GOCA, i.e. the* Pegasor Mi3*, the* TSI NPET *and the* TEN LPA*.*

High and low idle speed tests are performed on cars during the experiments. The phases of the low and high idle speed tests are represented with a gray dashed curve on the graphs with the sensor's measurements. For a low idle speed test, the right-hand y-axis represents the analyzed environment being either zero for ambient air or one for the exhaust gases in the tailpipe. For a high idle speed test, the right-hand y-axis represents the rotational speed of the car.

The reported concentrations of the low-cost sensors are not corrected by the performed dilution because the exact dilution ratio has not been identified. Measurements of the CO before and after the dilution have identified a dilution ratio of 4:1 and 5:1. This dilution ratio does however not remain constant during the tests since the exhaust flow varies during accelerations. Differences in order of magnitude should therefore be interpreted with caution since they sometimes include a not exactly identified dilution ratio.

5.1 Experiments with Nova Laser PM2.5 Sensor SDS011 at Low Load

The Nova Laser PM2.5 Sensor SDS011 is tested in this section during low and high idle speed on two diesel cars complying with the Euro 6b and Euro 3 norm. This Nova sensor has a concentration range of 0-1,000 $\mu g/m^3$ with a precision of 0.1 $\mu g/m^3$ and costs approximately 15-20 €.

A dilution based on a fresh air flux of 100 L/h is made for this low-cost sensor on the Citroën Berlingo during both tests. For the Opel Astra, tests without dilution are completed in order to have indicative measurements.

5.1.1 Low Idle Speed Test

The low idle speed test consists of periods of 200 seconds during which the probe is either inserted in the exhaust pipe or placed on the ground measuring the ambient air.

Opel Astra, Diesel Euro 6b

Figure 5.1 depicts the relative measurements of the Nova sensor and the state-of-the-art sensors during low idle speed of the **Opel Astra**, i.e. a Euro 6b diesel engine. Significant results are obtained when the dilution is reduced to zero. Indeed, for a car with DPF the PM emissions are very low which makes it difficult to observe the impacts of the exhaust gases. A potential effect of condensation is not observed in the trends of the Nova sensor but should be taken into account for tests of a longer duration. Previous experiments have indeed shown lower particulate mass concentrations when no dilution is performed due to the presence of droplets on the lens of the optical sensor. It still appears that the measurement curve of the Nova sensor has a behaviour that is very close to the curve obtained with the TEN LPA sensor. Both indicate that the ambient air contains less PM than the exhaust gases. Meanwhile, the Pegasor Mi3 and the TSI NPET PN measurement curves, represented in Figure 5.2, affirm the contrary. Even though these measurements are expressed in particles per cubic meter, the particulate mass concentration and the PN concentration are linked which allows the comparison. Moreover, the Pegasor Mi3 calculates both concentrations and indicates a similar behaviour for the measured particulate mass and PN concentration (Fig. 5.1 and Fig. 5.2).

On the graph with the relative particulate mass concentrations (Fig. 5.1), the variation of the measurement curves of the Nova sensor is delayed as a result of the variation in the test environment while the reference sensors have a quasi-instantaneous reaction. However, the Nova sensor is the only sensor for which a moving average filter is not applied. A potential explanation is that the data acquisition system of the Nova sensor processes a strong filter for reducing the noise, delaying the measurements. Another explanation could be that it is intrinsic to the low-cost sensor for which the conversion of the signal takes more time. The setup of the test bench, such as the length of the tubes or the presence of pumps, is indeed very similar to the state-of-the-art sensors and are not supposed to induce the delay of the Nova sensor.

Peaks are observed for the nondimensional mass concentration curve of the Nova sensor in Figure 5.1, when the analyzed environment switches from the tailpipe to the ambient air. Let's recall that, for the Nova sensor, this change of environment occurs by increasing the fresh air flow to a maximum of 320 L/h corresponding to an ambient air measurement, as opposed to 100 L/h when the sensor is measuring the tailpipe's emissions. These peaks are probably due to the increase of gas flow in the tubes which pulls along the PM that dropped on the walls when the gas flow was weaker. Indeed, the filtered air flow goes from 100 L/h to 320 L/h and the exhaust gas flow is not strong enough to compensate this difference of 220 L/h. Consequently

the flow is supposed weaker when it is a mixture of exhaust gases and filtered air than in case of only filtered air. In reality, the impact is very small (in the range of 1 $\mu g/m^3$). However, since the particulate mass concentration measured by the Nova sensor is very small too (≤ 5 $\mu g/m^3$), the impact is considerable in Figure 5.1.

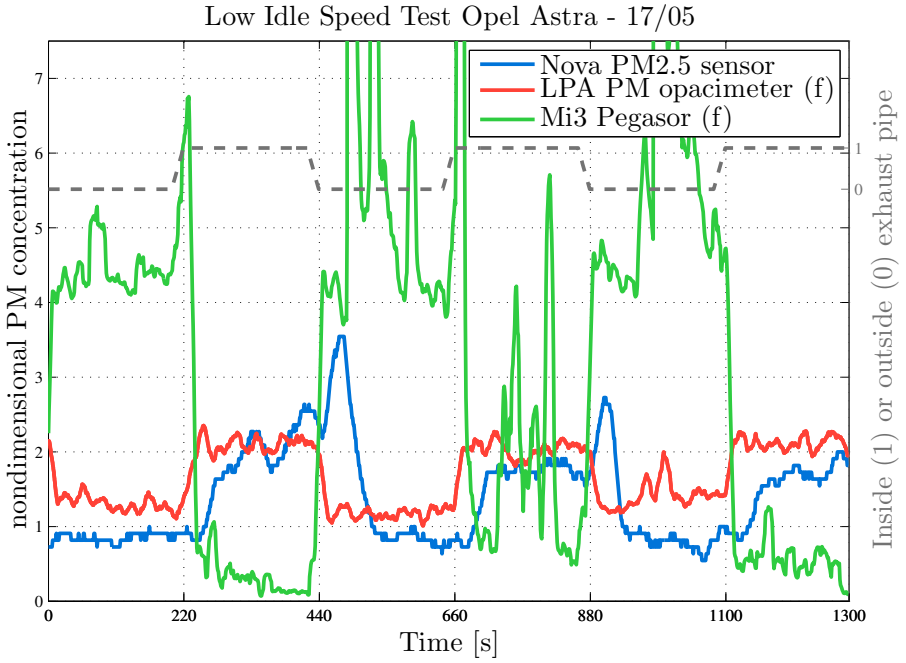

Figure 5.1: *The particulate mass measurement of the Nova sensor without dilution during low idle speeds on the Opel Astra show a similar trend compared to the* TEN LPA *but an opposed trend compared to the* Pegasor Mi3. *The particulate mass concentration is nondimensionalized with the first measurement which corresponds to a measurement of ambient air.*

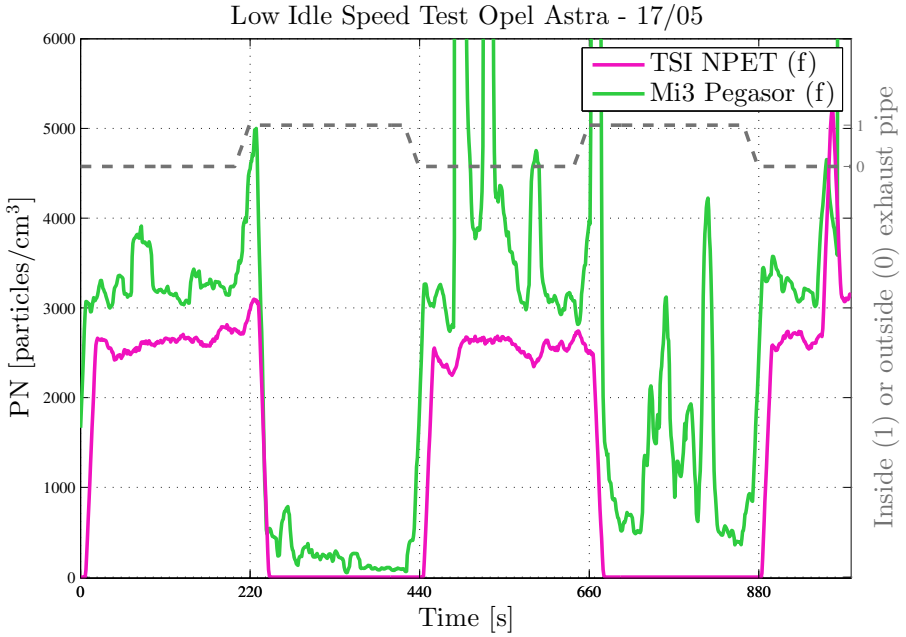

Figure 5.2: *The PN measurements of the* TSI NPET *and the* Pegasor Mi3 *sensors during low idle speeds on the Opel Astra.*

The measurements of the Nova sensor are less stable than the TSI NPET and the TEN LPA sensors where the steps are clearly visible. On the other hand, the measurements of the Pegasor Mi3 are less stable than the Nova sensor. For the measurements of the exhaust gases, this is due to the difficulty to insert appropriately all the probes inside the tailpipe. Figure 5.3 illustrates the probes of the three state-of-the-art measurement systems where the probe of the Pegasor Mi3, i.e. the probe in the middle, is distinguished from the other probes by its lack of flexibility. An increase of sensitivity of the Pegasor Mi3 possibly explains its increase in noise during ambient conditions.

Figure 5.3: *The probe of the* Pegasor Mi3*, i.e. the probe in the middle, is rigid and does not have a handle fixing the probe in the tailpipe compared to the* TEN LPA *and* TSI NPET *probes, respectively the left and right probes.*

The TSI NPET measured a zero concentration for the PN concentration when inserted in the tailpipe during the low idle speed test (Fig. 5.2). The PN concentration range of the TSI NPET has a lower limit of 1,000 particles/m^3 and most probably returns a zero concentration below this value. The PN emissions of the Opel Astra exceed this lower threshold as measured by the Pegasor Mi3.

Figure 5.4 illustrates the measurements of the dimensional mass concentration of the Nova sensor and two state-of-the-art sensors during low idling of the Opel Astra and it shows surprising results for the Pegasor Mi3. Let's recall that no dilution was performed with the Nova sensor and that the concentrations can therefore directly be compared with the reference sensor. On this graph, the mass concentration measured by the Pegasor Mi3 is within the same order of magnitude as the concentration measured by the Nova sensor, i.e. very low, while the measurements of the LPA TEN are three orders of magnitude higher. This result contradicts the expected behaviour of the Pegasor Mi3 on the Opel Astra since this reference sensor is measuring particles as small as 23 nm in diameter. This should result in a slightly higher mass concentrations than the other sensors since a smaller size range is measured. The concentration is near the lower limit of the measurable concentration range (1 $\mu g/m^3$) when the sensor is measuring ambient air. The lower limit is exceeded when the probe is entered in the tailpipe. These measurements can therefore not be considered to be completely reliable.

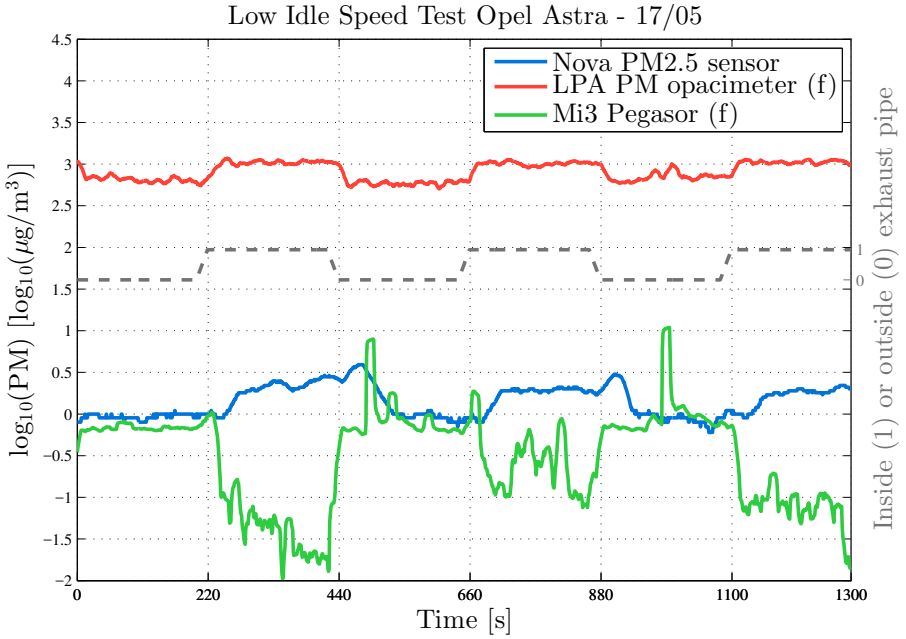

Figure 5.4: *The absoluteparticulate mass measurements of the Nova sensor without dilution during low idle speeds on the Opel Astra. The Nova sensor indicates a similar particulate mass concentration as the* Pegasor Mi3 *sensor but the* TEN LPA *sensor measures higher mass concentrations.*

Citroën Berlingo, Diesel Euro 3 without DPF

The measurements of the Nova sensor at low idle speed on the **Citroën Berlingo** show a similar behaviour as the reference sensors (Fig. 5.5). The sensors do not have opposite reactions anymore (cfr. the results obtained for the Euro 6b car) and all sensors indicate that the particulate mass concentration is higher in the tailpipe than in the ambient air. Let's notice that, unlike the low idle speed tests on the Opel Astra, a dilution is performed on the Citroën Berlingo introducing a fresh air flux of 100 L/h. The two peaks measured when the sensors are inside the tailpipe (Fig. 5.5) are due to the activation of the electric fan. This indeed induces a higher load on the engine since additional power is required for the electric generator. An increase in particulate mass measurements due to the activation of the electric fan is observed for all sensors.

An analogue behaviour during low idling on the Citroën Berlingo is measured by the particle counters when compared to the particulate mass measurement systems (Fig. 5.6). This expected result is explained by the absence of a DPF for the Citroën Berlingo (Euro 3) compared to the Opel Astra (Euro 6b). However, a different behaviour is observed during the activation of the cooling fan with the TSI NPET measuring a trough whereas the Pegasor Mi3 measures a peak. A potential justification is that inducing a higher load on the engine due to the cooling fan causes a deterioration of the combustion producing less and bigger particles. The particulate mass is therefore increased whereas the PN is decreased. Since the Pegasor Mi3 is based on the electric escape current of the charged particles, the mass concentration is computed considering that it is proportional to the escape current. The PN concentration measured by the Pegasor Mi3 is therefore supposed to be a conversion of the particulate mass concentration based on a PSD. The PN concentration measured by the Pegasor Mi3 is thus considered less reliable than the TSI NPET.

Even though the behaviours of the Nova sensor and the accurate sensors are likewise for the low idle test on the Citroën Berlingo, the absolute measurements are significantly different. Indeed, the Nova sensor measures a particulate mass concentration that is at least 30 to 100 times lower

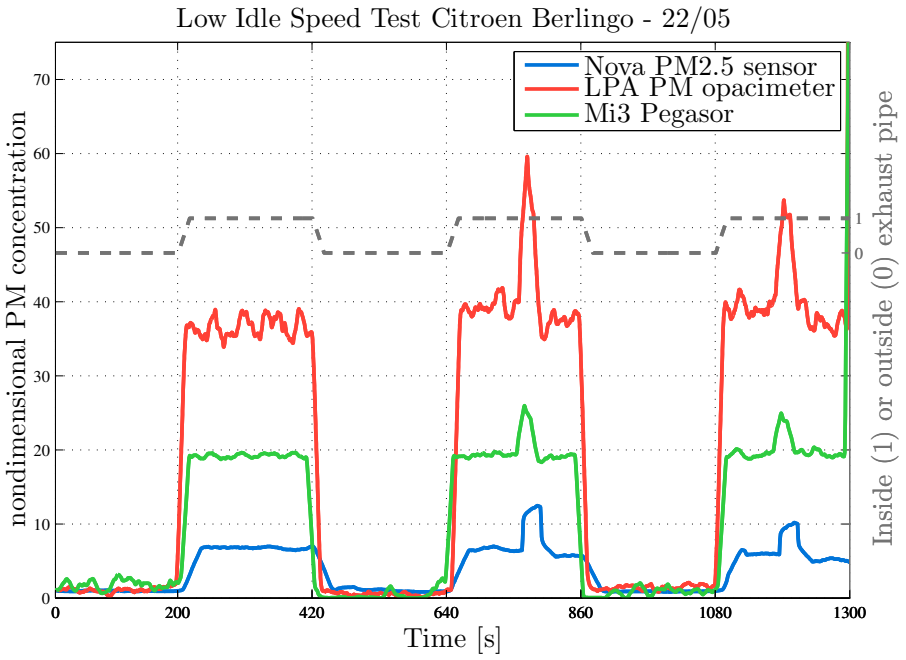

Figure 5.5: *The nondimensional particulate mass measurement of the Nova sensor with a dilution during low idle speeds on the Citroën Berlingo. A similar trend compared to the* TEN LPA *and the* PEGASOR MI3 *is observed.*

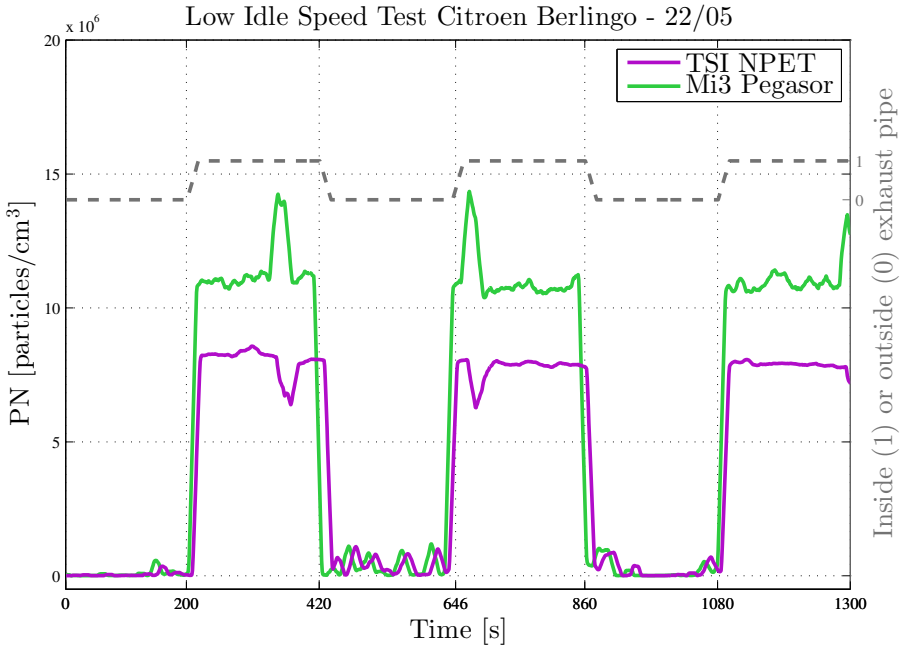

Figure 5.6: *The dimensional PN concentration measured by the* PEGASOR MI3 *and* TSINPET *during low idle speeds on the Citroën Berlingo. Opposite behaviours are observed at the small peaks and correspond to the activation of the cooling fan.*

than the one measured by the state-of-the-art sensors (Fig. 5.7). When the particulate mass concentration is higher, the difference in absolute measurements becomes more pronounced. This difference results from the fact that the range of measured particle's size of the state-of-the-art measurement systems is larger than the range of the Nova sensor. They are indeed able to detect smaller PM. Moreover, for the Nova sensor, the dilution is not yet taken into account which emphasizes the difference. The results also reveal less sensitivity to ambient air for the Nova

sensor compared to the LPA TEN and the Pegasor Mi3. The latter sensor is indeed more sensitive to ambient noise as observed earlier.

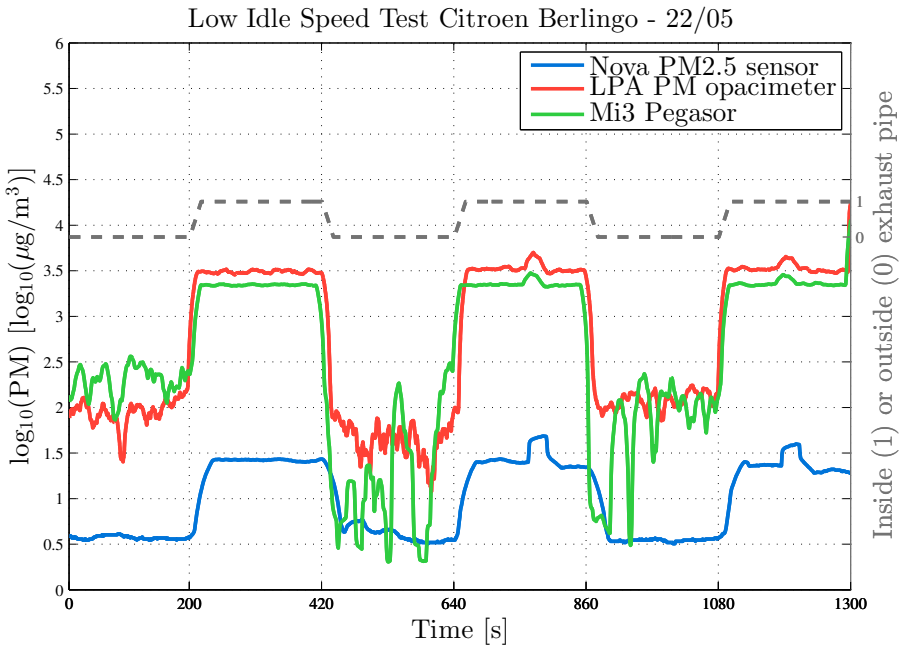

Figure 5.7: *The dimensional particulate mass measurement of the Nova sensor with a dilution during low idle speeds on the Citroën Berlingo. The Nova sensor indicates a lower particulate mass concentration than the* TEN LPA *and the* Pegasor Mi3 *sensors that are close to each other.*

5.1.2 High Idle Speed Test

The high idle speed test consists of acceleration periods where a rotational speed of 3,000 rpm is maintained during 30 seconds. This is followed by a period of 280 seconds of idling.

High idle speed tests are not ideal for the Pegasor Mi3 since the measurement system returned error messages concerning the overloading of the electrometer during the acceleration periods. The increase of heat during high idling is supposed to exceed the temperature limit of the Pegasor Mi3 resulting in error messages and unrealistic measurements. As a general rule, the two most precise measurement instruments made available by GOCA, i.e. the Pegasor Mi3 and the TSI NPET, needed more maintenance and were more restricted in test conditions which resulted in several system errors.

Opel Astra, Diesel Euro 6b

Figure 5.8 illustrates the nondimensional particulate mass measurements of the Nova sensor during high idle speeds on the **Opel Astra**, a car with DPF, when no dilution is performed on the low-cost sensor. Troughs are measured by the Nova sensor as opposed to the TEN LPA opacimeter that measures small peaks in particulate mass concentrations. The contradiction between the sensors is explained by the input during high idle speeds of a more important as well as hotter exhaust flux leading to more condensation in the tubes and measurement chamber of the low-cost sensor, especially in the case of zero dilution. The Nova sensor has moreover an operating temperature range limited to 45 °C and does not guarantee adequate measurements beyond this limit. The Pegasor Mi3 stopped recording the measurements during the high idle speed tests for a reason that has not been identified which explains its absence on the graph.

In Figure 5.9, a dilution is performed on the Nova sensor by introducing in the exhaust flow a filtered air flow of 100 L/h. Thanks to the dilution, less condensation occurs and the flow temperature is lowered avoiding wrong measurements. The peaks in particulate mass concentration obtained at high idle speed are more pronounced for the Nova sensor with dilution than for the TEN LPA and the Nova sensor without dilution.

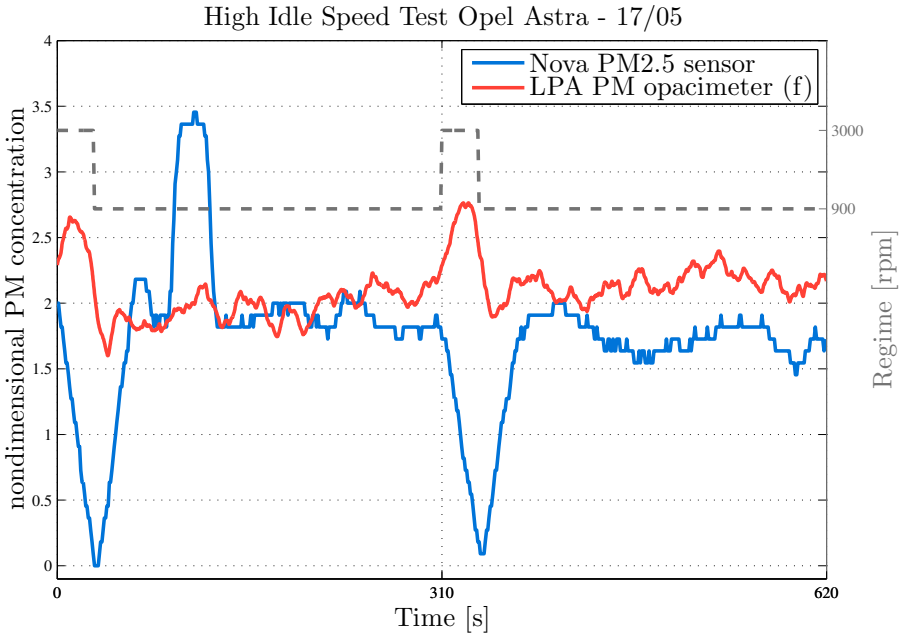

Figure 5.8: *The nondimensional particulate mass measurements of the Nova sensor without dilution during high idle speeds on the Opel Astra. The low-cost sensor has an opposite behaviour compared to the* TEN LPA*, a second generation opacimeter. The particulate mass concentration is nondimensionalized with the first measurement which corresponds to a measurement of ambient air.*

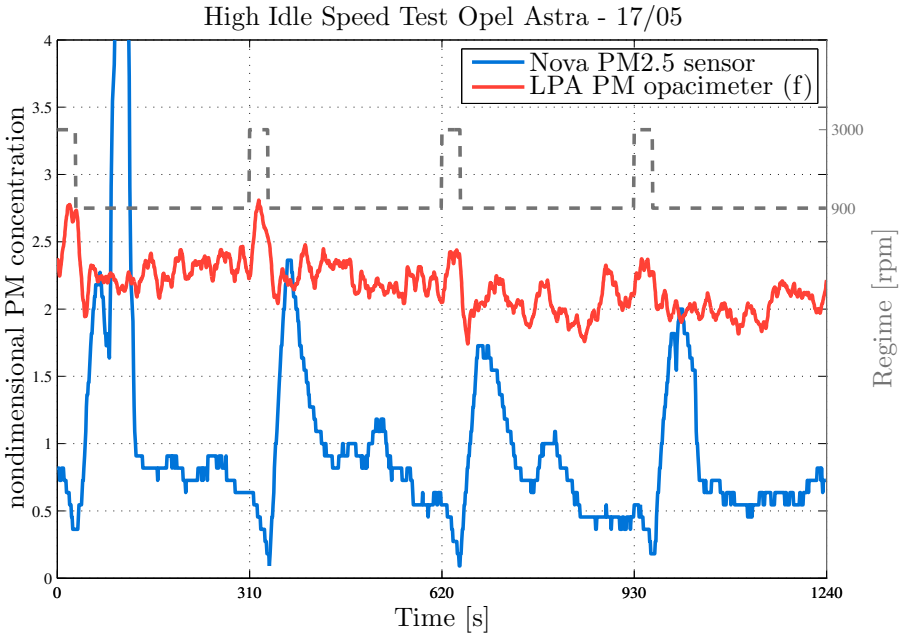

Figure 5.9: *The nondimensional particulate mass measurements of the Nova sensor with dilution on an Opel Astra (Euro 6b) during high idle speed. The* TEN LPA*, a second generation opacimeter, shows similar behaviours with smaller peaks during the accelerations. The particulate mass concentration is nondimensionalized with the first measurement which corresponds to a measurement of ambient air.*

Besides differences in behaviours of the low-cost sensor and the accurate sensors during high idle speed on the Opel Astra, significant differences in absolute measurements are observed too. The absolute values of the Nova sensor are indeed nearly three order of magnitudes lower than the TEN LPA (Fig. 5.10). Let's notice that no dilution was performed with the Nova sensor for the dimensional comparison and that the concentrations can therefore directly be compared with the reference sensor.

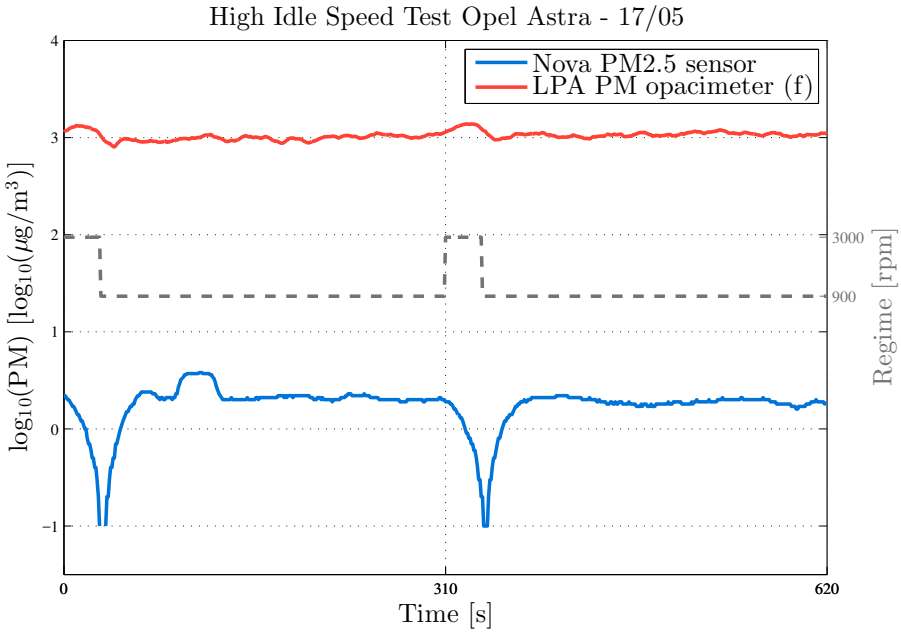

Figure 5.10: *The logarithm of the absolute measurements at high idling on the Opel Astra (Euro 6b) show significant differences for the Nova sensor and the* TEN LPA *with a difference of three order of magnitudes.*

Citroën Berlingo, Diesel Euro 3 without DPF

The Nova sensor with dilution measures equivalent trends as the state-of-the-art measurement systems during high idle speed tests on the **Citroën Berlingo**, a car without DPF (Fig. 5.11). The peaks of the Nova sensor are shifted downwards due to the lower particulate mass concentrations obtained during the low idle speed test compared to the state-of-the-art sensors. The Pegasor Mi3 has three very high peaks exceeding the plotted figure and are due to an overload of the electrometer (error message of the sensor). Between or during every high idle speed, the cooler of the Citroën Berlingo turned on resulting in small peaks in particulate mass concentration as observed between 630 s and 930 s. The cooler affected all measurement systems and was activated at every high idle speed. This influence on the measurements needs to be taken into account when interpreting the peaks since it may cause higher peaks.

An analogue behaviour during high idling on the Citroën Berlingo is measured by the particle counters when compared to the particulate mass measurement systems (Fig. 5.12). Higher absolute PN concentrations are measured with the Pegasor Mi3 than with the TSI NPET.

Besides similar trends between the sensors during high idling on the Citroën Berlingo, significant differences are observed in the absolute particulate mass concentrations measured by the Nova sensor compared to the Pegasor Mi3 and TEN LPA. Let's notice that the measurements of the Nova sensor are not corrected by the dilution ratio and should therefore be compared to the other measurements with caution. The supposed and measured dilution ratio was approximately

4:1 or 5:1 but it is decreased during high idle speed. The Nova sensor's peaks are approximately two orders of magnitude lower than the reference sensors as observed in Figure 5.13.

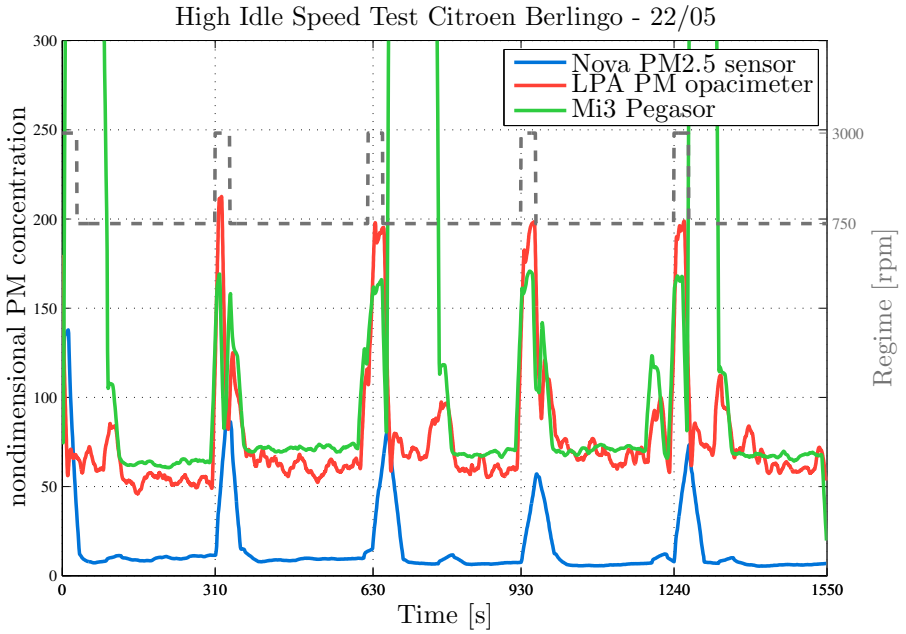

Figure 5.11: *Nondimensional particulate mass measurements of the Nova sensor with dilution on a Citroën Berlingo (Euro 3) during high idle speed. The* TEN LPA*, a second generation opacimeter, and the* Pegasor Mi3 *measure Similar behaviours as the Nova sensor. The particulate mass concentration is nondimensionalized with the first measurement which corresponds to a measurement of ambient air.*

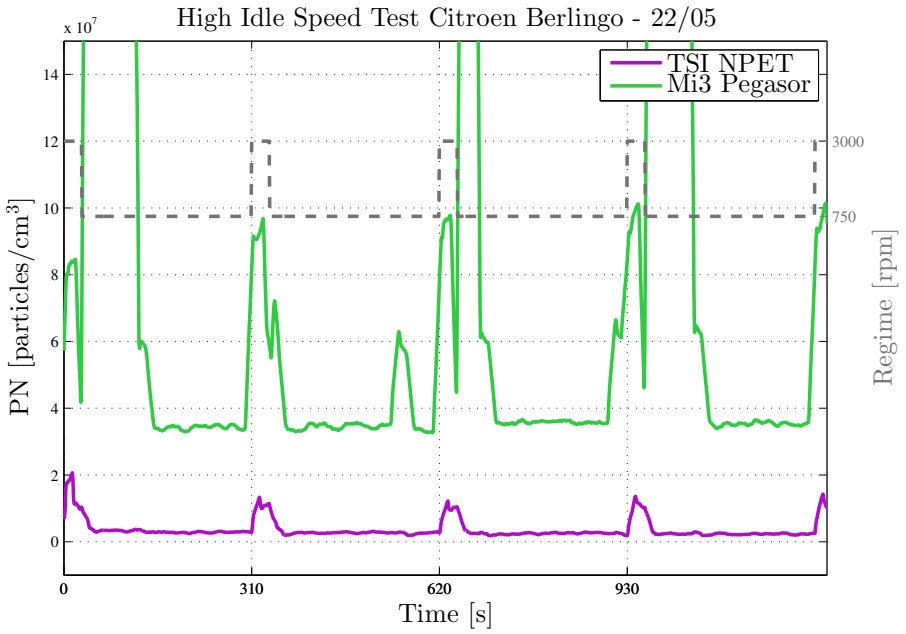

Figure 5.12: *The dimensional PN concentration measured by the* Pegasor Mi3 *and* TSI NPET *during high idle speeds on the Citroën Berlingo. The peaks exceeding the graph limits for the* Pegasor Mi3 *are due to the overloading of the electrometer.*

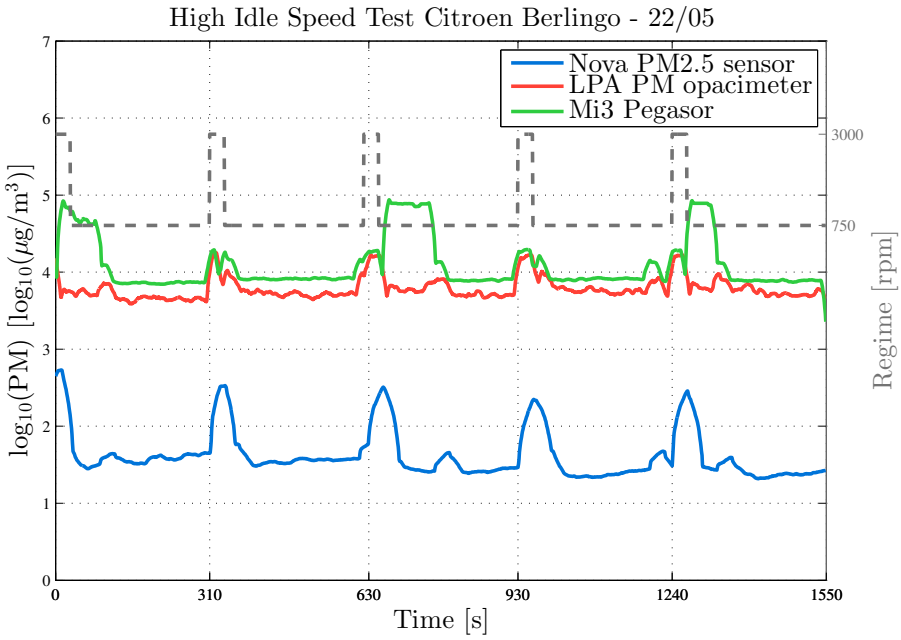

Figure 5.13: *The logarithm of the absolute measurements at high idle on the Citroën Berlingo (Euro 3). Significant differences are observed for the Nova sensor compared to the* Pegasor Mi3 *and* TEN LPA *with approximatively three orders of magnitudes dissimilarity.*

5.1.3 Summary

At low idle speed, the Nova PM2.5 sensor behaves differently depending on the car on which the measurements are made. In the absence of a DPF, the measurement curve of this sensor behaves likewise the expensive sensors. When a DPF is present, the variation of particulate mass concentration measured by the Nova sensor differs from the variation measured by the Pegasor Mi3 and the TSI NPET which are supposed to be the most accurate among the used sensors. This is because the minimum concentration limit of the Pegasor Mi3 and the TSI NPET are reached or exceeded. Similar trends measuring more particles in the tailpipe than in the ambient air are observed with the TEN LPA. Absolute measurements of the Nova sensor are, however, significantly lower than the TEN LPA. It has moreover been necessary to reduce the dilution to zero on the car with DPF in order to obtain an observable variation in the particulate mass concentration.

At high idle speed, all sensors measure peaks in particulate mass and PN concentrations on both cars with one exception. On a car with DPF, the Nova sensor is indeed characterized at high idle speed by troughs when no dilution is performed instead of peaks as is the case for the reference sensors. When a dilution is performed the same behaviours are observed as the reference sensors.

To summarize the relative comparisons, the Nova sensor is able, during both tests, to distinguish the PM emissions of the Euro 3 and Euro 6b cars. The measurements of the Nova sensor are very low for the car with DPF and should therefore be interpreted with care. Further tests on a same recent car with and without DPF should indicate whether this sensor is distinguishing the cars thanks to the presence/absence of a DPF or due to the tiny size of the particles produced by this category of cars.

Table 5.2 compares the absolute measurements of the Nova sensor to the state-of-the-art measurement systems for each type of test and for each car. Let's notice that the measurements

of the Nova sensor are not corrected by the performed dilution for the tests on the Citroën Berlingo because the exact dilution ratio could not be measured. During both low and high idle speed tests on the Opel Astra, the Nova sensor measured concentrations that were nearly three orders of magnitude lower than the reference sensors. On the Citroën Berlingo the Nova sensors measured concentrations that were approximately two orders of magnitude lower than the reference sensors during both tests. No simple constant calibration factor can therefore be applied but rather a calibration function should be considered. The differences in order of magnitude for each car can be explained by the differences in particle size distribution of the exhaust gases of each car. Another explanation could be that the measurements of the Nova sensor are less reliable for low concentrations giving underrated concentrations at low particulate mass concentrations.

Type of test	Diesel car	Differences in order of magnitude
Low idle speed	Opel Astra (Euro 6b, 2016)	2.75 to 3
	Citroën Berlingo (Euro 3, 2001)	1.5 to 2
High idle speed	Opel Astra (Euro 6b, 2016)	2.75
	Citroën Berlingo (Euro 3, 2001)	1.8 to 2

Table 5.2: *Comparison in absolute measurements between the Nova sensor and the state-of-the-art measurement systems for each type of test on each diesel car. The orders of magnitude stay approximately constant for each car and varying type of test. The differences in order of magnitude of the Citroën Berlingo include a dilution.*

5.2 Experiments on MakeBlock Me PM2.5 Sensor at Low Load

The MakeBlock Me PM2.5 sensor is tested in this section during low and high idle speed on two diesel cars complying with the Euro 6b and the Euro 3 norm. This low-cost sensor has a concentration range of 0-6,500 $\mu g/m^3$ with a precision of 1 $\mu g/m^3$ and costs approximately 40-45 €.

A dilution based on a fresh air flux of 100 L/h is performed for this low-cost sensor on the Citroën Berlingo during both tests. For the Opel Astra, tests without dilution are done.

The low-cost sensor studied in this section showed insensitive results for tests performed on the Opel Astra, i.e. a car with DPF. The values returned by the sensor expressed in micro-grams per cubic meter are either zero, one or two because the low-cost sensor is unable to detect a small amount of particles neither small particles precisely.

5.2.1 Low Idle Speed Test

The low idle speed test consists of periods of 200 seconds during which the probe is either inserted in the exhaust pipe or placed on the ground measuring the ambient air.

Opel Astra, Diesel Euro 6b

As mentioned earlier, the MakeBlock sensor did not measure significant particulate mass concentrations during high and low idle speed test on the **Opel Astra**, i.e. a diesel Euro 6b car. The absolute measurements do not reflect a particular trend and are either 0 $\mu g/m^3$ or 1 $\mu g/m^3$ (Fig. 5.14). No comparison is therefore done with state-of-the-art measurement systems.

Citroën Berlingo, Diesel Euro 3 without DPF

The nondimensional particulate mass concentrations measured during low idle speed on the **Citroën Berlingo** by the MakeBlock, the TEN LPA and the Pegasor Mi3 sensors have

similar trends measuring more PM in the exhaust gases than in the ambient air (Fig. 5.15). The MakeBlock sensor measures, however, higher steps than the TEN LPA compared to the Nova low-cost sensor studied before. This low-cost sensor is consequently more sensitive to particulate mass concentration variations and notices just like the other sensors the activation of the cooling fan of the Citroën by measuring higher particulate mass concentrations.

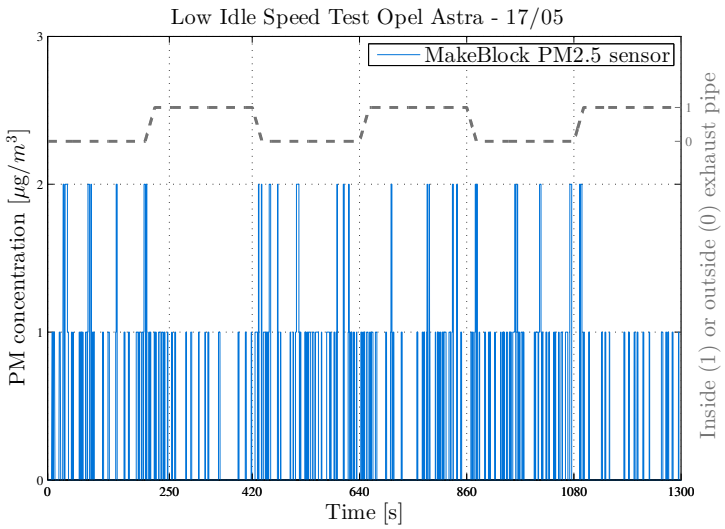

Figure 5.14: *The particulate mass measurements of the MakeBlock sensor at low idle speed on the Opel Astra. The absolute particulate mass concentration is too low to be analyzed. No filter is applied on the results because the variation of the measurements is not revelatory enough.*

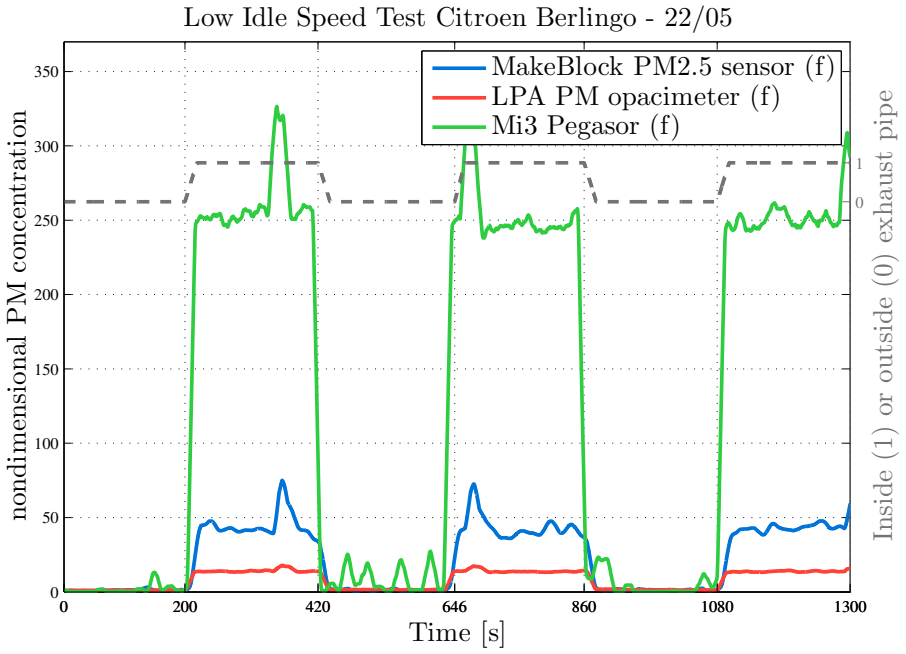

Figure 5.15: *The particulate mass measurement of the MakeBlock sensor with a dilution during low idle speeds on the Citroën Berlingo shows a similar trend compared to the* TEN LPA *and to the* Pegasor Mi3. *The particulate mass concentration is nondimensionalized with the first measurement which corresponds to a measurement of ambient air.*

Concerning the absolute measurements during low idle speed on the Citroën Berlingo, the MakeBlock sensor measures much lower concentrations than the two state-of-the-art sensors

(Fig. 5.16). An approximate ratio of 100 exists between measurements of the MakeBlock sensor compared to the reference sensors which was also observed for the Nova sensor. Let's notice that the measurements of the Nova sensor include a dilution and should therefore be compared with care to the other measurements. The supposed and measured dilution ratio was approximately 4:1 or 5:1. Surprisingly, the particulate mass concentration of the ambient air measured by the Pegasor Mi3 is also below the concentration measured by the TEN LPA opacimeter while, for the tests with the Nova sensor, the measurement curve of the Pegasor Mi3 and the TEN LPA sensors were very close.

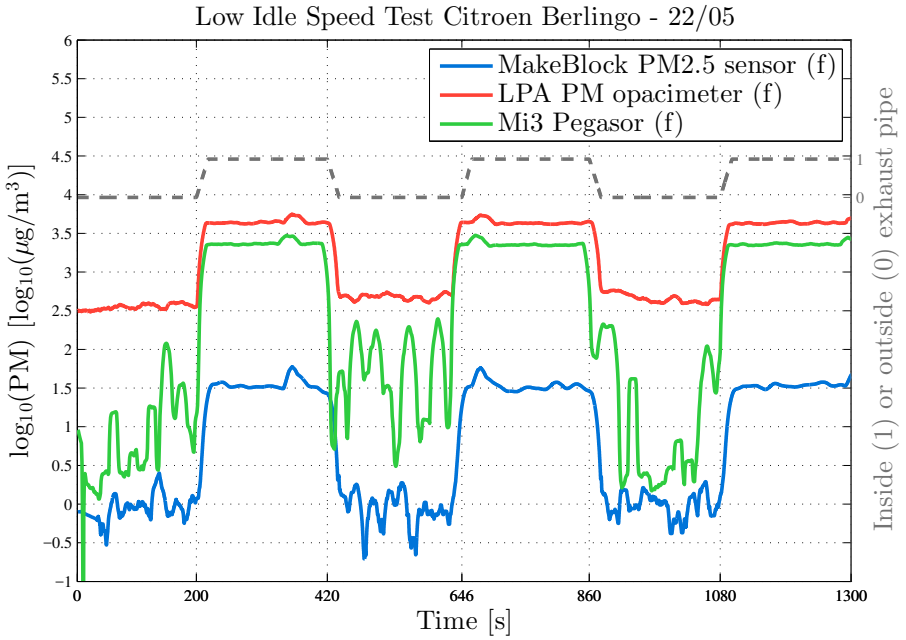

Figure 5.16: *The absolute particulate mass measurement of the MakeBlock sensor with a dilution during low idle speeds on the Citroën Berlingo. The MakeBlock sensor indicates lower particulate mass concentration than the* TEN LPA *and the* Pegasor Mi3 *sensors which are close to each other only when the probes are in the tailpipe.*

5.2.2 High Idle Speed Test

The high idle speed test consists of acceleration periods where a rotational speed of 3,000 rpm is maintained during 30 seconds. This is followed by a period of 280 seconds of idling.

Based on the experiments, the increase of heat during high idling is supposed to exceed the temperature limit of the Pegasor Mi3 resulting in error messages and unrealistic measurements.

Opel Astra, Diesel Euro 6b

No particular trend can be identified from measurements of the MakeBlock sensor during high idle speed on the **Opel Astra**, a car with DPF. The obtained figure can be found in Appendix B.1. The values obtained by the sensor are either zero, one or two micro-grams per cubic meter because the low-cost sensor is not able to detect a small amount of particles neither small particles precisely. No comparison is therefore applicable with state-of-the-art measurement systems.

Citroën Berlingo, Diesel Euro 3 without DPF

Similar behaviours of the MakeBlock sensor are observed during high idle speed tests on the Citroën Berlingo (Euro 3) with the Pegasor Mi3 (Fig. 5.17). During the large peaks of the

Pegasor Mi3 exceeding the Figure 5.17, the sensor returned an error message indicating an overload of the electrometer. The TEN LPA measures very small peaks during the accelerations.

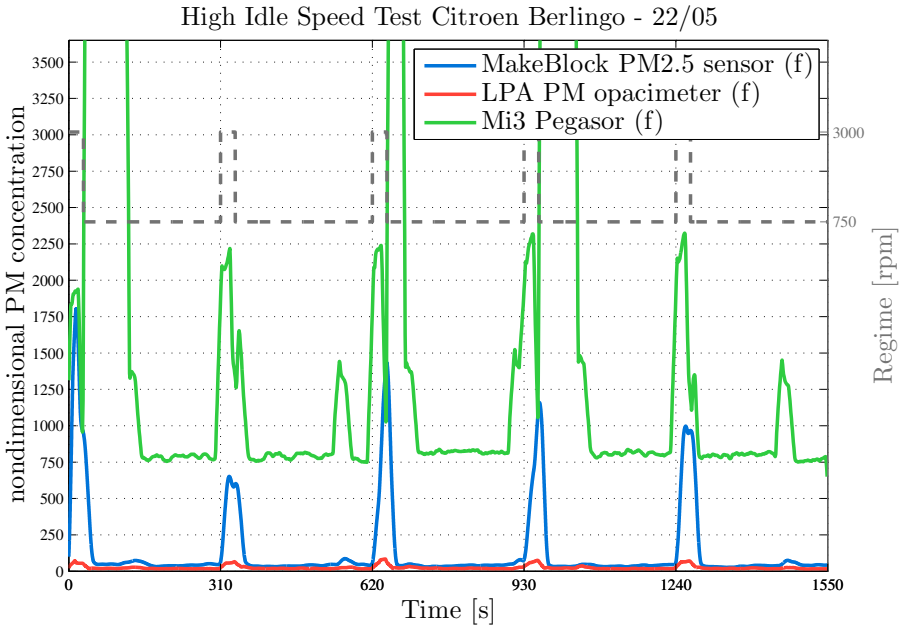

Figure 5.17: *The nondimensional particulate mass measurement of the MakeBlock sensor with dilution during high idle speeds on the Citroën Berlingo. The* Pegasor Mi3 *and the MakeBlock sensor have same behaviours whereas the* TEN LPA *measures only small peaks during the accelerations. The particulate mass concentration of each sensor is nondimensionalized with the first measurement which corresponds to a measurement of ambient air and is represented on the left-hand y-axis.*

Besides similar trends between the MakeBlock sensor and the reference sensors during high idling on the Citroën Berlingo, notable differences are observed in the absolute particulate mass concentration measurements of the MakeBlock sensor compared to the Pegasor Mi3 and TEN LPA. The MakeBlock sensor's peaks are between 2 and 2.5 orders of magnitude lower than the reference sensors as observed in Figure 5.18. Let's recall that the measurements of the MakeBlock sensor include a dilution and should therefore be compared to the other measurements with care. The supposed and measured dilution ratio was approximately 4:1 or 5:1 but is decreased during high idling.

5.2.3 Summary

At low idle speed, the MakeBlock Me PM2.5 sensor has different reactions depending on the car. On a recent car with DPF, such as an Opel Astra, the measurements are too low to be analyzed even when no dilution is performed. For a car without DPF, such as the Citroën Berlingo, the MakeBlock sensor reacts however in the same way as expensive sensors. It is, in addition, more sensitive than the TEN LPA sensor.

At high idle speed, the same conclusions apply as at low idle speed in relation to the type of car. On a car without DPF, the MakeBlock sensor is considerably more sensitive than the TEN LPA sensor but utterly less sensitive than the Pegasor Mi3.

To summarize the relative comparison, both type of tests are effective to distinguish the PM emissions of the two cars. The results of the MakeBlock sensor are nevertheless insignificant for the Euro 6b car. Further tests on a same recent car, with and without DPF, should indicate

whether this is due to the presence of a DPF or to the tiny size of the particles produced by recent cars.

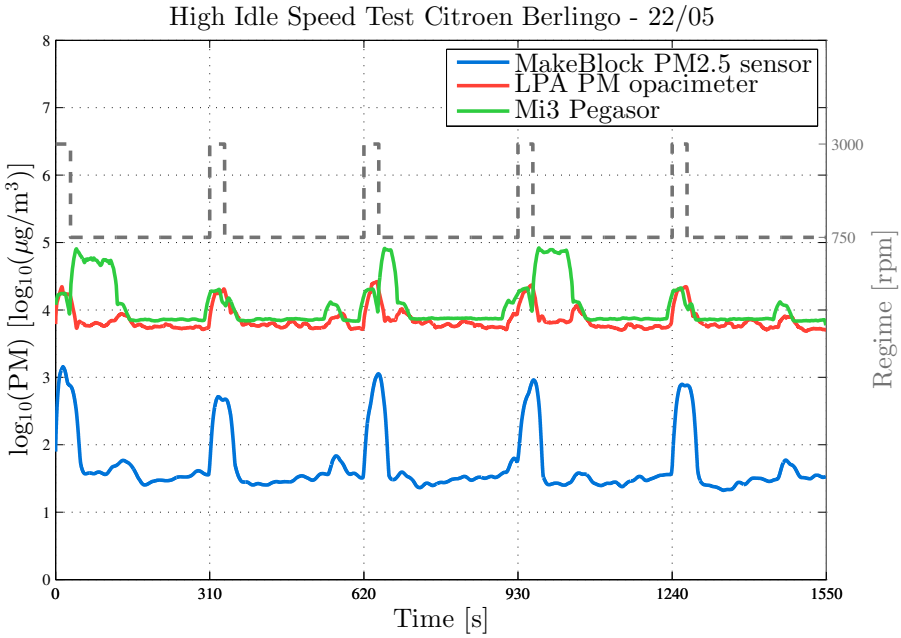

Figure 5.18: *The logarithm of the absolute measurements of the MakeBlock sensor at high idle on the Citroën Berlingo (Euro 3). Significant differences of one to two orders of magnitudes are observed between the MakeBlock sensor and the* Pegasor Mi3 *and* TEN LPA. *The left-hand y-axis represents the 10-base logarithm of the particulate mass concentration expressed in micro-grams per cubic meter.*

Table 5.3 compares the absolute measurements of the MakeBlock sensor to the state-of-the-art measurement systems for each car and each type of test. No difference in order of magnitude is reported for the tests performed on the Opel Astra due to the insignificant measurements. Let's notice that the measurements of the MakeBlock sensor are not corrected by the performed dilution because the exact dilution ratio could not be measured. The dilution ratio is expected to be approximately 4:1 or 5:1. During the experiments on the Citroën Berlingo, the MakeBlock sensor measured different orders of magnitude between the low-cost sensor and the reference sensors for each type of test. During the low idle speed test, the MakeBlock sensor measured concentrations that were 2 to 2.5 orders of magnitude lower than the reference sensors whereas, during the high idle speed test, differences of 1.5 to 2 orders of magnitude were observed. This indicates the higher sensitivity of the MakeBlock sensor at high temperatures, i.e. during high idle speed, resulting in higher and thus less reliable concentration measurements.

Type of test	Diesel car	Differences in order of magnitude
Low idle speed	Opel Astra (Euro 6b, 2016)	-
	Citroën Berlingo (Euro 3, 2001)	2 to 2.5
High idle speed	Opel Astra (Euro 6b, 2016)	-
	Citroën Berlingo (Euro 3, 2001)	1.5 to 2

Table 5.3: *Comparison in absolute measurements between the MakeBlock sensor and the state-of-the-art measurement systems for each type of test on each diesel car. The differences in order of magnitude vary for the Citroën Berlingo depending on the type of test.*

5.3 Laboratory Tests

Laboratory tests are performed on the low-cost sensors to examine whether they react to PM by using incense and to identify the potential shortcomings of the low-cost sensors on car engines. As discussed in Chapter 4, the low-cost sensors are not appropriate for car's exhaust gases due to, inter alia, the temperature and concentration limits of the sensors. Issues with condensation, clogging and reflux have also been encountered during the tests on laboratory engines and have allowed to design the test bench in such a way that these confounding effects are minimized. Performing tests on laboratory engines when compared to cars allows to have a better and separate control on the engine's parameters such as the rotational speed, the torque and the air excess ratio. The characteristics of the two laboratory engines used for this Master's thesis are the following:

- Citroën engine
  - An atmospheric gasoline engine with 4 aligned cylinders, 16 valves, reference TU5J4 and a displacement volume of 1,587 cm^3;
  - A brake which is of the "eddy-currents" type and its control panel to model the external system of the interface;
  - A calculator ECU of the brand Sybele, model Commander44, completely programmable thanks to the Winjall software (allowing a real-time control of the injection and of the ignition advance). This ECU is however programmed in an open loop and does not allow a precise control of the air excess coefficient.
- Varimax engine
  - A single-cylinder piston engine coupled to a three-phase asynchronous electric motor and to a system of acquisition and measurement;
  - The bore of the cylinder is 9.52 cm and the stroke is 11.43 cm. Thus, the engine's displacement is 814.45 cm^3;
  - Characteristic allowing to change in real time several parameters such as the compression ratio or the ignition advance;
  - Configuration in spark ignition mode with RON 95 gasoline as fuel.

A major limitation of the laboratory Citroën engine is the unreliable measure of the air excess ratio. Since the ECU works in an open loop, the displayed air excess ratio cannot be considered as an absolute measure. The measurements obtained on different days or at different moments with the same rotational speed and torque gave indeed different values. Moreover, since the laboratory Citroën engine works on gasoline fuel much more water was present in the exhaust gases. The duration of the tests were therefore considerably restricted and the results were less reliable when the measurements were performed at the end of the experiment.

The major limitation of the Varimax engine is the important quantity of water in the exhaust gases. Indeed, the engine sputtered lots of water droplets at the exhaust which is due to the engine's characteristics (old gasoline engine) and to the exhaust pipe design. The latter is specific to the laboratory and does not allow to extract the exhaust gases further downstream the tailpipe. Due to the strong limitations of this engine, no significant measurements could be obtained with the low-cost sensors. The experiments have therefore only been useful for determining the packaging of the bought sensors.

Due to these limitations, the tests on the laboratory engines could not be used for a validation of the low-cost sensors. They have, however, allowed to identify important issues encountered by the low-cost sensors on engine's exhaust gases.

5.3.1 Citroën Gasoline Laboratory Engine

The particulate mass measurements of the Makeblock sensors on the Citroën gasoline laboratory engine are proportional to the load even though no precise steps are obtained at the different torques (Fig. 5.19). During the experiment, the load is varied between 72 Nm and 95 Nm while adapting the injection advance in order to keep the air excess ratio at unity. However, this latter tuning was not fully reliable since the ECU worked in an open loop as mentioned earlier. Due to the time constraint cited above, it was not possible to wait for stabilization of the particulate mass concentrations at the different torques.

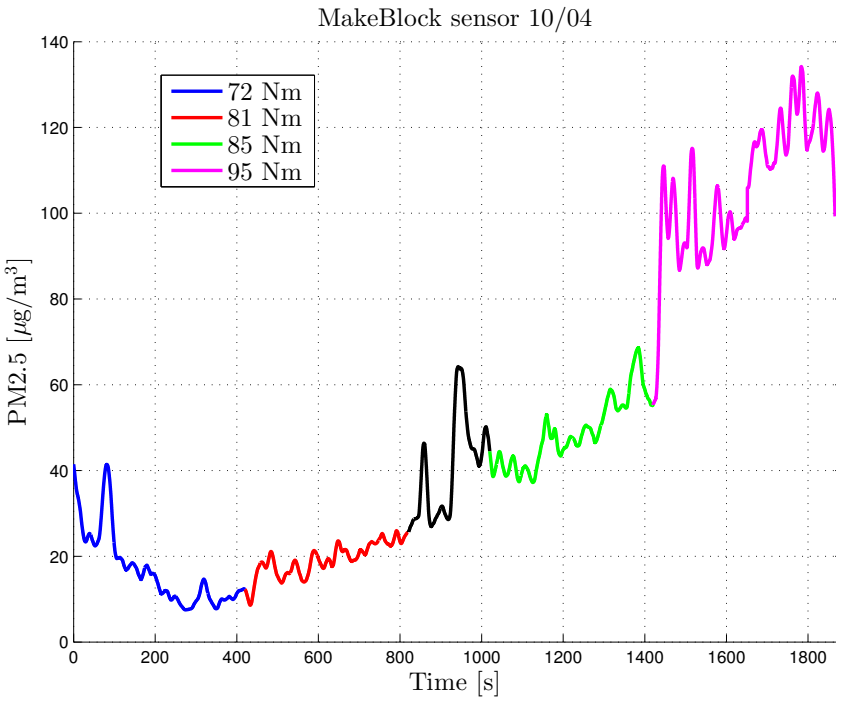

Figure 5.19: *Particulate mass concentration measured by the Makeblock sensor on the Citroën gasoline laboratory engine when varying the torque between 72* Nm *and 95* Nm*. The particulate mass measurements are proportional to the load even though precise steps are not obtained. The black curve represents an intermediate transition torque level.*

The particulate mass measurements of the Nova sensors on the Citroën gasoline laboratory engine are proportional to the load showing distinctive steps at the different torque levels (Fig. 5.20). The load is varied between 72 Nm and 95 Nm, i.e. identically as for the MakeBlock sensor.

The two tests described above for the Nova and MakeBlock sensors on the Citroën gasoline laboratory engine were done on the same day respectively in the morning and in the afternoon. Closer orders of magnitude of both measurements are hence obtained for the first torque levels but they move apart when the torque is going higher. The absence of steps for the MakeBlock sensor is explained by its higher sensitivity, as observed during the tests with incense needing more time to reach stabilization.

5.3.2 Incense

Experiments with incense have allowed to compare both low-cost sensors simultaneously near a source of PM. Each low-cost sensor had its own measurement chamber and aspiration pump and no dilution was performed. Drawbacks of testing the sensors with incense are the absence

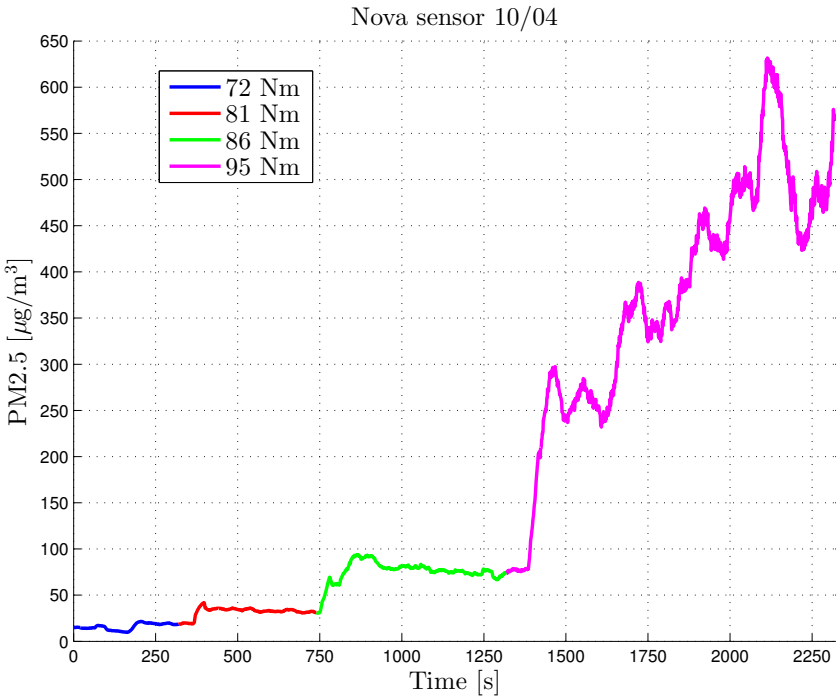

Figure 5.20: *Particulate mass concentration measured by the Nova sensor on the Citroën gasoline laboratory engine when varying the torque between 72* Nm *and 95* Nm*. The particulate mass measurements are proportional to the load and distinctive and precise steps are obtained.*

of knowledge concerning the expected PM emissions and PSD. The measured particulate mass concentration can therefore not be challenged with correct values.

As depicted in Figure 5.21, the two low-cost sensors are measuring same concentrations of PM. The concentration limit of both sensors are respectively 1,000 $\mu g/m^3$ and 6,500 $\mu g/m^3$ for the Nova and MakeBlock sensor. This information results in significant differences in measurement during the first 140 seconds (Figure 5.21 (a)). Although the measurements of the MakeBlock sensor are filtered with a moving average filter, the obtained particulate mass concentration varies significantly more than for the Nova sensor (Fig. 5.21 (b)). For that reason, a greater sensitivity of the MakeBlock is therefore assumed.

5.3.3 Summary

The experiments on the laboratory engines have allowed to determine an appropriate packaging for low-cost sensors avoiding as much as possible clogging, condensation and exceeding of the sensor's temperature and concentration limits. Varying load experiments on the Citroën gasoline laboratory engine have showed that the measured particulate mass concentration was proportional to the load. The limitations of this laboratory engine has not allowed to perform a precise validation of the low-cost sensors. Moreover, due to the time restrictions for the laboratory tests, no distinctive steps have been obtained for the MakeBlock sensor. Experiments with incense have indeed shown the greater sensitivity of the MakeBlock sensor to particulate mass concentration in spite of applying a moving average filter.

5.4 Review of the Experimental Study

The experimental study allowed to test, validate and identify the flaws of the low-cost sensors. Two low-cost sensors on diesel cars with and without DPF are confronted with state-of-the-art measurement systems during low and high idle speed tests. Preliminary experiments with incense

and laboratory engines have allowed to validate the behaviour of the sensors.

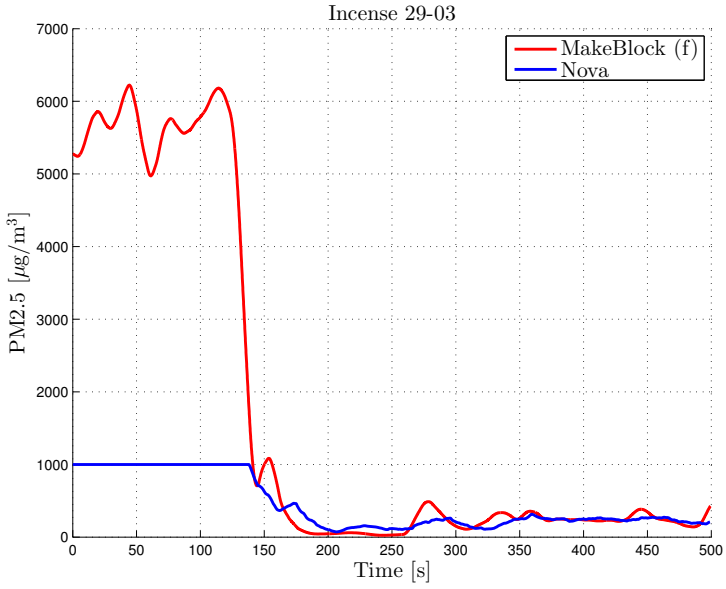

(a)

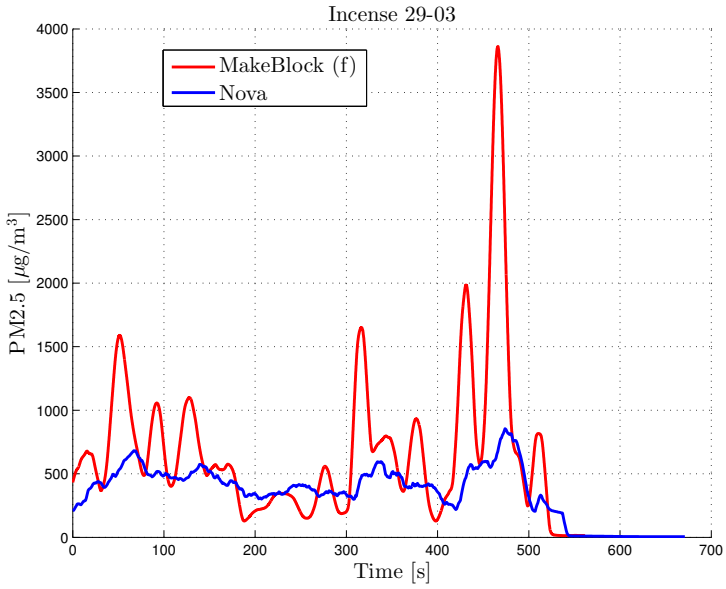

(b)

Figure 5.21: *Experiment with incense on the Nova and MakeBlock low-cost sensors. Similar measurements are obtained for both sensors with a higher sensitivity of the MakeBlock sensor.*

During the experimental study, a relative comparison with the reference sensors demonstrated that both low-cost sensors are able to distinguish the diesel car with and without DPF based on their PM emissions. This was the case for both types of tests, i.e. at low and high idle speed. Further tests should however identify whether this distinction is due to the presence/absence of a particulate filter or consequent to the technological improvements of cars ever since the year 2001. In addition, the MakeBlock sensor measured insignificant concentrations on the car with DPF ranging between zero, one and two micro-grams per cubic meter. The Nova sensor, on the other hand, measured very low concentrations whose reliability is not necessarily ascertained. It is indeed possible that the Nova sensor filters the measured concentrations whose precision

is only of 1 $\mu g/m^3$. The filter would then virtually increase the precision of the measurements to 0.1 $\mu g/m^3$. At low concentrations, between zero and two micro-grams per cubic meter, the precision is therefore not assured. Let's also notice that, except the second generation opacimeter, no state-of-the-art measurement system was able to measure reliable particulate mass or PN concentrations on the car with DPF.

An absolute comparison between the low-cost and accurate measurement systems showed significant differences. The Nova sensor measured, on the car with DPF, concentrations that were approximately three orders of magnitude lower than the reference measurements. On the car without DPF the difference in order of magnitude dropped to approximately two. This can be explained by the difference in PSD between both cars which is taken into account by the measurements of the accurate sensors but not measured by the low-cost sensors. The MakeBlock sensor, on the other hand, measured concentrations that were 1.5 to 2 orders of magnitude lower than the reference sensors on the Citroën Berlingo. A difference is observed between the types of tests which highlights the higher sensitivity of the MakeBlock sensor.

Preliminary experiments with incense and laboratory engines showed that the MakeBlock proved to be more sensitive than the Nova sensor.

Conclusion

The present Master's thesis analyzes Particulate Matter (PM) emissions of diesel cars and develops a low-cost measurement system for engine's exhaust. The main objective of the experimental study is to detect the presence as well as the efficiency of a Diesel Particulate Filter (DPF). A collaboration with the group of recognized enterprises for PTI and driving licenses GOCA allowed to compare the obtained measurements with state-of-the-art sensors at rest on cars with and without DPF.

The first chapter of the Master's thesis discusses the European vehicle emission regulations and the methods for controlling PM in diesel engines. The Euro norms and corresponding test procedures are described and the low emissions zones are presented focusing on those presently activated in Antwerp and Brussels. Direct and indirect control methods for Particulate Matter emissions of diesel engines are thereafter presented concentrating on DPF. A final characterization of PM presents particle size distributions of diesel exhaust.

The second chapter converts the Euro norms to massic concentrations in order to have appropriate orders of magnitude of the allowed PM emissions for diesel cars. For that purpose a conversion model is implemented in Matlab that depends on the characteristics of a specific engine and that is based on a volumetric efficiency model found in the literature [38]. A 0D model of the engine cycle including in-cylinder heat transfer losses is also applied in order to obtain the evolution of the cylinder pressure and temperature needed for the volumetric efficiency model. The conversion model is thereafter applied to two engines complying with Euro 3 and Euro 6. The limitations of the conversion model do not allow to have an accurate conversion but this can be achieved by measuring the exhaust flow at a car's tailpipe.

In the third chapter, a state of art is reported concerning PM measurement techniques. Four main types are studied among which the optical backscatter sensor is identified as the most appropriate for the experimental study of the present Master's thesis. Sensors based on the accumulation of PM are described as well as two precise measurement techniques known as the Scanning Mobility Particle Sizer and the Electrical Low Pressure Impactor+.

The fourth chapter elaborates the experimental purpose and the methodology of this Master's thesis. The experiments at low load are firstly motivated by describing the state-of-the-art measurement systems made available by GOCA as well as the two cars on which the tests are performed. These two diesel cars date from the years 2001 (Euro 3) and 2016 (Euro 6b) and are respectively characterized by the absence and the presence of a DPF. The self-established test protocol is thereafter addressed developing the low and high idle speed tests followed up by a description of the test bench. The latter justifies the choices for the setup based on experiments with laboratory engines. Finally, the three selected low-cost sensors are presented with specification of their limits. The MakeBlock and Nova sensors are identified as the most efficient whereas the Shinyei sensor is discarded for further experiments.

In the last chapter, two low-cost sensors are compared with state-of-the-art measurement systems during tests at low-load on two diesel cars (Euro 3, Euro 6b). For each type of test, i.e. low and high idle speed test, a comparison is done between the results obtained on the car with and without DPF. Relative and absolute measurements of each low-cost sensor are challenged with those of the state-of-the-art sensors. The two low-cost sensors were able to distinguish the two diesel cars based on their PM emissions by measuring considerably less particulate mass for the car with DPF. The third section of this chapter described the experiments performed with incense and on laboratory engines. These experiments have allowed to perform a preliminary validation of the low-cost sensors and the added packaging.

The experiments showed that both low-cost sensors are able to distinguish the car with and without DPF and this during both types of tests. The Nova sensor measured considerably lower concentrations on the car with DPF whereas the MakeBlock sensor measured insignificant concentrations. Further tests with a recent car without DPF should however identify whether this distinction is due to the presence or absence of a particulate filter or resulting from the technological improvements of cars dating from the year 2016. The concentrations measured by the Nova sensor on the car with DPF were also very low hence decreasing the reliability of the measurements. Let's also notice that, except the second generation opacimeter, no other state-of-the-art sensor was able to measure reliable particulate mass or number concentrations on the car with DPF. The lower concentration limit was either exceeded or the concentrations were too close to the minimum measurable concentration.

Limitations

Limitations in the performed study are identified for the Matlab model and the experiments at low-load. The Matlab model is principally theoretical and no real challenge with experimental results was done. A lot of assumptions and simplifications were made to obtain the presented results such as the temperature and pressure inside a cylinder and the volumetric efficiency. Some parameters among which the valve timing and the regression parameters used in the volumetric efficiency were also considered to be identical for all the cars.

An important limitation of the performed experiments is the lack of known reference PM concentration. Indeed, the state-of-the-art measurement systems were not always able to measure a realistic concentration, especially on the car with DPF, and sometimes they gave contradictory conclusions. This information therefore did not allow to validate the sensors.

A major limitation of the MakeBlock sensor is its inability to measure significant PM concentrations on the car with DPF. The Nova sensor is also limited by its minimum measurable concentration but still measured significant trends. The measured concentration of the Nova sensor on the car with particulate filter were indeed very low even without any dilution. The reliability of the measured concentrations is therefore not certified.

The lower concentration limit of the two low-cost sensors constrained to suppress the dilution on the car with DPF since this allowed the measurement of significant concentrations for the Nova sensor. However, this highlighted a second important limitation of the low-cost sensors which is their sensitivity to condensation leading to clogging and water droplets in the sensor. The absence of dilution does also not allow to reduce the exhaust temperature and the PM measurements are therefore not fully reliable since the temperature range of the sensor is exceeded.

The performed tests require the human hand which makes it impossible to repeat exactly the same conditions for each tests, especially for the free acceleration and high idle speed test for which a precise and repeated regime of 3,000 rpm cannot be guaranteed.

Future Prospects

This work may lead to the conclusion that the conception of a low-cost measurement system can be achieved. Furthermore, this latter system may be able to detect the presence of a DPF. However, more experiments are required to confirm these statements. Indeed, an interesting experience would be to do the same tests twice on the same car but with and without a DPF. This could permit to verify whether the low PM concentration measured on the car with a DPF is simply the result of the technological advance.

Another point of improvement would be the test bench and more particularly the dilution. The mixture between the exhaust gases and the filtered air is indeed not optimal because it does not completely exclude reflux. The T-branch has the inconvenient to create lot of turbulence which causes head losses. The dilution ratio should moreover be maintained constant by adapting the fresh air flux with the engine regime. The use of Nondispersive Infrared (NDIR) sensors measuring the CO concentration before and after the dilution would allow to measure the dilution ratio instantaneously. The fresh air flux could then be adapted in order to maintain a constant dilution ratio.

Among the future prospects, the low-cost sensors could also be used on gasoline engines in order to assess the efficiency of the GPF. However, this would be more ambitious than on diesel engines since the size of the emitted PM emissions of a gasoline engine are smaller.

The present Master's thesis offers a series of perspectives for the future development of the measurement of PM emissions of engines. PM has recently become a topical subject due to its detrimental effects on health and due to the high emissions caused by vehicles. Diesel engines that are not equipped with a particulate filter are blamed albeit wood stoves and current gasoline engines are also responsible for high PM emissions. In accordance with this increased attention, the issue of PM emissions of diesel and gasoline vehicles is evolving rapidly in time. This trend was observed during this Master's thesis with the introduction of new tests procedures in September 2017 and the discovery of the DPF fraud in July 2017.

Acronyms

ACEA European Automobile Manufacturers Association. 80

AFR Air-Fuel Ratio. 26

AMTD Atmospheric Measurement Techniques Discussion. 82

ATDC After Top Dead Center. 16, 17, 86

BC Black Carbon. 10, 15, 17, 86

BDC Bottom Dead Center. 22, 25

CA Crank Angle. 16, 17, 86

CF Conformity Factor. 7

CI Compression Ignition. 26

CNG Compressed Natural Gas. 10

CPC Condensation Particle Counter. 36, 37, 39, 40, 87

CVS Constant Volume Sampler. 32

DMA Differential Mobility Analyzer. 36, 87

DMPS Differential Mobility Particle Sizer. 83

DOC Diesel Oxidation Catalyst. 13, 17, 31

DPF Diesel Particulate Filter. I, 1–5, 7, 12, 13, 17, 29–32, 34, 39–42, 52, 55, 57, 59, 61, 62, 64–66, 69–74, 85, 86, 90

EC Elementary Carbon. 14, 15, 17, 86

ECU Engine Control Unit. 3, 67, 68

EGR Exhaust Gas Recirculation. 14, 16, 17, 31, 86

ELPI Electrical Low Pressure Impactor. 28, 36–38, 40, 72, 83, 87

EMPA Eidgenössische Materialprüfungs- und Forschungsanstalt. 84

EPL Ecole Polytechnique de Louvain. 42, 49

ETH Eidgenössische Technische Hochschule. 83

EU European Union. 8, 25

EUDC Extra-Urban Driving Cycle. 8, 90

EVC Exhaust Valve Closing. 20, 22, 24

EVO Exhaust Valve Opening. 20–23, 86

GDI Gasoline Direct Injection. 1, 2, 85

GOCA "Groupement des Entreprises agréées de Contrôle Automobile et du Permis de Conduire". I, II, 3, 4, 31, 32, 39–41, 51, 57, 72, 90

GPF Gasoline Particulate Filter. 2, 74

HEPA High Efficiency Particulate-free Air. 33, 87

IAC Institute for Atmospheric and Climate Science. 83

IC Inorganic Carbon. 14

IEA International Energy Agency. 80

IVC Intake Valve Closing. 19–22, 24, 86

IVO Intake Valve Opening. 19, 20, 22, 23, 86

LED Light-Emitting Diode. 28, 31, 32, 49, 86

LEZ Low Emission Zone. 10–12, 85, 90

LNG Liquefied Natural Gas. 10

LPO Low Pulse Occupancy. 29, 30, 86

LRTAP Long-Range Transboundary Air Pollution. 81

MEMS Micro Electromechanical Sensor. 34, 35, 37, 83, 87

MEVG Motor Emissions Vehicle Group. 8, 90

MEVG-A Motor Emissions Vehicle Group A. 8

MEVG-B Motor Emissions Vehicle Group B. 8

MPS Micro-Proportional Sampling. 32, 33, 86, 87

MTZ Motortechnische Zeitschrift. 83

NDIR Nondispersive Infrared. 74

NEDC New European Driving Cycle. 7–9, 18, 19, 26, 85, 86, 90

NOx Nitrogen Oxides. 2, 3, 7, 10, 11, 13, 14, 85

NPET Nanoparticle Emissions Tester. 40, 51–57, 59–61, 88, 90

OBD On-Board Diagnostics. 31

OC Organic Carbon. 14, 15, 17

PEMS Portable Emmision Measurement System. 3, 8

PFI Port Fuel Injected. 1, 2, 85

PM Particulate Matter. I, 1–8, 10, 12–18, 26–37, 40, 42–48, 52, 56, 61, 63, 65, 67–70, 72–74, 83–87, 90

PMP Particle Measurement Program. 8, 9, 32

PMR Power-to-Mass Ratio. 8, 9, 85

PN Particulate Number. 7, 8, 41, 48, 52–56, 59–61, 71, 88

PPS Pegasor Particle Sensor. 40

PSD Particulate Size Distribution. 15, 17, 32, 55, 69, 71

PTI Periodic Technical Inspection. 3, 7, 10, 30–32, 39, 72, 82, 90

QCM Quartz Crystal Microbalance. 34, 87

RDE Real Driving Emissions. 3, 7, 8, 80

SAE Society of Automative Engineers. 81–84

SCR Selective Catalytic Reduction. 31

SDSS Soot Deposit Spark Sensor. 35

SMPS Scanning Mobility Particle Sizer. 16, 28, 36, 37, 72, 87

SOF Soluble Organic Fraction. 12

TC Total Carbon. 14

TDC Top Dead Center. 20, 22, 25

TEOM Tapered Element Oscillating Microbalance. 34, 83

TFL Thermodynamics and Fluid mechanics Laboratory. 42

TNO Toegepast Natuurwetenschappelijk Onderzoek. 82

UART Universal Asynchronous Receiver-Transmitter. 44, 47

UDC Urban Driving Cycle. 8, 90

US EPA United States Environmental Protection Agency. 3, 6, 81, 85

VDC Volt Direct Current. 35

VRT Vlaamse Radio- en Televisieomroeporganisatie. 3

WHO World Health Organisation. 1, 6, 80

WLTC World harmonized Light vehicle Test Cycle. 8

WLTP World harmonised Light vehicle Test Procedure. 3, 7–9, 85

Nomenclature

Physical Quantities

A	Area
B	Cylinder bore
C_d	Discharge coefficient
D	Diameter
F_st	Stoichiometry factor
L	Piston shaft length
L_exv	Exhaust valve lift
L_inv	Intake valve lift
N_cyl	Number of cylinders
Q	Heat
R	Specific gas constant of air
S	Surface area
T	Temperature
V	Volume
V_c	Displacement volume
V_d	Dead volume
$\dot{V}$	Volume flow
W	Work
c_p	Isobaric heat capacity of air
c_v	Isochoric heat capacity of air
m	Mass
$\dot{m}$	Mass flow
n_e	Engine speed
p	pressure
r	Crank radius

r_{EGR}	EGR ratio
v	Velocity
x	Piston position inside the cylinder
η_{eff}	Volumetric efficiency
λ	Normalized air-to-fuel ratio
ϕ	Crank angle
κ	Isotropic exponent of air
φ	Dimensionless compressible flow number
ρ	Density
ω_{e}	Angular engine speed

Indices

EVC	Exhaust valve closing
EVO	Exhaust valve opening
IVO	Intake valve opening
IVC	Intake valve closing
TDC	Top dead center
bf	Back-flow
c	Cylinder
clt	Coolant
ex	Exhaust
exv	Exhaust valve
fg	Fresh Gas
in	Intake
inv	Intake valve
m	Manifold
pi	Piston
r	Runner
ram	Ramming
rg	Residual gas

Bibliography

[1] Michaël Torfs, Luc Pauwels, and VRT News Desk. Massive dpf fraud in diesel cars unnoticed by inspection centres. http://deredactie.be/cm/vrtnieuws.english/News/1.3014387, 2 July 2017.

[2] William Laenen. Wetenschappers tonen verband aan tussen luchtvervuiling en sterftecijfers per dag. https://www.vrt.be/vrtnws/nl/2017/12/28/fijnstof-verhoogt-al-na-een-dag-de-sterftekans-/, 28 December 2017.

[3] Sonal Patel. IEA: World's power sector trails others in air emissions. http://www.powermag.com/iea-worlds-power-sector-trails-others-in-air-emissions/, 2016.

[4] Dieter Quartier. Keep calm and diesel on. https://www.fleeteurope.com/en/fleet-strategy/europe/analysis/keep-calm-and-diesel, 10th April 2018.

[5] W. Addy Majewski. Diesel particulate matter. https://www.dieselnet.com/tech/dpf_sys.php, 2016.

[6] Catherine Dawson. New euro6 emissions standards set to clean up diesel. https://www.clm.co.uk/blog/euro6-emissions-ad-blue/, 2015.

[7] the free encyclopedia Wikipedia. Volkswagen emissions scandal. https://en.wikipedia.org/wiki/Volkswagen_emissions_scandal#VW_anti-pollution_system, 2018.

[8] Les Furets, Jonathan Rodriguez, Amel Hebbali, Lucas Perrin, Boris Vallano, and Mathilde Hodouin. Signification des normes antipollution euro 4, 5 et 6. https://www.lesfurets.com/assurance-auto/guide/que-signifient-les-normes-antipollution-euro-45-et-6, 21st September 2017.

[9] European Automobile Manufacturers Association (ACEA). Car emissions testing facts eu, what is the Real Driving Emissions (RDE) test? http://www.caremissionstestingfacts.eu/rde-real-driving-emissions-test/#, September 2017.

[10] Timelab vzw (Gent). Ik adem, bouwen van een fietssensor. http://ik-adem.be/#fietssensor.

[11] Civic Tech Netzwerks OK Lab Stuttgart. Luftdaten selber messen. http://luftdaten.info/.

[12] Leuvenair Civic Lab Leuven. Samen luchtkwaliteit meten in leuven. https://leuvenair.be.

[13] WHO Media centre. Ambient (outdoor) air quality and health. http://www.who.int/mediacentre/factsheets/fs313/en/, September 2016.

[14] M. Matti Maricq. Chemical characterization of particulate emissions from diesel engines: A review. Science Direct Aerosol Science 38 1079 – 1118, Research and Advanced Engineering, Ford Motor Company, 2007.

[15] United States Environmental Protection Agency (US EPA). Particulate matter (pm) basics. https://www.epa.gov/pm-pollution/particulate-matter-pm-basics#PM, September 2016.

[16] The European Parliament and the Council. Directive 2007/46/ec. https://eur-lex.europa.eu/legal-content/EN/TXT/PDF/?uri=CELEX:32007L0046&from=EN, 5 September 2007.

[17] Ecoscore. Directives européennes. http://ecoscore.be/fr/legislation/european, 2018.

[18] Dieselnet. Emission test cycles : Ece 15 + eudc / nedc. https://www.dieselnet.com/standards/cycles/ece_eudc.php, 2018.

[19] Dieselnet. Emission standards eu : Cars and light trucks. https://www.dieselnet.com/standards/eu/ld.php, 2018.

[20] Oliver F. Bischof. Recent developments in the measurement of low particulate emissions from mobile sources: A review of particle number legislations. https://link.springer.com/content/pdf/10.1007%2Fs40825-015-0016-9.pdf, 2015.

[21] B. Giechaskiel, J. Vanhanen, M. Väkevä, and G. Martini. Investigation of vehicle exhaust sub-23nm particle emission. *Aerosol Science and TEchnology*, 51, 2017.

[22] Belga News. Pollution de l'air: l'ue menace la belgique de sanctions financières. https://www.rtbf.be/info/belgique/detail_pollution-de-l-air-l-ue-menace-la-belgique-de-sanctions-financieres?id=5624733, 2011.

[23] Jean-Claude Verset. Le contrôle technique belge est-il vraiment pire qu'ailleurs? https://www.rtbf.be/info/dossier/la-redaction-vous-propose-aussi/detail_faut-il-changer-la-procedure-de-controle-technique?id=9015563, 2015.

[24] European Environment Agency. Air pollutant emissions data viewer (gothenburg protocol, LRTAP convention). https://www.eea.europa.eu/data-and-maps/dashboards/air-pollutant-emissions-data-viewer, 2017.

[25] Nico Cardone. Lage-emissiezone in antwerpen heeft positieve impact op luchtkwaliteit. https://www.vrt.be/vrtnws/nl/2018/05/18/lage-emissiezone-in-antwerpen-heeft-positieve-impact-op-luchtkwa/, Mei 2018.

[26] Elodie Debiere. La wallonie va aussi interdire les véhicules diesel les plus polluants, mais en 2020 et avec un système de vignette. http://fr.newsmonkey.be/article/21433, 2017.

[27] Carlo Di Antonio. Adoption de mesures fortes pour lutter contre la pollution atmospherique - zones de basses emissions & restriction du diesel en wallonie. http://diantonio.wallonie.be/home/presse--actualites/publications/publication-presse--actualites-6.publicationfull.html, 2017.

[28] Athanasios G. Konstandopoulos, Margaritis Kostoglou, Evangelos Skaperdas, Eleni Papaioannou, Dimitrios Zarvalis, and Evdoxia Kladopoulou. Fundamental studies of diesel particulate filters: Transient loading, regeneration and aging. SAE Mobilus 2000-01-1016, Foundation for Research and Technology – Hellas/Chemical Process Engineering Research Institute, 2000.

[29] W. Addy Majewski. Diesel particulate filters. https://www.dieselnet.com/tech/dpf.php#performance, 2011.

[30] Michael Fiebig, Andreas Wiartalla, Bastian Holderbaum, and Sebastian Kiesow. Particulate emissions from diesel engines: correlation between engine technology and emissions. Journal of Occupational Medicine and Toxicology 10.1186/1745-6673-9-6, 2014.

[31] W. Addy Majewski. Diesel filter systems. `https://www.dieselnet.com/tech/dpf_sys.php`, 2015.

[32] A. Karanasiou, M. C. Minguillón, M. Viana, A. Alastuey, J.-P. Putaud, W. Maenhaut, P. Panteliadis, G. Močnik, O. Favez, and T. A. J. Kuhlbusch. Thermal-optical analysis for the measurement of elemental carbon (ec) and organic carbon (oc) in ambient air a literature review. Technical Report 8, 9649–9712, Atmospheric Measurement Techniques Discussion, 2015.

[33] California Air Resources Board (CARB). Lev iii pm technical support document : development of particulate matter mass standards for future light-duty vehicles (appendix p). Technical report, 2011.

[34] Colin R. Ferguson and Allan T. Kirkpatrick. *Internal Combustion Engines Applied Thermosciences*. John Wiley & Sons, third edition, 2016.

[35] David B. Kittelson, Megan Arnold, and Winthrop F. Watts. Review of diesel particulate matter sampling methods. Final report, University of Minnesota, 1999.

[36] Xinling Li, Zhen Xu, Chun Guan, and Zhen Huang. Effect of injection timing on particle size distribution from a diesel engine. Science Direct Fuel 134 (2014) 189–195, Key Laboratory of Power Machinery and Engineering, Ministry of Education, Shanghai Jiao Tong University, 2014.

[37] Donaldson Company. Engine horsepower & exhaust flow guide. `http://www.asia.donaldson.com/en/exhaust/support/datalibrary/1053747.pdf`.

[38] Raymond C. Turin, Rhon Zhang, and Man-Feng Chang. Volumetric efficiency model for variable cam-phasing and variable valve lift apllications. SAE Mobilus 2008-01-0995, General Motors, 2008.

[39] Joseph Martin. Moteurs à combustion interne, 2004.

[40] António Emanuel Figueiredo Costa. Computer simulation of an internal combustion engine. Master's thesis, Faculdade de Engenharia da Universidade do Porto and University of Maryland, Baltimore County, 2008.

[41] Jim Parks, Bill Partridge, and Vitaly Prikhodko. An optical backscatter sensor for particulate matter measurement. SAE Mobilus 2009-01-0687, Oak Ridge National Laboratory, 2009.

[42] World Air Quality China. The shinyei experiment : Real-time air quality readings from beijing. `http://aqicn.org/sensor/shinyei/`, 2018.

[43] G. Kadijk, M. Elstgeest, N.E. Ligterink, and P.J. van der Mark. Investigation into a Periodic Technical Inspection (PTI) test method to check for presence and proper functioning of diesel particulate filters in light-duty diesel vehicles – part 2. TNO report R10530 | 1.0, Earth, Life & Social Sciences, The Hague, 2017.

[44] Belgian Royal Decree MB 28.03.1968 Chapter VI. article 39. `https://www.code-de-la-route.be/textes-legaux/sections/ar/reglement-technique-des-vehicules/142-hs4`.

[45] W. Addy Majewski and Hannu Jääskeläinen. Smoke opacity. https://www.dieselnet.com/tech/measure_opacity.php, 2013.

[46] Emily D. Pertl, Franz A. Pertl, Daniel K. Carder, James E. Smith, and Mridul Gautam. Design of a portable micro-dilution tunnel particulate matter emissions measurement system. SAE Mobilus 2005-3795, West Virginia University, 2005.

[47] Dr. Wolfgang Schindler, Dr. Alexander Bergmann, Manfred Linke, Ferdinand Mosbacher, and Katia Giovanella. Facing the challenge particle measurement for euro 5 / 6 and alternative particle measurement technology. MTZ 06|2008 Volume 69, 2008.

[48] Timothy T. Diller, Matthew J. Hall, and Ronald D. Matthews. Further development of an electronic particulate matter sensor and its application to diesel engine transients. SAE Mobilus 2008-01-1065, The University of Texas at Austin, 2008.

[49] D. R. Booker, R. A. Giannelli, and J. Hu. Road test of an on-board particulate matter mass measurement system. SAE Mobilus 2007-01-1116, Sensor's, Inc. and U.S. Environmental Protection Agency, 2007.

[50] Gerard W. Malaczynski and Gregory Roth. Real-time sensing of particulate matter in a vehicle exhaust system. SAE Mobilus 2017-01-1639, Delphi Automotive Systems, 2017.

[51] Sera Lim, Sundong Kwon, Kukjin Chun, Seungbeom Yoo, and Jin-ha Lee. MEMS sensor for particulate matter measurement of exhaust gas. SAE Mobilus 2013-01-0011, Hyundai Motor Co. and Seoul National Univ., 2013.

[52] Atmospheric physics lab work Differential Mobility Particle Sizer (aerosol measurements). Institute for Atmospheric and Climate Science (IAC) ETH.

[53] Heinz Burtscher, W. Addy Majewski, and Hannu Jääskeläinen. PM measurement: In-situ methods. https://www.dieselnet.com/tech/measure_pm_ins.php, 2017.

[54] Dekati Company. ELPI®+. https://www.dekati.com/products/Fine%20Particle%20Measurement/ELPI%C2%AE%2B.

[55] Wikipedia (Kaet). Corona discharge. https://en.wikipedia.org/wiki/Corona_discharge, 2003, latest revision 2017.

[56] A. Järvinen, M. Aitomaa, A. Rostedt, J. Keskinen, and J. Yli-Ojanperä. Calibration of the new electrical low pressure impactor (elpi+). Journal of aerosol science 69 (150-159), Tampere University of Technology, Department of Physics, Aerosol Physics Laboratory, 2014.

[57] Ltd. Nova Fitness Co. Laser pm2.5 sensor specification (sds011, v1.0). http://dokuwiki.hatlab.fr/lib/exe/fetch.php?media=projet:stationmesure:sds011_spec_v1.0.pdf, 2014.

[58] Messungen und Naturschutz Baden-Württemberg (LUBW) Landesanstalt für Umwelt. Messungen mit dem feinstaubsensor sds011. Technical report, Juni 2017.

[59] Shinyei Company. Datasheet shinyei ppd42ns dust sensor. http://wiki.timelab.org/images/f/f9/PPD42NS.pdf, 2010.

[60] Wikipedia. Tapered Element Oscillating Microbalance. https://en.wikipedia.org/wiki/Tapered_element_oscillating_microbalance, 2017.

[61] Martin Mohr, Anna-Maria Forss, and Dominik Steffen. Particulate emissions of gasoline vehicles and influence of the sampling procedure. SAE Mobilus 2000-01-1137, Swiss Federal Laboratories for Materials Testing and Research (EMPA), 2000.

[62] Mir-Akbar Hessami and Carolyn Child. Statistical analysis of diesel vehicle exhaust emission: Development of empirical equations to calculate particulate emission. SAE Mobilus 2004-01-3066, Monash University, 2004.

[63] David L. McKain, Scott Wayne, and Nigel Clark. Relationship between carbon monoxide and particulate matter levels across a range of engine technologies. SAE Mobilus 2012-01-1346, West Virginia University, 2012.

[64] Claudio Mazzoleni, Hans Moosmüller, Hampden D. Kuhns, Robert E. Keislar, Peter W. Barber, Djordje Nikolic, Nicholas J. Nussbaum, and John G. Watson. Correlation between automotive co, hc, no, and PM emission factors from on-road remote sensing: implications for inspection and maintenance programs. Science Direct 477–496, Desert Research Institute, University and Community College System of Nevada, 2004.

[65] European Environment Agency. Emission de particules fines. `http://www.indicators.be/fr/i/BGD_ENV_PME/Emissions_de_particules_fines`, 2016.

[66] Burkhard Stiller, Thomas Bocek, Fabio Hecht, Guilherme Machado, Peter Racz, and Martin Waldburger. Mobile Systems IV. Technical report, University of Zurich, Department of Informatics, 01 2010.

[67] Transport & Environment. How to tackle the illegal diesel filter removal 'industry' in belgium and beyond, July 2017. https://www.transportenvironment.org/news/how-tackle-illegal-diesel-filter-removal-industry-belgium-and-beyond.

List of Figures

1 Energy-related PM2.5 by region in 2015 considering 3 major sectors: buildings, industry and transport. The transport sector contributes with a significant amount to the PM2.5 emissions In Europe, the United States and the Middle East. [3] . 1

2 Visual comparison of the PM emissions for modern and old diesel and gasoline light duty vehicles. Diesel engines with DPF emit considerably less PM emissions than diesel engines without a DPF. Old gasoline PFI engines are characterized by low PM emissions whereas modern GDI engines are emitting significantly more PM especially during the cold start phase (see FTP bag 1). [5] 2

3 History of Euro emissions standards for diesel passenger cars concerning NOx and PM emissions from 1992 until 2014 covering the Euro norms 1 until 6. The non-scaled graph shows that the norms have decreased exponentially with the years. [6] 2

4 The PM concentration in Northern Belgium with the measurement system developed by OK Lab based on the optical backscatter sensor Nova Laser PM2.5 on 6th April 2018. The detailed measurement of the sensor in Louvain-la-Neuve is given on the right side of the Figure. The guideline values fixed by the WHO for 24-hour mean and annual mean are respectively 25 $\mu g/m^3$ and 10 $\mu g/m^3$ for PM2.5 and 50 $\mu g/m^3$ and 20 $\mu g/m^3$ for PM10. [11] 4

1.1 Size comparisons for PM between fine sand beach, human hair, PM2.5 and PM10 as defined by US EPA. [15] 6

1.2 The WLTC concerning Class 3b vehicles, i.e. typical vehicles driven in Europe (PMR $\geq$ 34 W/kg and $v_{max} \geq$ 120 km/h). 9

1.3 Differences between NEDC and WLTP introduced respectively in the year 2000 and 2017. The main difference is that WLTP is more dynamic reaching higher average and maximum speeds and including motorways and freeways. 9

1.4 Small particle emissions (PM2.5) of European countries in 2015 [24]. The more the color tends to green, the lower is the rate of emission of particles of matter and vice versa when the color tends towards the red. Belgium being colorized in green, it is among the countries that emitted the lowest PM concentration. . . . 10

1.5 Decrease of the soot and NOx emissions in Antwerp since the introduction of the LEZ. The observed decrease is at its highest at places with a lot of congestion. A maximum decrease of 19.2 % for soot emissions is observed in Borgerhout whereas the maximum decrease of NOx emissions (27.6 %) is observed in de Belgiëlei. . . 11

1.6 The honeycomb wall-flow monolith is the most popular geometric configuration for actual DPFs since its compactness allows to have a low pressure drop without reducing the filtration rate nor the available space. [28] 12

1.7 Particles are trapped by a DPF thanks to a combination of filtration mechanisms among which diffusional and inertial deposition and flow-line interception [29]. The filtration efficiency of each filtration mechanism varies according to the particle's aerodynamic diameter. [30] 13

1.8 A tree-shape summary of the different types of options in the case of a blocked diesel particulate filter. The filter can then either be replaced, either be regenerated through active and passive processes. The latter process consists in lowering the soot oxidation temperature with a catalyst whereas active regeneration consists in increasing the soot temperature. 14
1.9 Comparison between EC, BC and soot. [33] 15
1.10 The particle size distribution of diesel exhaust expressed in mass and number weightings have three distinctive modes. The nucleation mode contains more than 90 % of the number weighting whereas the accumulation mode contains a considerable amount of the mass weighting. The coarse mode particles are formed through deposition and re-entrainement of accumulation mode particles. [35] . . 16
1.11 The effects of EGR and injection timing, expressed in CA ATDC, on particle size distribution. The PM emissions of a a four-cylinder, four-stroke diesel engine are measured with a scanning mobility particle sizer after a two-stage dilution. [36] . 17

2.1 Representation of the speed during the NEDC which is composed of four urban driving cycle and one extra-urban driving cycle. ECE-15 represents one elementary urban cycle. 19
2.2 The evolution of the cylinder volume in function of the CA with the specified opening and closing times of the inlet and exhaust valves of a four-stroke engine. 21
2.3 The evolution of the pressure inside the cylinder from IVC to EVO. The peak in pressure is not aligned with the crank angle at top dead center ϕ_{TDC} because the combustion is delayed which is generally the case in cars. 21
2.4 The cylinder pressure between IVO and EVO approximated as the superposition of three linear pressure functions. [38] 23
2.5 The pressure inside the cylinder in function of the cylinder volume for a four-stroke engine. Figure (b) is a zoom at low pressure of Figure (a) and allows to have a better image of the corresponding valve timings. 24
2.6 Representation of the temperature variation versus the crank angle with the valve timings represented in red and green. 24

3.1 The optical backscatter sensor is composed of a photodiode which measures the light emitted by the LED source whenever a particle scatters its light beam. The output signal is directly proportional to the amount of particles. 28
3.2 The optical backscatter PM sensor developed by the Oak Ridge National Laboratory (U.S. Department of Energy) that is based on the light scattering principle. The sensor uses optic fibers for the signal transmission and measures a PM concentration at the exhaust manifold, i.e. before a DPF. [41] 29
3.3 The photodiode voltage in function of time for the Shinyei PM2.5 PPD42NS sensor, a low-cost PM2.5 sensor. The measurement principle of the sensor is based on the scattering of light by particles. The more scattered light the photodiode intercepts, the higher the spikes and also the greater the particle's size. [42] . . . 29
3.4 The photodiode voltage in function of time for the Shinyei PM2.5 PPD42NS sensor with a representation of the LPO. The latter represents the amount of time the photodiode detects a moving particle and is analogous to an opacity percentage. The red line represents the pass band filter excluding small particles and noise. [42] 30
3.5 The measurement technique of the opacimeter that is distinguished from optical backscatter sensors by the location of the receiver and emitter on either side of the exhaust pipe. 31
3.6 The model 7610 Mott Corporation Micro-Proportional Sampling (MPS) of the Micro-dilution Tunnel PM Measurement System. The cross-flow design of the micro-dilution tunnel avoids that the porous walls get clogged. [46] 33

3.7 The block diagram of the micro-dilution tunnel PM measurement system developed by West-Virginia University. Next to a MPS, the measurement sensor is composed of a HEPA filter, a chiller and a filter. [46] 33
3.8 QCM where the externally driven crystal oscillates at a frequency depending on the thickness of the electrodes, the crystal and the deposited PM. 34
3.9 The measurement technique of the Delphi PM sensor that is based on the accumulation of PM on electrodes altering their conductance. [50] 35
3.10 The charge induced electrodynamic MEMS composed of a heater to remove the deposited particles and a semiconductor that measures a change in electric field as particles move along. [51] 35
3.11 Block diagram of the SMPS composed of a DMA to size the particles and a CPC to count them. [52] 36
3.12 Schematic illustrating the working principle of a CPC. The pool saturated with alcohol vapor allows to increase the size of the sub-micron particles which makes them visible to the lamp of the optical system. [53] 37
3.13 The block diagram of the ELPI+ of Dekati ® which is composed of an unipolar charger, a low pressure impactor and electrometers. [56] 38

4.1 The packaging developed for the low-cost sensors consisting of a measurement chamber, a T-branch, a valve and two membrane pumps. The filtered air flux is represented in blue, the exhaust gases in red and the diluted exhaust gases in green. 43
4.2 The Nova laser PM2.5 sensor with its ventilator represented by the black square and its wind inlet with a possible connection to a hose (a). An inside view of the Nova sensor identifies the laser and photodiode (b). 45
4.3 A comparison of the PM2.5 and PM10 measurement of the Nova sensor during an experiment with incense. Based on the behaviour at low and high concentrations it is supposed that two measurements are done or that a non linear conversion function is applied. 45
4.4 Both Figures show the influence of air humidity on the PM10 concentrations measured by the Nova sensor, see *PM 10_OK*, compared to a reference Grimm PM sensor, see *PM 10_GRIMM*. The air humidity is represented with the *Luftfeuchtigkeit* curve. Figure (a) shows the overrated particulate mass measurements of the Nova sensor for a relative humidity above 70 % whereas Figure (b) shows the underrated particulate mass measurements for a relative humidity below 50 % compared to the reference Grimm sensor. 46
4.5 The MakeBlock Me PM2.5 sensor measuring three types of particulate mass concentration, i.e. PM1.0, PM2.5 and PM10. The sensor has a small circular opening for the inlet on the back of the sensor and a small ventilator at the exit which guarantees air circulation in the sensor. 47
4.6 Tests with incense reveal that the different particulate mass measurements of the MakeBlock Me PM2.5 sensor are offset with a proportional factor. This, however, does not represent the reality as observed on the particle size distribution of Chapter 1. 48
4.7 The Shinyei PPD42NS Dust Sensor (a) with an inside cut of the sensor (b). The sensor measures a particle number concentration and has a small resistance for the air circulation. 49
4.8 A comparison of the photodiode and laser of the three low-cost sensors, i.e. the Shinyei, MakeBlock and Nova sensors. 50

5.1 The particulate mass measurement of the Nova sensor without dilution during low idle speeds on the Opel Astra show a similar trend compared to the TEN LPA but an opposed trend compared to the Pegasor Mi3. The particulate mass concentration is nondimensionalized with the first measurement which corresponds to a measurement of ambient air. 53
5.2 The PN measurements of the TSI NPET and the Pegasor Mi3 sensors during low idle speeds on the Opel Astra. 53
5.3 The probe of the Pegasor Mi3, i.e. the probe in the middle, is rigid and does not have a handle fixing the probe in the tailpipe compared to the TEN LPA and TSI NPET probes, respectively the left and right probes. 54
5.4 The absoluteparticulate mass measurements of the Nova sensor without dilution during low idle speeds on the Opel Astra. The Nova sensor indicates a similar particulate mass concentration as the Pegasor Mi3 sensor but the TEN LPA sensor measures higher mass concentrations. 55
5.5 The nondimensional particulate mass measurement of the Nova sensor with a dilution during low idle speeds on the Citroën Berlingo. A similar trend compared to the TEN LPA and the Pegasor Mi3 is observed. 56
5.6 The dimensional PN concentration measured by the Pegasor Mi3 and TSINPET during low idle speeds on the Citroën Berlingo. Opposite behaviours are observed at the small peaks and correspond to the activation of the cooling fan. 56
5.7 The dimensional particulate mass measurement of the Nova sensor with a dilution during low idle speeds on the Citroën Berlingo. The Nova sensor indicates a lower particulate mass concentration than the TEN LPA and the Pegasor Mi3 sensors that are close to each other. 57
5.8 The nondimensional particulate mass measurements of the Nova sensor without dilution during high idle speeds on the Opel Astra. The low-cost sensor has an opposite behaviour compared to the TEN LPA, a second generation opacimeter. The particulate mass concentration is nondimensionalized with the first measurement which corresponds to a measurement of ambient air. 58
5.9 The nondimensional particulate mass measurements of the Nova sensor with dilution on an Opel Astra (Euro 6b) during high idle speed. The TEN LPA, a second generation opacimeter, shows similar behaviours with smaller peaks during the accelerations. The particulate mass concentration is nondimensionalized with the first measurement which corresponds to a measurement of ambient air. . . . 58
5.10 The logarithm of the absolute measurements at high idling on the Opel Astra (Euro 6b) show significant differences for the Nova sensor and the TEN LPA with a difference of three order of magnitudes. 59
5.11 Nondimensional particulate mass measurements of the Nova sensor with dilution on a Citroën Berlingo (Euro 3) during high idle speed. The TEN LPA, a second generation opacimeter, and the Pegasor Mi3 measure Similar behaviours as the Nova sensor. The particulate mass concentration is nondimensionalized with the first measurement which corresponds to a measurement of ambient air. 60
5.12 The dimensional PN concentration measured by the Pegasor Mi3 and TSI NPET during high idle speeds on the Citroën Berlingo. The peaks exceeding the graph limits for the Pegasor Mi3 are due to the overloading of the electrometer. 60
5.13 The logarithm of the absolute measurements at high idle on the Citroën Berlingo (Euro 3). Significant differences are observed for the Nova sensor compared to the Pegasor Mi3 and TEN LPA with approximatively three orders of magnitudes dissimilarity. 61

5.14 The particulate mass measurements of the MakeBlock sensor at low idle speed on the Opel Astra. The absolute particulate mass concentration is too low to be analyzed. No filter is applied on the results because the variation of the measurements is not revelatory enough. 63
5.15 The particulate mass measurement of the MakeBlock sensor with a dilution during low idle speeds on the Citroën Berlingo shows a similar trend compared to the TEN LPA and to the Pegasor Mi3. The particulate mass concentration is nondimensionalized with the first measurement which corresponds to a measurement of ambient air. 63
5.16 The absolute particulate mass measurement of the MakeBlock sensor with a dilution during low idle speeds on the Citroën Berlingo. The MakeBlock sensor indicates lower particulate mass concentration than the TEN LPA and the Pegasor Mi3 sensors which are close to each other only when the probes are in the tailpipe. 64
5.17 The nondimensional particulate mass measurement of the MakeBlock sensor with dilution during high idle speeds on the Citroën Berlingo. The Pegasor Mi3 and the MakeBlock sensor have same behaviours whereas the TEN LPA measures only small peaks during the accelerations. The particulate mass concentration of each sensor is nondimensionalized with the first measurement which corresponds to a measurement of ambient air and is represented on the left-hand y-axis. . . . 65
5.18 The logarithm of the absolute measurements of the MakeBlock sensor at high idle on the Citroën Berlingo (Euro 3). Significant differences of one to two orders of magnitudes are observed between the MakeBlock sensor and the Pegasor Mi3 and TEN LPA. The left-hand y-axis represents the 10-base logarithm of the particulate mass concentration expressed in micro-grams per cubic meter. 66
5.19 Particulate mass concentration measured by the Makeblock sensor on the Citroën gasoline laboratory engine when varying the torque between 72 Nm and 95 Nm. The particulate mass measurements are proportional to the load even though precise steps are not obtained. The black curve represents an intermediate transition torque level. 68
5.20 Particulate mass concentration measured by the Nova sensor on the Citroën gasoline laboratory engine when varying the torque between 72 Nm and 95 Nm. The particulate mass measurements are proportional to the load and distinctive and precise steps are obtained. 69
5.21 Experiment with incense on the Nova and MakeBlock low-cost sensors. Similar measurements are obtained for both sensors with a higher sensitivity of the MakeBlock sensor. 70

B.1 The MakeBlock PM2.5 sensor shows no trend in its PM measurements on a high idling Euro 6b car. The results of the sensor are neither filtered nor nondimensionalized since mainly two integer values are returned, zero or one. 93

List of Tables

1.1 The Euro norms of the European Union for vehicles from category M1 corresponding to passenger cars with a mass that is greater or equal to 2,500 kg [17]. A sharp drop is observable over time for the limit of the mass of PM from 140 mg/km in 1992 to 5 mg/km in 2014. 7
1.2 Characterization of the MEVG cycle test composed of urban and extra-urban segments. MEVG test cycles are characterized by one EUDC and four repetitions of the UDC. The NEDC follows the MEVG cycle test and imposes a cold start. . 8
1.3 Table with the evolution of the prohibition of the most polluting diesel vehicles in Brussels' LEZ. 12

2.1 Conversion of the norms into volume concentration for a Volvo V40 commercialized in 2000. 25
2.2 Conversion of the norms into volume concentration for a Volvo V40 commercialized in 2016. 26
2.3 Ratios of the allowable mass of particulate matter to the mass of diesel fuel for a Volvo V40 commercialized in 2000. 26
2.4 Ratios of the allowable mass of particulate matter to the mass of diesel fuel for a Volvo V40 commercialized in 2016. 27

3.1 During the PTI, the maximum allowed smoke emissions becomes very close to the margin of error (0.5 m^{-1}) for recent vehicles. [43] 31
3.2 Comparative table between first and second generation opacimeters which are respectively used during PTI and investigated by GOCA for their ability to detect the presence of a DPF. 32

4.1 Characteristics of the two diesel M1-category cars used for testing the low-cost sensors during a low and high idle speed test. 40
4.2 Specifications of the Nova laser PM2.5 sensor including its concentration range and working temperature range which will be a limiting factor for dilution during the experiments. 44
4.3 Specifications of the MakeBlock Me PM2.5 sensor including its concentration range and working temperature range which will be a limiting factor for dilution during the experiments. The concentration range of the sensor as well as its serial data output frequency is determined from experiments with the sensors. 47
4.4 Specifications of the Shinyei PPD42NS Dust Sensor including its concentration range and working temperature range. 48

5.1 The measurement's frequency and the window size of the moving average filter for the two low-cost sensors, i.e. the Nova and Makeblock PM2.5 sensors, and the three state-of-the-art measurement systems of GOCA, i.e. the Pegasor Mi3, the TSI NPET and the TEN LPA. 51

5.2 Comparison in absolute measurements between the Nova sensor and the state-of-the-art measurement systems for each type of test on each diesel car. The orders of magnitude stay approximately constant for each car and varying type of test. The differences in order of magnitude of the Citroën Berlingo include a dilution. 62
5.3 Comparison in absolute measurements between the MakeBlock sensor and the state-of-the-art measurement systems for each type of test on each diesel car. The differences in order of magnitude vary for the Citroën Berlingo depending on the type of test. 66

A.1 Technical details of a Volvo V40 1.9 D 102ch Summum 92
A.2 Technical details of a Volvo V40 II D2 102ch Kinetic 92

Appendix A

Technical Details of the Cars of the Conversion of the Euro Norms

A.1 Volvo V40 1.9 D 102ch Summum

Fuel	Diesel
Norm	Euro 3
Dimensions of the wheels	195/60 R15
Displacement volume	1,870 cm^3
Number of cylinders	4
Number of valves	8
Bore	80 mm
Stroke	93 mm
Volumetric ratio	19.0:1
End of market date	01/05/2002

Table A.1: *Technical details of a Volvo V40 1.9 D 102ch Summum*

A.2 Volvo V40 II D2 102ch Kinetic

Fuel	Diesel
Norm	Euro 6
Dimensions of the wheels	205/55 R16
Displacement volume	1,969 cm^3
Number of cylinders	4
Number of valves	16
Bore	82 mm
Stroke	93.2 mm
Volumetric ratio	16:1
End of market date	01/04/2017

Table A.2: *Technical details of a Volvo V40 II D2 102ch Kinetic*

Appendix B

Experiments with State-of-the-art Measurement Systems

B.1 High Idle Speed Test of MakeBlock Sensor on Opel Astra

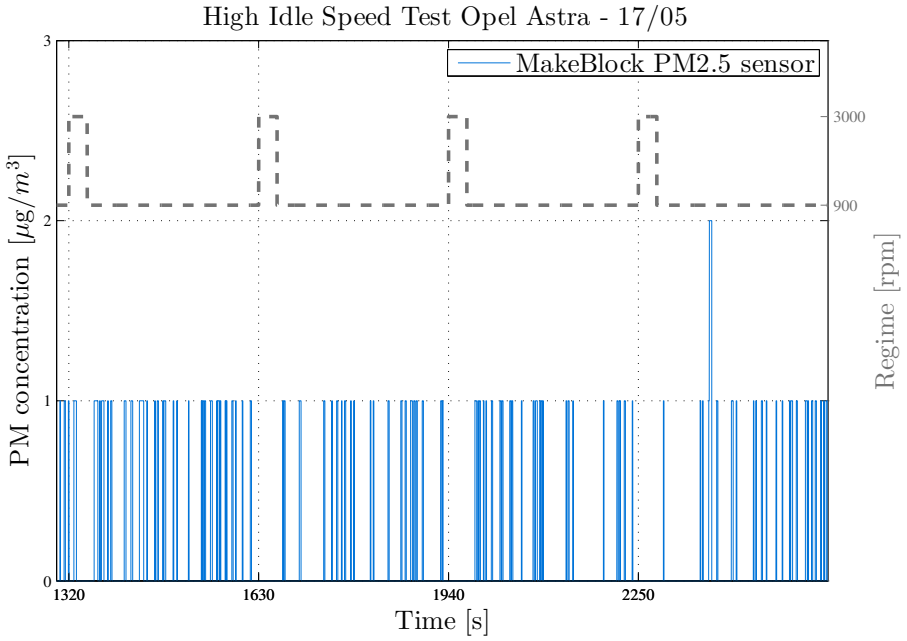

Figure B.1: *The MakeBlock PM2.5 sensor shows no trend in its PM measurements on a high idling Euro 6b car. The results of the sensor are neither filtered nor nondimensionalized since mainly two integer values are returned, zero or one.*

B.2 Schedule of the Tests at the GOCA Center

Wednesday, 16th May 2018

At 8h12 The weather conditions are 13°C, 1016 hPa, 91% humidity and a wind of 10 km/h in the west-north-west direction

At 10h14 The test begins on the Opel Astra. The following sensors are used :

- Nova Laser PM2.5
- Pegasor Mi3
- TEN LPA

At 12h23 The weather conditions are 20°C, 1016 hPa, 57% humidity and a wind of 19 km/h in the north direction

At 13h26 The test begins on the Citroën Berlingo. The following sensors are used :

- MakeBlock Me PM2.5
- Pegasor Mi3
- TEN LPA

Thursday, 17th May 2018

At 8h45 The weather conditions are 11°C, 1023 hPa, 72% humidity and a wind of 16 km/h in the north direction

At 9h49 The test begins on the Opel Astra. The following sensors are used :

- MakeBlock Me PM2.5
- Pegasor Mi3
- TEN LPA

At 10h32 The weather conditions are 13°C, 1023 hPa, 62% humidity and a wind of 16 km/h in the north direction

At 12h14 The test begins on the Opel Astra. The following sensors are used :

- Nova Laser PM2.5
- Pegasor Mi3
- TSI NPET
- TEN LPA

Tuesday, 22th May 2018

At 8h13 The weather conditions are 14°C, 1013 hPa, 96% humidity and a wind of 3 km/h in the west-south-west direction

At 8h47 The test begins on the Citroën Berlingo. The following sensors are used :

- Nova Laser PM2.5
- Pegasor Mi3
- TSI NPET
- TEN LPA

At 9h32 The weather conditions are 17°C, 1013 hPa, 82% humidity and a wind of 6 km/h in the west-north-west direction

At 10h12 The weather conditions are 18°C, 1013 hPa, 74% humidity and a wind of 5 km/h in the north-west direction

At 10h35 The test begins on the Citroën Berlingo. The following sensors are used :

- Nova Laser PM2.5
- Pegasor Mi3
- TSI NPET
- TEN LPA

Rue Archimède, 1 bte L6.11.01, 1348 Louvain-la-Neuve **www.uclouvain.be/epl**